CHARACTERIZATION OF *GRAPEVINE VEIN CLEARING VIRUS* EXPRESSION STRATEGY AND DEVELOPMENT OF CAULIMOVIRUS INFECTIOUS CLONES

A Dissertation

presented to

the Faculty of the Graduate School

at the University of Missouri-Columbia

In Partial Fulfillment

of the Requirements for the Degree

Doctor of Philosophy

in Plant, Insect and Microbial Sciences

---

by

YU ZHANG

Dr. James E. Schoelz, Dissertation Supervisor

DECEMBER 2016

The undersigned, appointed by the dean of the Graduate School,

have examined the dissertation entitled

CHARACTERIZATION OF *GRAPEVINE VEIN CLEARING VIRUS* EXPRESSION STRATEGY AND DEVELOPMENT OF CAULIMOVIRUS INFECTIOUS CLONES

Presented by Yu Zhang

A candidate for the degree of doctor of philosophy

In Plant, Insect and Microbial Sciences

And hereby certify that, in their opinion, it is worthy of acceptance.

Dr. James E. Schoelz, PhD

Dr. Wenping Qiu, PhD

Dr. David G. Mendoza-Cózatl, PhD

Dr. Trupti Joshi, PhD

ACKNOWLEDGEMENTS

I wish to express my appreciation to my advisor, Dr. James Schoelz, for his constant guidance and support during my doctoral studies. He is a role model to me as an enthusiastic and hard working scientist. Although I will leave MU, I will keep what I learnt from him with my future life.

I owe thanks to members of my doctoral committee, Dr. Wenping Qiu, Dr. David G. Mendoza-Cózatl, and Dr. Trupti Joshi, for their helpful comments and suggestions. I also want to thank Dr. Dmitry Korkin, who served in my committee for one year and helped me with bioinformatics and data interpretation.

Thanks are due to my colleagues in the lab, Dr. Carlos Angel, Dr. Andres Rodriguez, Mustafa Adhab, and Mohammad Fereidouni, who I really enjoyed working with. In addition, Mustafa Adhab contributed to chapter 5 by helping me with screening vein clearing symptoms on young leaves of *N. benthamiana* and taking pictures of symptomatic leaves. Mustafa has such a keen eye for early stage viral disease symptoms.

Finally, I'm grateful to my parents, family, and friends for their constant, unconditional support during my studies in Missouri

TABLE OF CONTENTS

LIST OF TABLES

LIST OF FIGURES

LIST OF FIGURES

LIST OF FIGURES

LIST OF FIGURES

LIST OF FIGURES

CHARACTERIZATION OF *GRAPEVINE VEIN CLEARING VIRUS* EXPRESSION STRATEGY AND DEVELOPMENT OF CAULIMOVIRUS INFECTIOUS CLONES

Yu Zhang

Dr. James E. Schoelz, Dissertation Supervisor

ABSTRACT

Grapevine Vein Clearing Virus (GVCV) is a newly discovered DNA virus in grapevine that is closely associated with grapevine vein clearing syndrome observed in vineyards in Missouri and surrounding states. However, Koch's postulates have never been completed. Four chapters discussing four projects related to GVCV are included in this dissertation. This is a step further toward efficient management of the grapevine vein clearing syndrome in the future.

Chapter 2 focuses on GVCV promoter characterization and GVCV mRNA transcript mapping. Portions of the GVCV large intergenic region were cloned and assessed for promoter activity, and the segment between nucleotides 7,332 and 7,672 was sufficient to drive expression of downstream ORF. 5' RACE and 3' RACE revealed that transcription was initiated predominantly at nucleotide 7,571 and terminated at nucleotide 7,676. Additional transient expression analysis studies were

supportive of a ribosomal shunt model for expression of ORF1 of GVCV

Chapter 3 is about *Cauliflower mosaic virus* (CaMV) and its P6 protein. P6 and P6-GFP were examined for the ability to complement a defect CaMV isolate that contains a lethal mutation in its P6 coding region. P6-GFP was able to perform all the functions of P6 and support coat protein expression and virion assembly. The co-agroinfiltration assay of *Nicotiana benthamiana* developed in this chapter was used to evaluate the infectivity of an infectious clone of GVCV.

Chapter 4 describes the construction of a terminally redundant clone of GVCV. The GVCV genome was assembled via three overlapping DNA fragments amplified from GVCV-infected tissues and the terminally redundant clone, designated pGVCV-1, was inserted into an Agrobacterium binary vector for delivery into plant cells. The co-agroinfiltration assay described in chapter 3 was applied, and pGVCV-1 was shown to be capable of replication and encapsidation. Furthermore, a systemic veinal chlorosis symptom was observed in several of the *N. benthamiana* plants agroinoculated with pGVCV-1, indicating that the virus clone was infectious. Two types of virus-like particles, long flexuous rods and bacilliform particles, were purified from either pGVCV-1 infiltrated *N. benthamiana* leaves or GVCV-infected grape leaves showing typical vein clearing symptoms, and further research is planned to characterize the nature of the flexuous rods in these plants.

Two species of mealybugs were tested for their ability to acquire and transmit

Grapevine vein clearing virus in chapter 5. The longtailed mealybugs were collected from a cycad plant in Tucker greenhouse (University of Missouri), whereas a mixed population of longtailed and citrus mealybugs were collected from infested grapevines in the Ashland-Gravel greenhouses (University of Missouri). Both populations were able to acquire GVCV after short feeding periods of as little as three days. However, the tucker population was not able to persist on grapevines and was not tested for transmission of GVCV. The Ashland-Gravel population was tested for transmission but none of the plants developed symptoms indicative of GVCV, and PCR assays showed GVCV was not transmitted to any of the 31 grapevine plants. I conclude that the citrus and longtailed mealybugs are unlikely to be the vectors for GVCV.

CHAPTER 1: LITERATURE REVIEW

1. THE FAMILY CAULIMOVIRIDAE

The *Caulimoviridae* family contains all plant viruses that have a double-stranded DNA genome and replicate by reverse transcription in their life cycles. Viruses belonging to this family are termed pararetroviruses, to distinguish them from retroviruses (RNA reverse-transcribing viruses) (Haas *et al.*, 2002). There are two major differences between pararetroviruses and retroviruses. First, pararetroviruses contain DNA in the capsid whereas retroviruses contain RNA within the capsid. Second, the DNA intermediate of retroviruses is integrated into the host DNA, whereas the DNA of pararetroviruses acts as a free chromosome in the nucleus of the host cell (Haas *et al.*, 2002). The latter property is shared by the hepadnaviruses, of which the type member is the human pathogen *Hepatitis B virus*. The caulimoviruses and hepadnaviruses together form the so-called pararetrovirus supergroup.

There are six genera within the Caulimoviridae. They are the *Caulimovirus*, *Petuvirus*, *Soymovirus*, *Cavemovirus*, *Badnavirus*, and *Tungrovirus*. *Cauliflower mosaic virus* (CaMV) is the type species of *Caulimoviridae*. It is the first DNA plant virus to be discovered (Haas *et al.*, 2002); before this, all plant virus genomes were thought to be composed of RNA. Furthermore, CaMV is the first plant-associated organism to be completely sequenced (Franck *et al.*, 1980), as well as the first plant virus to be cloned in infectious form (Hohn *et al.*, 1980). The full-length genome of

CaMV was cloned into the bacterial plasmid pBR322 (Hohn *et al.*, 1980) and it was subsequently shown that a CaMV infection could be initiated from the cloned DNA by excising the CaMV DNA from the plasmid DNA and rubbing this mixture onto turnip leaves (Gardner & Shepherd, 1980). This simple experiment revolutionized plant virology because it meant that mutations could be precisely engineered into the virus genome and their effect on the virus studied. In addition, it led the way towards the development of plant viruses as vectors for foreign genes and ultimately as tools for Virus Induced Gene Silencing (VIGS). The following chapter discusses the molecular biology of CaMV, since this virus has been studied in greatest detail. This information serves as a guide for studies with badnaviruses and in particular for the badnavirus *Grapevine vein clearing virus* (GVCV).

2. THE BIOLOGY OF CAMV

2.1. *Cauliflower mosaic virus* (CaMV)

CaMV was first described by Tompkins (1937). A disease of cauliflower observed in a field in the San Francisco Bay section of California attracted great attention since cauliflower is a major winter crop in certain coastal valleys in central and southern California. The first symptom of infection is a clearing of the veins, which usually begins at or near the base of the leaf and gradually extends over the entire leaf. Vein clearing may be persistent for 10 to 20 days, and gradually changes to vein banding, which consists of narrow, continuous, dark-green areas parallel with

and adjoining the midrib and lateral veins. Eventually, small, irregular, necrotic lesions appear in the mottled areas. The infection usually causes severe stunting of the plants. This cauliflower mosaic disease was later discovered to be caused by a virus, which was termed *Cauliflower Mosaic Virus* (CaMV).

CaMV has a fairly narrow host range, which is limited to plants of *Cruciferae* family. Some CaMV strains such D4 and W260 are also able to infect solanaceous species of the genera *Datura* and *Nicotiana*, while other strains elicit a plant defense response that prevents the infection from spreading to the whole plant (Qiu & Schoelz, 1992).

CaMV is transmitted in a non-circulative manner by several aphid species (*Myzus persicae*), and the transmission of CaMV by any other type of vector has never been reported in nature (Haas *et al.*, 2002). CaMV can be easily inoculated mechanically to host plants, but it is unlikely for CaMV to be transmitted by the intermediate of seeds or pollen, or plant-to-plant contact (Blanc *et al.*, 2001; Haas *et al.*, 2002).

2.2. CaMV genome structure and protein functions

The CaMV genome consists of a double-stranded circular DNA approximately 8,000 bp in length. There are three sequence discontinuities at specific sites on both sense or (+) and anti-sense or (-) DNA strands (Fig. 1-1, discontinuities designated by the symbol Δ), and their number and position vary depending on the CaMV strains

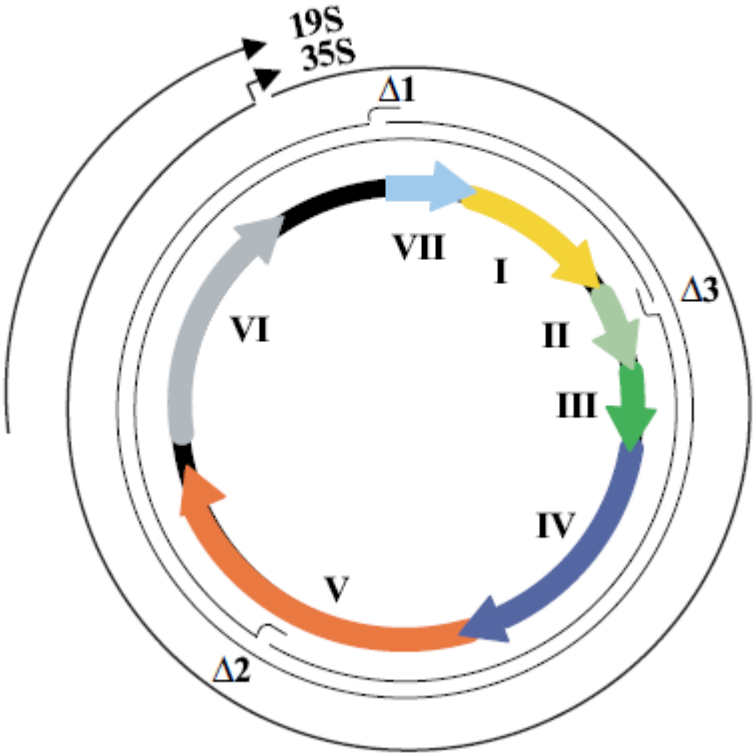

Fig.1-1 Genomic structure of CaMV. Thin lanes show the dsDNA with the respective discontinuities (Δ1-3). Colored arrows indicate ORFs I (cell-to-cell movement), II and III (aphid transmission), IV (Coat Protein), V (Precursor of proteinase, reverse transcriptase and RNase H) and VI (Inclusion body and translational transactivator protein). Length of RNAs 19S and 35S is also shown on the outside of the circular dsDNA. Regulatory sequences for the 19S and 35S is illustrated by the black intergenic regions (Hass *et al*, 2002). *Figure release approved by John Wiley and Sons Publishers*.

(Haas *et al.*, 2002). The discontinuities are associated with the replication strategy of CaMV and are a consequence of the initiation of synthesis of either the "+" or "–" DNA strands. There are seven major open reading frames (ORFs) within the CaMV genome, but only six encoded proteins detected in infected plants. A protein product associated with ORF VII has never been identified and may not exist, as deletions within ORF VII have no effect on CaMV infections (Wurch *et al.*, 1990). CaMV proteins are designated P1-P7, in agreement with the seven ORFs.

CaMV P1 is a movement protein (MP). P1 is a 38kDa protein responsible for virus spread (Citovsky *et al.*, 1991; Linstead *et al.*, 1988; Perbal *et al.*, 1993). CaMV construct containing mutated unfunctional gene I was not able to cause systematic infection, but the accumulation of encapsidated forms of virion DNA could still be detected, indicating that P1 is not involved in CaMV replication (Thomas *et al.*, 1993). When expressed in plant protoplast, P1 alone is sufficient to cause the formation of tubular extensions projecting out of cell membrane (Huang *et al.*, 2000; Kasteel *et al.*, 1996; Perbal *et al.*, 1993). Furthermore, P1 is also able to induce tubules in whole leaves upon agroinfiltration into *Nicotiana benthamiana* leaves (Rodriguez *et al.*, 2014).

CaMV P2 is an aphid transmission factor (ATF) (Armour *et al.*, 1983; Woolston *et al.*, 1983). The function of P2 was first discovered by a comparison between wild type CaMV and a naturally occurring CaMV isolate CM4-184, which contains a deletion in gene II and is non-transmissible by aphids (Howarth *et al.*, 1981). Later,

another CaMV isolate, NY8153, was found to contain a deletion within the gene II coding region. Symptoms caused by NY8163 were the same as symptoms caused by wildtype CaMV, only it cannot be transmitted by aphids (Armour *et al.*, 1983). When expressed in insect cells (Sf9 insect cell culture, derived from the pupal ovarian tissue of the fall army worm, *Spodoptera frugiperda*), P2 ATF colocalizes with an atypical cytoskeletal network which is composed with microtubules (Blanc *et al.*, 1996). P2 also interacts with P3, and the P2/P3/virion complex is essential for aphid transmission of virions (Leh *et al.*, 2001; Leh *et al.*, 1999).

CaMV P3 is a dual-role protein that participates in aphid transmission, encapsidation of the viral DNA, and intercellular movement. There are two forms of P3: a 15 kDa protein and an 11 kDa form derived from the 15 kDa protein by cleavage on the C-terminus. The 15 kDa P3 protein non-specifically interacts with double-stranded DNA. The DNA binding region of P3 is located in the C-terminus and it is responsible for its non-specific DNA affinity (Mesnard *et al.*, 1990; Mougeot *et al.*, 1993). By contrast, the 11 kDa P3 protein interacts with the coat protein in the virus capsid but has no DNA binding activity (Giband *et al.*, 1986). The 11 kDa P3 protein forms a complex with P2 and CP, and this complex is essential for aphid transmission (Leh *et al.*, 2001; Leh *et al.*, 1999). P3 forms a tetramer in infected plants and co-sediments with CaMV CP (Tsuge *et al.*, 1999). Taken together, P3 is considered to participate in viral DNA folding encapsidation, and are involved in virion formation and stabilization (Tsuge *et al.*, 1999). In addition, P1 (MP) was also

proved to interact with the N-terminus of P3 through formation of a coiled-coil structure, suggesting the involvement of P3 in viral entry into host cells and CaMV cell-to-cell movement (Stavolone *et al.*, 2005).

CaMV P4 is a coat protein (CP), which is employed by CaMV to encapsidate the genomic DNA (Daubert *et al.*, 1982). The P4 protein has a size of 58 kDa, and it is the precursor of the functional 42 kDa CP protein (Hahn & Shepherd, 1982). P4 interacts with other CaMV proteins, including P3 and P6 (Himmelback *et al.*, 1996; Leh *et al.*, 2001; Leh *et al.*, 1999). P4 has been found to influence the ability of the W260 isolate to systemically infect the solanaceous host, *N. bigelovii*, in cooperation with P2 and P6 (Qiu & Schoelz, 1992). The CaMV virion particle is an icosahedron with a diameter of 50 nm and the reconstructed surface showed a multilayered structure (Fig. 1-2A) (Cheng *et al.*, 1992).

CaMV P5 is the reverse transcriptase (RT), which is responsible for the synthesis of first strand DNA through reverse transcription of the 35S RNA (Toh *et al.*, 1983). Since the template for the first DNA strand is the 35S RNA, the first DNA strand is considered to be a minus strand (-), with respect to protein synthesis. P5 has an inactive 75 kDa precursor, which is composed of the reverse transcriptase domain, ribonuclease H domain, and aspartate protease domain (Hohn *et al.*, 1985; Takatsuji *et al.*, 1986; Toh *et al.*, 1983). This precursor can be processed to form a 60 kDa mature activated form of P5 (Takatsuji *et al.*, 1992). Interestingly, CaMV RT resembles the reverse transcriptase of *Hepatitis B virus* (HBV), which is a double-stranded DNA

A

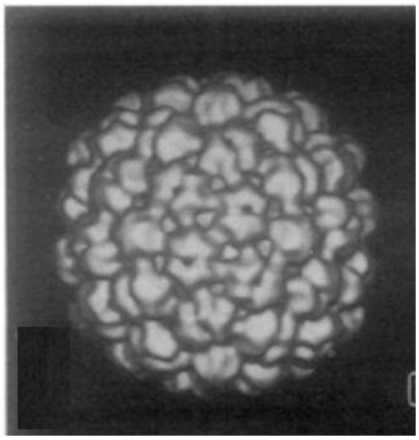

B

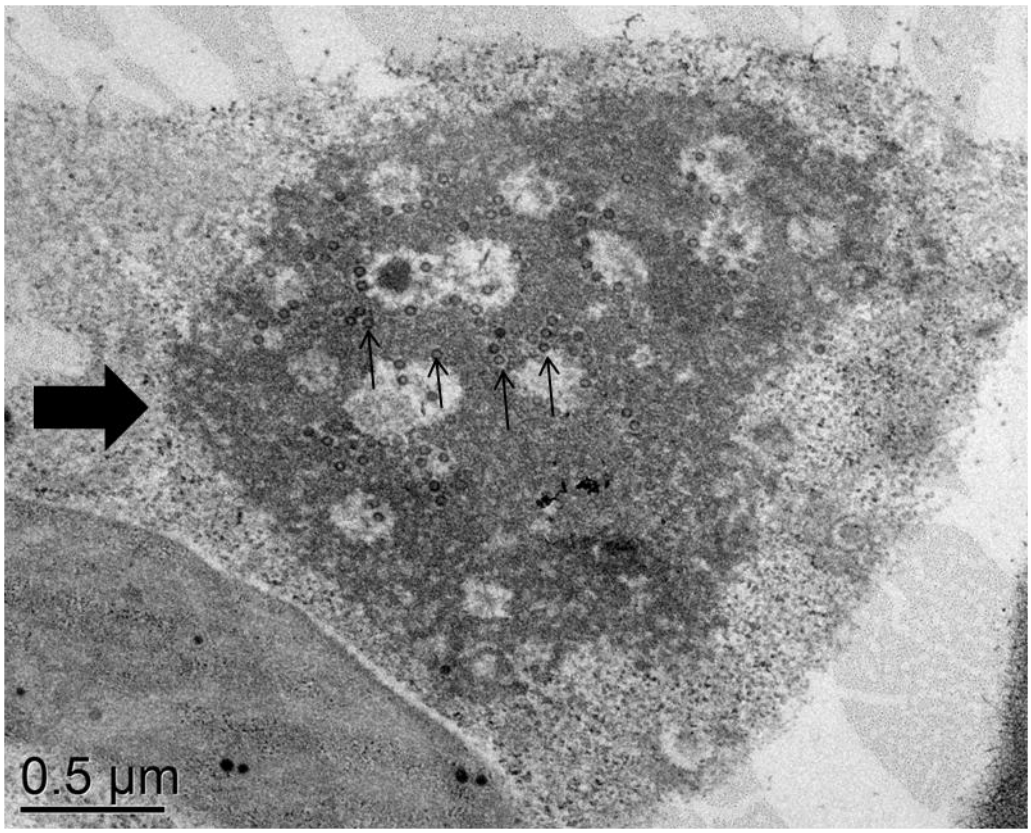

Fig. 1-2 CaMV virion and CaMV inclusion body. (A) CaMV isometric particles are about 50 nm in diameter with multilayered structure (Cheng *et al*., 1992) *Figure release approved by Copyright Clearance Center.* (B) CaMV virions and CaMV inclusion body in turnip leaf. Bold arrow indicates the inclusion body, small arrows indicates individual CaMV virions within inclusion body.

virus that infects animals and humans. The amino acid sequence alignment showed 40-60% similarity between CaMV RT and *Hepatitis B virus* (HBV) RT, and the probability that such similarity happened by chance is less than 10^{-8} (Toh *et al.*, 1983), which indicates a functional and evolutionary relationship.

CaMV P6 is a multifunctional protein. Unlike other CaMV proteins, P6 is only found within the genus Caulimovirus (Hohn, 2013). P6 is a multifunctional effector protein that plays varied roles in multiple steps during CaMV life cycle, targeting several major systems within the plant (Fig. 1-3) (Schoelz *et al.*, 2015). It was originally recognized as a major component of the inclusion bodies (IBs) that are diagnostic for CaMV infections (Fig. 1-2B) (Covey & Hull, 1981; Shockey *et al.*, 1980). Nearly all CaMV virions accumulate within the P6 IBs (Fig. 1-2B). In the early 80s, P6 was shown to be the first virus elicitor of the hypersensitive response (HR) in resistant hosts (Daubert *et al.*, 1983; Schoelz *et al.*, 1986), as well being responsible for the chlorosis symptom in susceptible hosts (Baughman *et al.*, 1988; Cecchini *et al.*, 1997; Goldberg *et al.*, 1991; Yu *et al.*, 2003). Later on, P6 was shown to reprogram ribosomes for the translation of polycistronic CaMV 35S RNA (Bonneville *et al.*, 1989). This function has been called the translational transactivator (TAV) function. In addition, P6 also has been shown to modulate plant defenses to other pathogens by altering the SA and JA pathways, as well as in the accumulation of H_2O_2 (Love *et al.*, 2005), and it also has been proven to be a silencing suppressor (Love *et al.*, 2007). Finally, it has been shown that P6 inclusion bodies can move

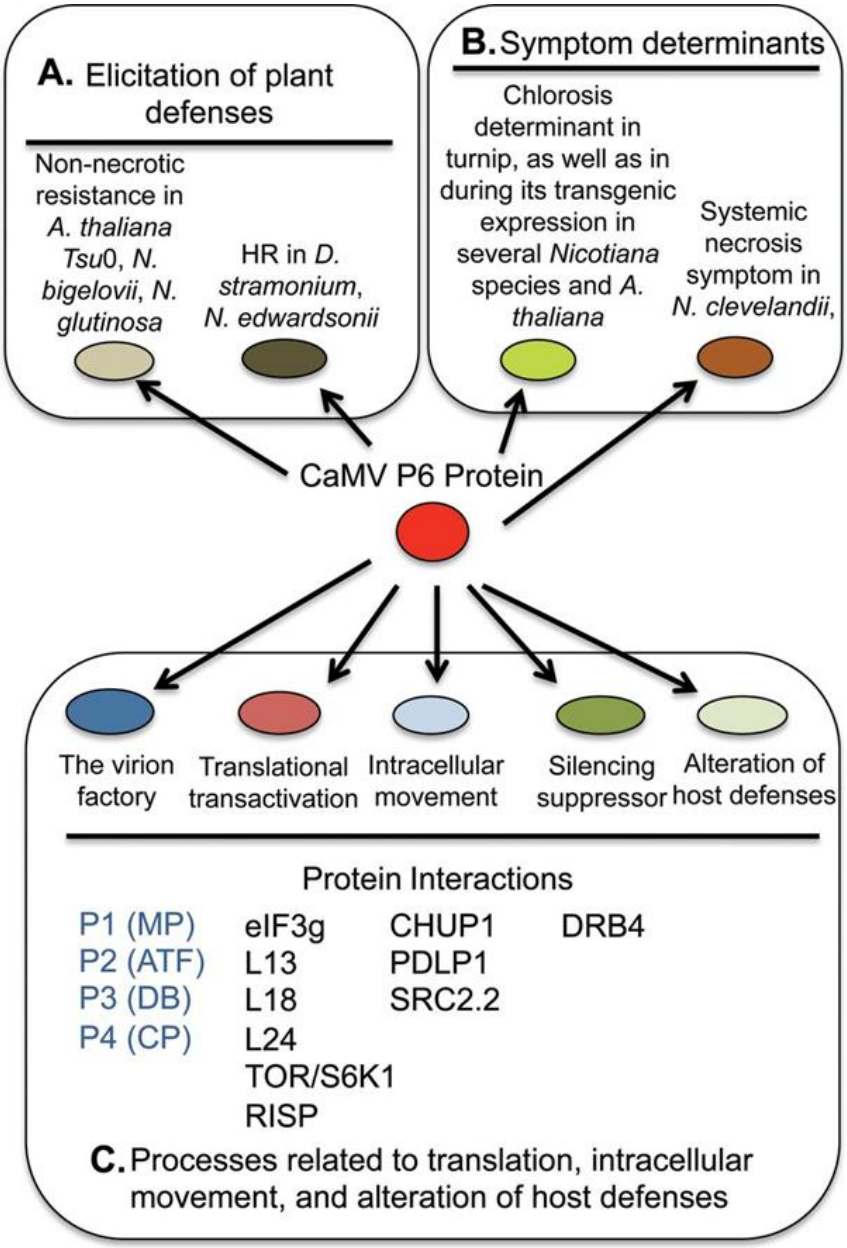

Fig.1-3 The multifunctional effect of the CaMV P6 protein. (A). Role of P6 in elicitation of plant defenses and restriction of virus spread. (B). Role of P6 in symptom development (C). Role of P6 in the viral infection cycle, suppression of silencing, and in alteration of plant defenses. Interactions with host or viral proteins identified to date are listed below each of the functions (Schoelz *et al.*, 2015). *Figure release approved by Copyright Clearance Center*.

intracellularly in association with microfilaments, and current models suggest that this intracellular movement may be necessary to deliver virions to plasmodesmata for transit to adjacent cells (Schoelz *et al.*, 2015).

2.3. CaMV transcription and replication

Two major mRNAs are transcribed from the CaMV genome: the 19S RNA and the genomic 35S RNA (Fig. 1-1). Transcription for the 19S RNA is initiated at nucleotide (nt) 5,764 and terminates at nt 7,615 (Covey & Hull, 1981; Guilley *et al.*, 1982). The 19S RNA is the mRNA for the P6 protein, the inclusion body matrix protein. The 35S RNA is initiated at nt 7,435 and is 3'-co-terminal with 19S RNA at nt 7,615 (Guilley *et al.*, 1982). The 35S RNA is a polycistronic mRNA template for CaMV proteins P1-P5 (Dixon & Hohn, 1984); at the same time, the 35S RNA is the RNA template for reverse transcription, serving as an intermediate in the viral replication process (Hull *et al.*, 1987).

There are two phases for the CaMV replication process: the nuclear phase and the cytoplasmic phase. When CaMV virions enter a plant cell by mechanical inoculation or vector transmission, the viral DNA is uncoated in the cytoplasm and subsequently transported into the nucleus (Fig. 1-4A). The single-stranded discontinuities in the viral DNA are covalently closed in the nucleus and a minichromosome is formed (Fig. 1-4B) (Menissier *et al.*, 1982; Olszewski *et al.*, 1982). Unlike retroviruses, the minichromosome of CaMV does not integrate into the

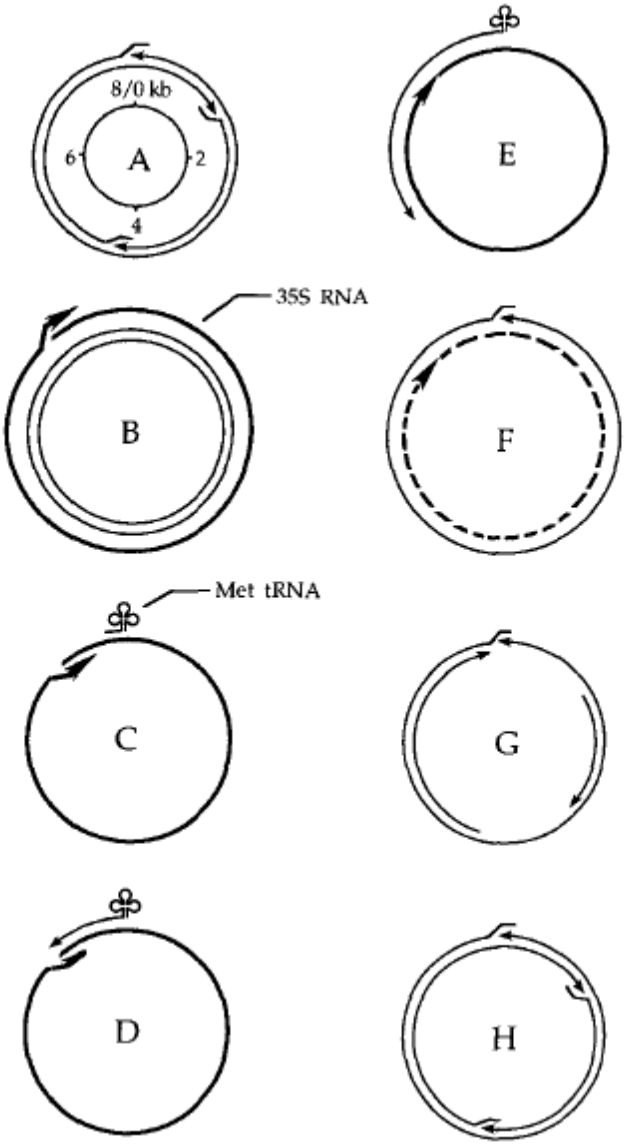

Fig.1-4 The replication procedure of CaMV by reverse transcription (Schoelz & Wintermantel, 1993). *Figure release approved by the American Society of Plant Biologists.*

host genome (Menissier *et al.*, 1982; Olszewski *et al.*, 1982). The 35S RNA is transcribed from the minichromosome within the nucleus by the host encoded RNA polymerase II and is subsequently transported outside of the nucleus (Menissier *et al.*, 1982; Olszewski *et al.*, 1982).

In the cytoplasm, the 35S RNA can serve as a template for translation of proteins or for reverse transcription of the (-) strand DNA. Reverse transcription is catalyzed by the virus-encoded reverse transcriptase (P5) and it occurs in the P6 IBs (Pfeiffer & Hohn, 1983; Takatsuji *et al.*, 1986; Toh *et al.*, 1983). DNA synthesis is primed by a methionine tRNA that binds to a 14-ribonucleotide sequence present approximately 600 nucleotides from the 5' end of the 35s RNA (Fig. 1-4C) (Guilley *et al.*, 1982; Pfeiffer & Hohn, 1983). The reverse transcriptase uses a methionine tRNA as the primer and synthesizes DNA up to the 5’ end of 35S RNA (Fig. 1-4D). A template switch happens from the 5’ end to the 3’ of the 35S RNA due to terminal redundancies and the CaMV reverse transcriptase proceeds to synthesize DNA along the 3’ end of 35S RNA template (Fig 1-4E). As the (-) strand DNA is completed, the 35S RNA template is degraded by the ribonuclease H activity of the reverse transcriptase, and small RNA fragments serve as primers near nucleotide positions 1,632 and 4,218 for the synthesis of (+) sense DNA (Fig. 1-4F). A second template switch occurs during the (+) DNA synthesis (Fig. 1-4G). The completion of CaMV replication results three single-stranded discontinuities: one in the (-) strand and two in the (+) strand (Fig. 1-4H) (Schoelz & Wintermantel, 1993).

2.4. Translation of the 35S RNA into proteins CaMV proteins

Two features distinguish the translation of the 35S RNA. The first is that this RNA is a true polycistronic mRNA. The second is that the leader sequence of the 35S RNA is unusually long for most eukaryotic mRNAs (600 nt in length) and it contains several short ORFs (sORFs) in front of ORFI. CaMV has evolved two unique strategies for translation of the 35S RNA.

The fact that the CaMV 35S RNA is polycistronic indicates CaMV must have developed a mechanism to express the downstream ORFs. There are two major mechanisms employed by viruses to express a polycistronic mRNA: an internal ribosome entry site (IRES) and translational reinitiation. Well-studied samples of viruses containing internal ribosome entry site include: the encephalomyocarditis virus (Jang *et al.*, 1988), poliovirus (Pelletier & Sonenberg, 1988), *Hepatitis A virus* (Glass *et al.*, 1993), *Turnip mosaic potyvirus* (Basso *et al.*, 1994), and *Tobacco mosaic virus* (Dorokhov *et al.*, 2002; Skulachev *et al.*, 1999; Zvereva *et al.*, 2004). Many other viruses developed mechanisms to reinitiate translation of downstream ORFs such as Influenza B virus (Powell, 2010). In the case of CaMV, the P6 protein is required to initiate expression of downstream ORFs through a process designated translational transactivation.

The role of the caulimovirus P6 as TAV was revealed in two papers (Bonneville *et al.*, 1989; Gowda *et al.*, 1989). The experiments involved the co-expression of a monocistronic CaMV gene VI construct with a bicistronic reporter construct. P6

increased the expression level of the downstream ORF of the bicistronic construct by 50 fold. Later on this phenomenon was also confirmed in transgenic plants (Fütterer & Hohn, 1991; Fuütterer & Hohn, 1992) and yeast (Sha *et al.*, 1995).

There are two domains of P6 that are required for the translational transactivation process: a mini-TAV domain (amino acid residues 111 to 242) (De Tapia *et al.*, 1993) and a C1 domain (residues 242-310) (Park *et al.*, 2001), which bind to the L18 ribosomal protein of the 60S subunit (Leh *et al.*, 2000) and eukaryotic initiation factor eIF3g subunit as well as the L24 ribosomal protein of the 60S ribosomal subunit (Park *et al.*, 2001), respectively. In the translational transactivation model proposed by Park *et al* (2001), the P6 protein (TAV) binds to the 40S ribosome subunit through eIF3g, and a ternary complex is recruited to initiate translation of ORF1 (Fig. 1-5A). The P6 protein remains attached to the polysome during elongation by translocation to the 60S ribosome subunit through L18 (Fig. 1-5B), and after termination of translation of ORF1, P6 returns to the eIF3g site of the 40S ribosome subunit to reinitiate the translation of the next ORF (Fig. 1-5C).

CaMV has also evolved a unique strategy to deal with the unusual complexity of the leader sequence of the 35S RNA. The 35S mRNA of CaMV has a 600 bp leader sequence upstream of the ORF VII start codon, which contains up to nine small open reading frame (sORF) (capable of coding for small peptides of two to 35 amino acids) (Pooggin *et al.*, 1998). This leader sequence can be folded into a large stem-loop

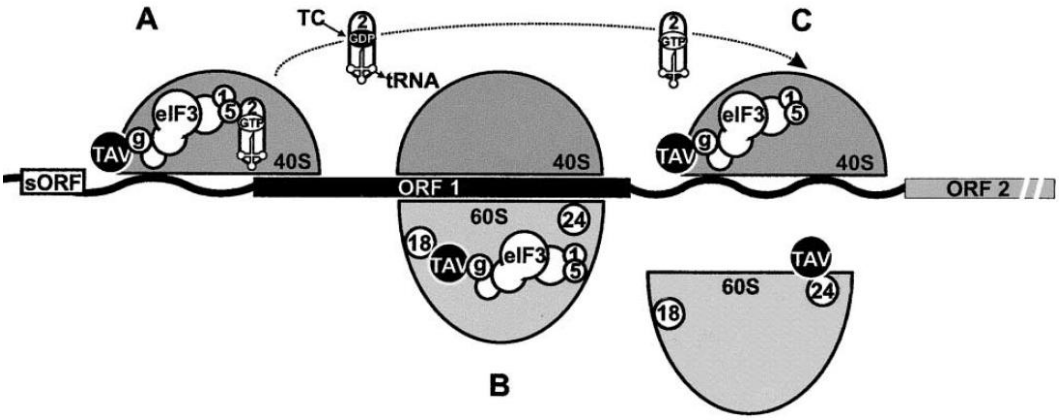

Fig.1-5 Model of translational transactivation of CaMV by the TAV function of P6 (Park *et al.*, 2001). *Figure release approved by Copyright Clearance Center*.

structure (Fütterer *et al.*, 1988). Both sORFs and stem-loop structures interfere with translation of downstream ORFs (Gray & Hentze, 1994; Kozak, 1986; 1987; 1989). CaMV has evolved a mechanism called the ribosomal shunt to bypass the stable secondary structure formed by the 35S leader sequence.

The ribosomal shunt model was proposed by Ryabova and Hohn (2000) (Fig. 1-6). The sORFs A - F are found upstream of ORF VII in the leader sequence, and sORF A is translated and properly terminated (Pooggin *et al.*, 2000). A modified shunt- and reinitiation-competent ribosome is able to bypass the hairpin and continue scanning until translation is reinitiated at the start codon of ORF VII (Ryabova & Hohn, 2000) (Fig. 1-6). Proper translation of sORF A is essential for an efficient shunt, and virus infectivity (Pooggin *et al.*, 2001). The P6 protein is also involved in this process by increasing the reinitiation efficiency 2-3 fold during the shunt process (Pooggin *et al.*, 2000).

2.5. Intracellular, intercellular, and long distance movement of CaMV virions

Plant viruses must transport their genomes from the site of replication within the plant cell to the plasmodesmata for transit to the next cell. This phase of the viral replication cycle is called intracellular movement. The model of intracellular movement for CaMV was first proposed by Harries *et al.* (2009) and updated by Schoelz *et al* (2015) (Fig. 1-7). The P6 IB is the site for translation of the 35S RNA, reverse transcription of the 35S RNA into DNA and for encapsidation of the newly

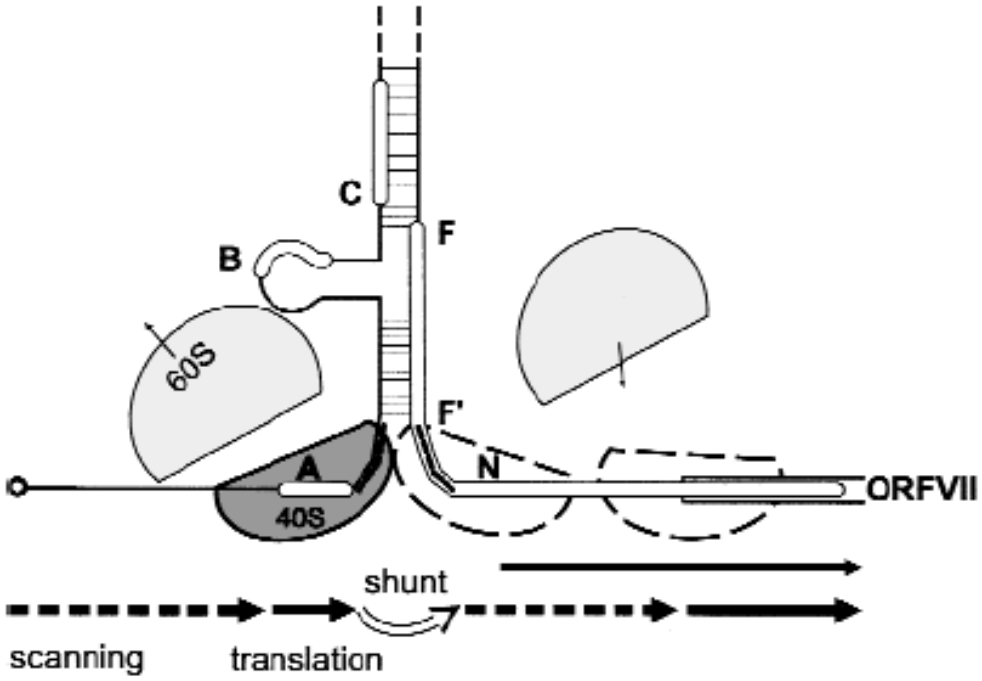

Fig.1-6 Model for CaMV ribosomal shunt (Ryabova & Hohn, 2000) *Figure release approved by Genes & Development, with copyright to Cold Spring Harbor Laboratory Press.*

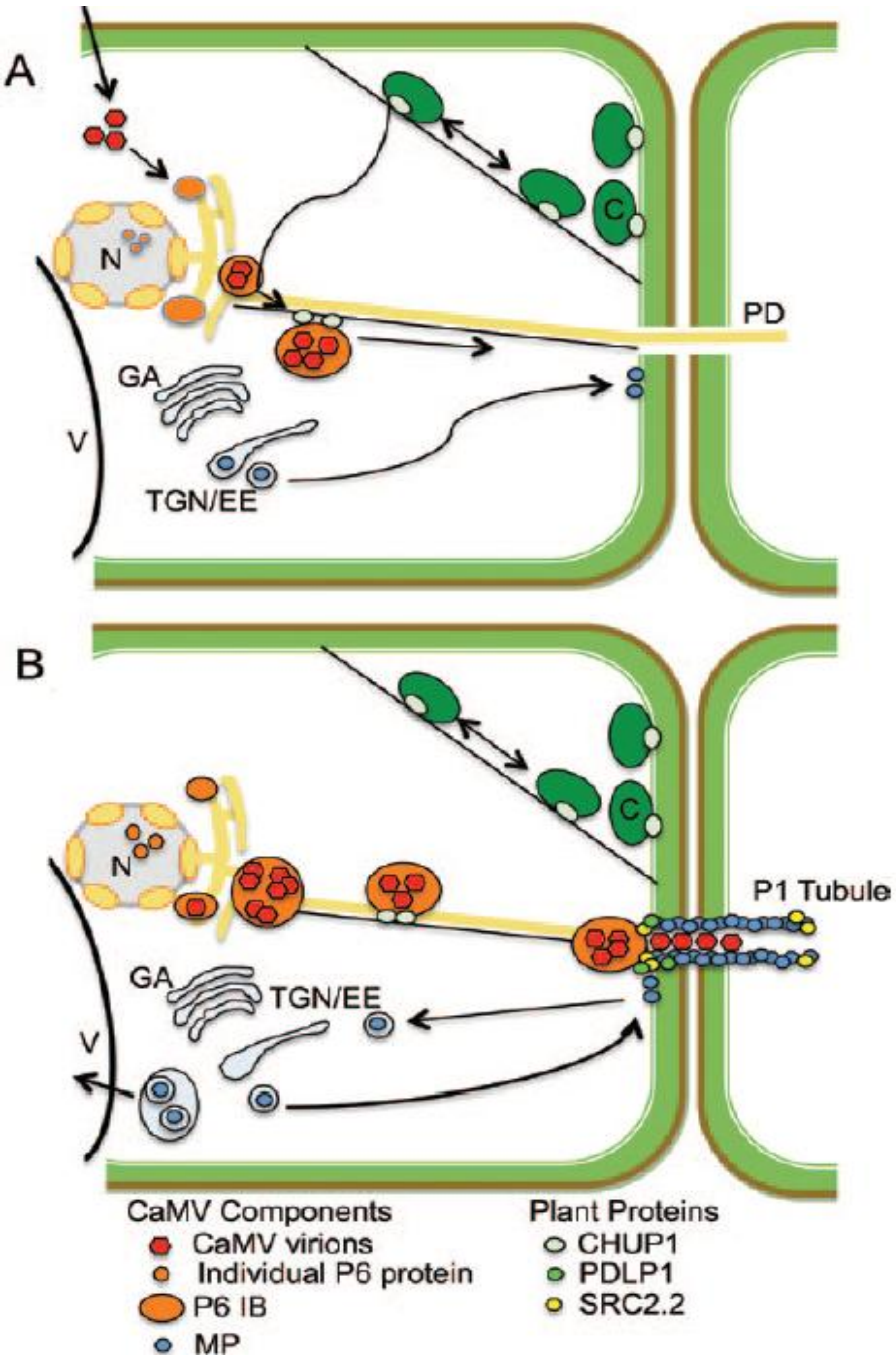

Fig.1-7 Model for intracellular movement of CaMV

(A) Early events include entry of virions into the cell through either an aphid vector or mechanical inoculation, followed by synthesis of the CaMV proteins, formation of the virion factory, incorporation of CHUP1 into the virion factor, and vesicular transport of the MP to the plasma membrane. N, nucleus; C, chloroplast, PD,

plasmodesmata; v, vacuole; GA, Golgi apparatus; TGN/EE, *trans*-Golgi network/early endosome. (B) Later events include formation of the tubule by the CaMV MP and docking of the virion factory for delivery of virions to the tubule (Schoelz *et al.*, 2015). *Figure release approved by Copyright Clearance Center*.

synthesized CaMV DNA into virions (Fig. 1-7A). The P6 IB was shown to interact with the endoplasmic reticulum (ER) (Harries *et al.*, 2009), and it has been suggested that this location may facilitate the recruitment of ribosomes into P6 IBs, considering that ER is studded with ribosomes and is the site of protein synthesis (Schoelz *et al.*, 2015). As the expressed CaMV proteins accumulate in the P6 IB, the 35S RNA serves as a template for reverse transcription and the newly synthesized viral DNA is packaged into virions. In this phase of the CaMV life cycle, the P6 IBs are considered virion assembly factories, and the proper formation of the virion factory may be essential for CaMV infections (Lutz *et al.*, 2015).

Harries and coworkers (2009) noted that P6 IBs were capable of movement in association with microfilaments. Interestingly, the P6 protein interacts with CHUP1 (Chloroplast Unusual Positioning protein), a plant protein that is essential for movement of plant chloroplasts on microfilaments in response to changes in light intensity (Angel *et al.*, 2013) (Fig. 1-7A). At some point in CaMV life cycle, CHUP1 is redirected away from its role in chloroplast movement and recruited by P6 for transport of the P6 IBs on microfilaments (Angel *et al.*, 2013). The interaction between P6 and CHUP1 is the first characterized direct interaction between a plant virus protein and a host protein known to attach physically to microfilaments (Schoelz *et al.*, 2015).

The CaMV MP is required for cell-to-cell movement of virions, and mutation of the MP abolishes CaMV infection (Thomas *et al.*, 1993). When expressed in plant

cells, the MP is localized in plasmodesmata (PD) and co-localizes with the plasmodesmata marker Plasmodesmata-Localized Protein 1 (PDLP1) as well as with Soybean Response to Cold (AtSRC2.2) (Rodriguez *et al.*, 2014). When expressed in protoplasts, the MP induces formation of tubules with a diameter of approximately 52 nm that project out of the protoplast membrane (Huang *et al.*, 2000; Kasteel *et al.*, 1996; Perbal *et al.*, 1993), and Rodriguez *et al* (2014) showed that ectopic expression of the MP can also induce formation of similar tubules *N. benthamiana* leaf tissues. Taken together, the CaMV MP restructures the PD and enlarges the PD to allow movement of CaMV icosahedral virions, which have a diameter of 50 nm (Fig. 1-7B) (Schoelz *et al.*, 2015; Schoelz *et al.*, 2011).

Interestingly, the CaMV MP is transported to PD independently of the P6 protein. CaMV MP is secreted from the *trans*-Golgi network into vesicles which are transported to the plasma membrane and PD, and the excess MP might be recycled back to the central vacuole (Fig. 1-7B) (Schoelz *et al.*, 2015). Furthermore, the MP does not encounter CaMV virions until they are transported to the PD (Schoelz *et al.*, 2015; Stavolone *et al.*, 2005), strengthening the model that P6 IBs deliver virions to PD for transit to adjacent cells through tubules formed from the MP.

CaMV moves systemically in turnip through phloem channels. It takes approximately five days for CaMV to exit inoculated leaves and to establish a systemic infection. Consistent with other plant viruses, CaMV accumulates in younger leaves that are “sinks” for photoassimilates (Leisner *et al.*, 1992).

3. THE GENUS, *BADNAVIRUS*

The genus *Badnavirus* belongs to family *Caulimoviridae*. As with other genera of *Caulimoviridae*, badnaviruses contain circular, double-stranded DNA, and replicate by reverse transcription; however, instead of forming an icosahedral virion (such as Caulimoviruses), badnaviruses form a bacilliform virion with a diameter of 30 nm and a length of 120-150 nm (Tidona & Darai, 2011). *Commelina yellow mottle virus* (CoYMV) was the first badnavirus to be identified (Medberry *et al.*, 1990; Migliori & Lastra, 1978), and it has been assigned as the type species of genus *Badnavirus*.

It is generally accepted that all badnaviruses have a single promoter that drives transcription of a terminally redundant pregenomic RNA (Tidona & Darai, 2011). Many studies related to the badnavirus replication strategy were focusing on their promoters and transcripts. Promoters of five Badnaviruses have been characterized: *Sugarcane bacilliform badnavirus* (SCBV) (Tzafrir *et al.*, 1998), *Commelina yellow mottle virus* (ComYMV) (Medberry *et al.*, 1992), *Banana streak virus* (BSV) (Schenk *et al.*, 2001), *Taro bacilliform virus* (TaBV) (Yang *et al.*, 2003), and *Rice tungro bacilliform virus (RTBV)* (Bhattacharyya-Pakrasi *et al.*, 1993). Promoters have been mapped to genome segments ranging in size from 773 base pairs (RTBV) to 1,421 base pairs (SCBV). Promoters of BSV (Schenk *et al.*, 2001) and SCBV (Schenk *et al.*, 1999; Tzafrir *et al.*, 1998) were demonstrated to be active in both monocots and dicots, which makes them great promoter candidates for transgene expression in monocots.

The promoters of RTBV and ComYMV also attracted interest because of their tissue specificities. For example, the RTBV promoter shows phloem-specific expression in rice (Bhattacharyya-Pakrasi *et al.*, 1993). Beside phloem tissue, ComYMV expression also tends to be stronger in reproductive tissues such as anthers of tobacco plants (Medberry *et al.*, 1992). More interestingly, the ComYMV promoter was proven to drive tissue-specific gene expression in the companion cells of leaves, stems, and roots of transgenic *Nicotiana tabacum* cv. Xanthi NN (Matsuda *et al.*, 2002), which makes it a perfect promoter for companion cell studies.

Transcripts of three badnaviruses have been characterized. The transcript of RTBV starts at nt 7,354, and ends at nt 7,620 (Qu *et al.*, 1991); for ComYMV, the transcript initiation site was mapped to nts 7,354 and 7,355, and the termination site was proven to be between nts 7,464 and 7,486 (Medberry *et al.*, 1990); Schenk *et al* (Schenk *et al.*, 2001) mapped the 5' end of the BSV transcript to nts 1,151 (BSV-Cav, AF215815), and 2,035 (BSV-Mys, AF214005).

Construction of an infectious clone is a common method for studying the functions of plant virus genes and is an essential tool for molecular virology. Infectious clones have been created for RTBV (Dasgupta *et al.*, 1991), Citrus yellow mosaic virus (CYMBV) (Huang & Hartung, 2001), and ComYMV (Medberry *et al.*, 1990). However, it has been difficult to create infectious clones from some of the Caulimoviridae, such as *Dahlia mosaic virus* (H. Pappu, Washington State University, personal communication). To create an infectious clone for badnaviruses and

caulimoviruses, a greater than full-length DNA clone, containing duplicated promoter regions on both ends of the insert, is cloned into a binary Agrobacterium vector and transferred into *Agrobacterium tumefaciens* for inoculation to plants. The terminally redundant RNA transcribed from the infectious clone is reverse transcribed into DNA to complete the replication process.

Most badnaviruses are known to be transmitted by different species of mealybugs. There are also reports about badnaviruses transmitted by aphids (Table 1-1).

4. GRAPEVINE VEIN CLEARING VIRUS (GVCV)

Grapevine vein clearing virus (GVCV) was discovered by a group at Missouri State University (Zhang *et al.*, 2011). The disease associated with GVCV was first observed in *Vitis vinifera* in Missouri vineyards in 2004. It was later observed in Indiana, Illinois, and Arkansas vineyards as well (Guo *et al.*, 2014; Lunden *et al.*, 2010; Qiu & Lunden, 2007; Zhang *et al.*, 2011). The symptoms include chlorosis in grapevine leaves which is most severe in newly emerged young leaves (Fig. 1-8), a zigzag pattern of shoot development, and smaller clusters of berries with fewer fruits. The infected grapevines end up dwarfed, and even dead in the worst scenario (Guo *et al.*, 2014; Lunden *et al.*, 2010; Qiu & Lunden, 2007; Zhang *et al.*, 2011). This syndrome has been identified in many grape cultivars including ‘Chardonnay’, ‘Chardonel’, ‘Cabernet Sauvignon’, ‘Vidal Blanc’, ‘Cabernet Franc’, ‘Riesling’, and

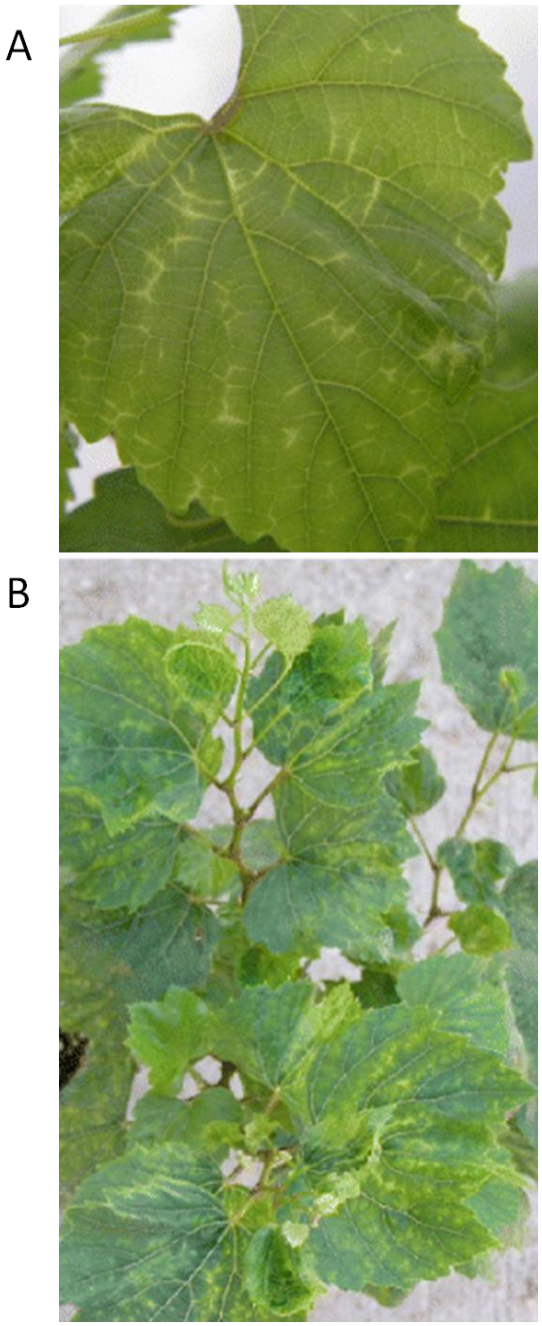

Fig.1-8 Symptoms of Grapevine vein clearing disease. (A) Typical vein-clearing symptom. (B) Leaves of the mature and woody vine show severe mosaic and chlorotic symptoms and short internodes with a zigzag pattern (Lunden *et al.*, 2010). *Figure release approved by Copyright Clearance Center*.

Virus	Vector	Citation
Banana streak virus	Mealybug	(Su, 1998)
Cacao swollen shoot virus	Mealybug	(Dongo & Orisajo, 2007)
Citrus yellow mosaic virus	Mealybug	(Aparna *et al*., 2012)
Dioscorea alata bacilliform virus	Mealybug	(Phillips *et al*., 1999)
Kalanchoe top-spotting virus	Mealybug	(Hearon & Locke, 1984)
Pineapple bacilliform virus	Mealybug	(Sether *et al*., 2012)
Piper yellow mottle virus	Mealybug	(Lockhart *et al*., 1997)
Schefflera ringspot virus	Mealybug	(Lockhart & Olszewski, 1996)
Sugarcane bacilliform virus	Mealybug	(Lockhart & Autrey, 1991)
Taro bacilliform virus	Mealybug	(Macanawai *et al*., 2005)
Rubus yellow net virus	Aphid	(Kalischuk *et al*., 2008) (Jones *et al*., 2002)
Spiraea yellow leaf spot virus	Aphid	(Lockhart & Geering, 2000) (Hull *et al*., 2005)

Table 1-1 Badnaviruses and their insect vector

'Corot noir'. The disease is consistently associated with GVCV, and the disease, along with GVCV can be transmitted by grafting (Zhang *et al.*, 2011). The economic loss caused by this disease was significant to vineyard owners in Midwest.

GVCV was identified through deep sequencing of small interfering RNAs (siRNA) purified from symptomatic leaves. The most conserved and prevalent siRNAs were identified by sequence alignment with badnaviruses. Virus-specific primers were designed based on conserved regions, and GVCV fragments were amplified using GVCV-specific primers. By primer walking, the complete nucleotide sequence of GVCV was assembled from clones amplified thought PCR (Zhang *et al.*, 2011).

The complete genome of GVCV is 7,753 bp in length and contains three open reading frames (ORFs) as well as a large intergenic region between ORFI and ORFIII (Fig. 1-9). The functions of proteins encoded by ORFI and ORFII are still unknown, but ORFIII is predicted to encode a polyprotein which contains movement protein, coat protein, reverse transcriptase (RT), and RNaseH domains (Fig. 1-9, Table 1-2). As with other caulimoviruses, the GVCV nucleotide sequence contains a domain complementary to the 3' end of the plant tRNAmet consensus sequence (tRNAmet: 3′-ACCAUAGUCUCGGUCCAA-5′), and the T which binds to the A of tRNAmet 3' end was considered as the nucleotide 1 of GVCV sequence

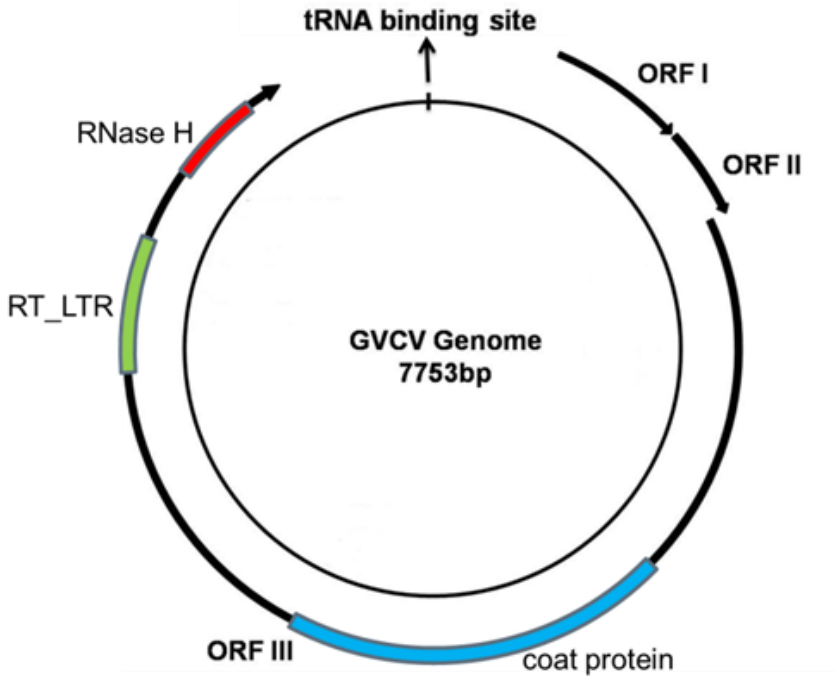

Fig.1-9 GVCV genome structure. RT_LTR: long terminal repeats of reverse transcriptase. Conserved region was predicted by BLAST.

ORF	1	2	3
First nucleotide	485	1,112	1,495
Last nucleotide (including the stop codon)	1111	1,495	7,320
Size (nucleotides)	624	381	5,823
Amino acids	208	127	1,941
Molecular mass (kDa)	24.2	14.3	219.5
Active sites	Unknown	Unknown	MP motif, CP, RT, RNase H

Table 1-2 Predicted proteins encoded by GVCV ORFs. MP: movement protein; CP: coat protein; RT: reverse transcriptase (Zhang *et al.*, 2011) (Reprinted from Zhang, Yu, Kashmir Singh, Ravneet Kaur, and Wenping Qiu. "Association of a novel DNA virus with the grapevine vein-clearing and vine decline syndrome." *Phytopathology* **101**, no. 9 (2011): 1081-1090.)

(GVCV nucleotide 1-12: 5'-TGGTATCAGAGC-3') (Fig. 1-9) (Zhang *et al.*, 2011).

Since the most abundant vsRNAs (viral small RNAs) in grapevine showing typical vein clearing symptoms are homologous to badnaviruses (Zhang *et al*., 2011), GVCV was predicted to be a badnavirus even before its genomic sequences were assembled. When the GVCV genomic sequences were assembled, a phylogenetic tree was constructed, comparing the putative amino acid sequence of the reverse transcriptase of GVCV to those of six genera in the family *Calimoviridae*. This analysis showed that GVCV is most closely related to *Commelina yellow mottle virus* (ComYMV), the type species of genus *Badnavirus* (Fig 1-10A). Another phylogenetic analysis comparing the putative reverse transcriptase and RNaseH active sites between GVCV and other members of *Badnavirus* showed that GVCV is most closely related with *Taro bacilliform virus* (TaBV) (Fig 1-10B) (Zhang *et al.*, 2011).

A second publication examined the population structure of GVCV isolate, showing that although GVCV populations are diverse and heterogeneous, they do not cluster by geography or grape species. Furthermore, the hybrid grape Chambourcin was proven to be resistant to GVCV, since GVCV was not transmitted by grafting to Chambourcin shoots. Finally, it was shown that GVCV accumulates most abundantly in grape leaf petioles (Guo *et al.*, 2014).

GVCV has been closely associated with the vein-clearing syndrome of grapevine. GVCV is consistently amplified from DNA samples extracted from grapevine leaves showing vein-clearing symptoms, but cannot be amplified from

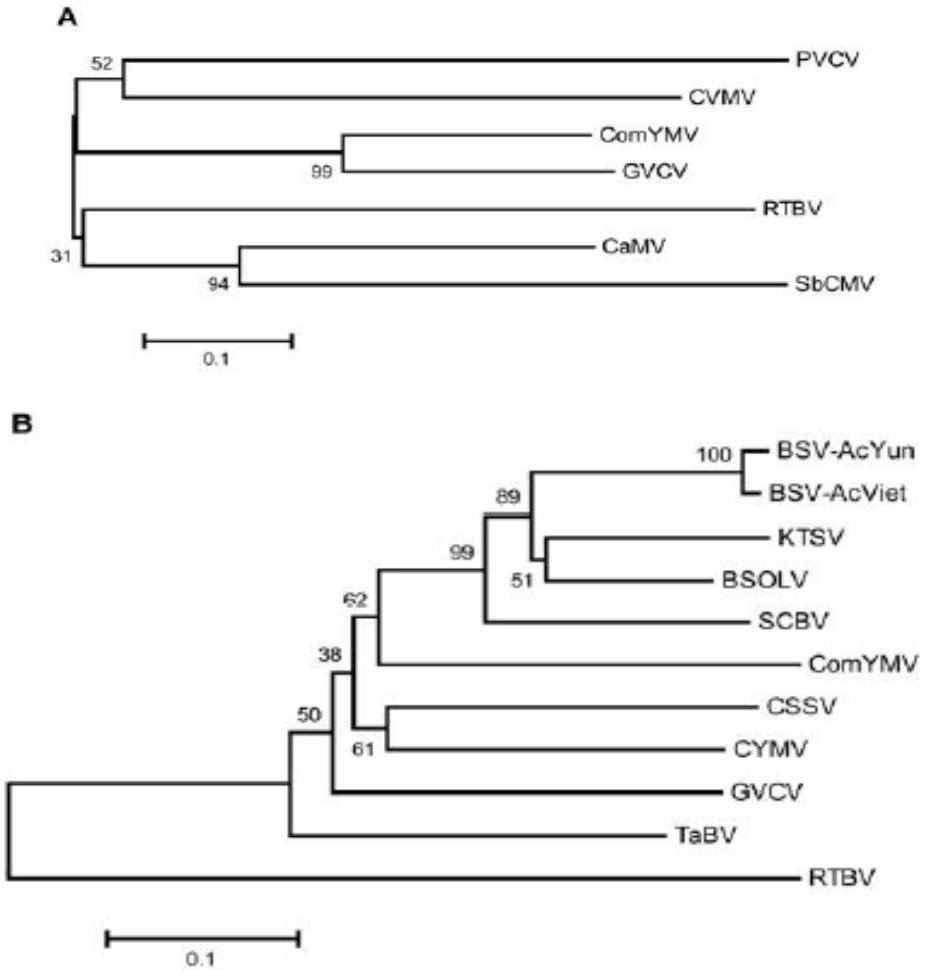

Fig.1-10 Phylogenetic analyses for putative classification of *Grapevine vein clearing virus* (GVCV) in the family *Caulimoviridae*. (A), Phylogenetic tree showing the relationship of GVCV with type species of six genera in the family: *Cauliflower mosaic virus* (CaMV) of *Caulimovirus*, *Soybean chlorotic mottle virus* (SbCMV) of *Soymovirus*, *Commelina yellow mottle virus* (ComYMV) of *Badnavirus*, *Rice tungro bacilliform virus* (RTBV) of *Tungrovirus*, *Cassava vein mosaic virus* (CVMV) of *Cavemovirus*, and *Petunia vein clearing virus* (PVCV) of *Petuvirus*. The tree was constructed using reverse transcriptase amino acids. (B) Phylogenetic analysis of GVCV and other closely related *Badnavirus* spp. (including *Banana streak*

virus-AcYun [BSVAcYun], *Banana streak virus-Vietnam* [BSV-AcViet], *Kalanchoe top-spotting virus* [KTSV], *Banana streak OL virus* [BSOLV], *Sugarcane bacilliform virus isolate Batavia D* [SCBV], *Cacao swollen shoot virus* [CSSV], *Citrus yellow mosaic virus* [CYMV], and *Taro bacilliform virus* [TaBV]) using the conserved region of reverse transcriptase and RNase H amino acid sequences. (Reprinted from Zhang, Yu, Kashmir Singh, Ravneet Kaur, and Wenping Qiu. "Association of a novel DNA virus with the grapevine vein-clearing and vine decline syndrome." *Phytopathology* **101**, no. 9 (2011): 1081-1090.)

asymptomatic grapevines. The vein-clearing symptom is also graft transmissible, and the GVCV sequences recovered from the previously asymptomatic rootstock was identical to the GVCV sequences from symptomatic scion (Zhang *et al.*, 2011). However, Koch's postulates have not been completed for GVCV, because it has not been possible to purify virions and reinoculate them to healthy grapevines to reproduce the disease. One issue that complicates the application of Koch's postulates for grape viruses is that they cannot be mechanically inoculated to grape leaves, a technique that is the method of choice for most plant virus tests. Instead, the only method that has been effective has been agroinfection, a technique in which a DNA clone of the virus is inserted into the T-DNA of Agrobacterium tumefaciens and the infections is initiated by infiltrating Agrobacterium carrying this clone into leaves (Grimsley *et al.*, 1987).

5. AGROINFILTRATION AND AGROINFILTION SYSTEM FOR TRANSIENT GENE EXPRESSION

Agroinfiltration is a plant biological technique which is widely used in transgene experiments. By taking advantage of *Agrobacterium tumefaciens* and *A. tumefaciens* Ti plasmid-derived vectors, which are able to integrate target genes into plant DNA, it becomes possible to transfer foreign genes to plant cells (Weising *et al.*, 1988). Agroinfiltration has been used to study the function of viral *avr* gene (Palanichelvam *et al.*, 2000), plant gene silencing mechanism (Schöb *et al.*, 1997),

promoter and transcription factors (Yang *et al.*, 2000; Zhang *et al.*, 2015), sub-cellular localization (Rodriguez *et al.*, 2014), protein intracellular trafficking (Luis *et al.*, 2004), as well as plant ion channel (Latz *et al.*, 2007). Agroinfiltration has been reported to work in a variety of plant species, such as *Arabidopsis*, potato, tomato, and lettuce (Santos-Rosa *et al.*, 2008), but the most widely used plant for agroinfiltration is *Nicotiana benthamiana*. Different agrobacterial strains can be co-infiltrated and the expression level of proteins remains unaffected; Same Agrobacterium strains that contain different binary vector constructs can also be co-infiltrated. Liu *et al* (2010) showed that up to five constructs can be co-infiltrated.

Agroinfiltration is a commonly used technique for transient expression of transgenes in plants, detached plant leaves, even culture of plant leave cells. It takes advantage of *A. tumefaciens*, with its natural ability of horizontal gene transfer and delivers and expresses gene of interest into plant cells. Agroinfiltration is widely used in studies including, but not limited to, plant gene functional analysis, plant resistance gene mapping, pathogenic effector identification, pathogenic virulence and host range determinant screening, and studies about silencing suppressors. Agroinfection is a more specific technique involving the use of Agrobacterium vectors to initiate plant virus infections. It was first demonstrated with the successful inoculation of CaMV in 1987 (Grimsley *et al.*).

5.1. The role of *A. tumefactions* in gene transfer

The genus *Agrobacterium* belongs to the order *Rhizobiales*, Family *Rhizobiaceae*. *Agrobacterium* is characterized by gram-negative soil-borne saprophytic and parasitic species. Many plant diseases are caused by parasitic species of *Agrobacterium*, such as "hairy root disease" (*A. rhizogenes*), "cane gall disease" (*A. rubi*), "Crown gall of grape" (*A. vitis*), and "crown gall" (A. *tumefaciens*) (Escobar & Dandekar, 2003). The infection of parasitic species of *Agrobacterium* often causes the formation of a crown gall tumor. Agrobacteria are well known as the only organisms capable of interkingdom gene transfer, and *A. tumefaciens* has served as a system for the study of the type IV bacterial secretory system, horizontal gene transfer and bacterial–plant signal exchange. Under lab conditions, Agrobacterium may be used for gene transfer into fungal and human cells, as well as plants. (Abuodeh *et al.*, 2000; Bundock *et al.*, 1995; Kunik *et al.*, 2001).

Generally, Agrobacterium pathogenesis is consistent with three steps: 1) The cellular contents released from wounded plant cells, such as amino acids, organic acids, and sugars, act as chemoattractants and trigger the binding of agrobacteria to the plant cells (Gelvin, 2000; Winans, 1992). 2) The formation of the type IV bacterial secretory system and delivery of tumorigenic DNA into the plant genome. 3) The alteration of plant cell metabolism and gall formation due to the transfer of Agrobacterium genes into the plant cell. The Agrobacterium Ti (tumor-inducing) plasmid plays the most important role in this process since it is the key component of horizontal gene transfer. Agrobacterium may remain *in planta* in the intercellular

spaces of plant tissue without causing disease. However, they will initiate tumorigenesis upon tissue wounding (Escobar & Dandekar, 2003).

5.2. Ti plasmid and horizontal gene transfer

The tumor-inducing plasmid, or Ti plasmid, is required for tumor formation. The Ti plasmid, rather than Agrobacterium chromosomal genes, serves as the major genetic determinant of host range (Loper & Kado, 1979; Özyiğit, 2012; Thomashow *et al.*, 1980), and it is also the source for the DNA that is transferred into plant cells and integrated into the plant genome. The formation of a DNA transfer apparatus requires both *cis*-elements and *trans*-elements encoded by the Ti plasmid: the two general categories are the T-DNA and *vir* region.

The T-DNA is flanked by 25-base-pair repeats (termed the left border and right border); it is the particular DNA segment that is delivered into the host nucleus and integrated into the plant genome. In *A. tumefaciens*, the T-DNA contains two types of genes: 1) oncogenic genes encoding genes of enzymes that catalyze the synthesis of plant hormones responsible for tumor formation, and 2) genes encoding enzymes that are responsible for synthesis of novel amino acid-sugar conjugates, termed opines (De La Riva *et al.*, 1998; McCullen & Binns, 2006; Özyiğit, 2012; Pitzschke & Hirt, 2010). Once the T-DNA is integrated into host genome, opines are synthesized and excreted by the crown gall cells. They serve as carbon and nitrogen sources for *Agrobacterium* to the exclusion of most other microorganisms; as a result they

provide a selective advantage for *Agrobacterium* (Pitzschke & Hirt, 2010; Tempé & Petit, 1982).

The virulence (*Vir*) region functions in trans during horizontal gene transfer. The proteins encoded by Vir genes are responsible for host recognition, host attachment, T-DNA targeting into the host cell, and chromosomal T-DNA integration (Pitzschke & Hirt, 2010). There are multiple *vir* factors encoded in the Ti plasmid, but not all of them are necessary for gene transfer. Four *vir* factors (*vir* A, *vir* B, *vir* D, and *vir* G) are essential for the T-DNA transfer, and *vir* C and *vir* E are important for increasing transfer efficiency (Özyiğit, 2012). *Vir* A and *vir* G are constitutively expressed in *Agrobacterium* at a basal level, and they are required for recognition and activation by plant signals. The signals perceived by *vir* A are phenol, aldose monosaccharides, low pH, and low phosphate. Acetosyringone, which belongs to phenol compounds, is routinely used as an inducer of gene transfer in agroinfiltration (Pitzschke & Hirt, 2010). The detailed process of *Agrobacterium*-induced tumor formation is reviewed by Pitzschke & Hirt (2010). Since proteins encoded by the T-DNA are not required by T-DNA transfer and integration, it becomes possible to replace T-DNA oncogenes by desired gene and transfer them into plants.

5.3. Binary vector systems

Although the Ti plasmid can be used by scientists to deliver target genes into plant cells, it also has many disadvantages. The Ti plasmid is very large

(approximately 200kbp), difficult to manipulate, has a low copy number, and is not able to replicate in *Escherichia coli*. However, the fact that *vir* factors are *trans*-acting factors makes it possible to split the Ti plasmid into two parts. In 1983, two groups separated the T-DNA region and *vir* regions into two plasmids and discovered that tumors could be induced when both two plasmids are present in *Agrobacterium* (de Framond *et al*., 1983; Hoekema *et al.*, 1983). These two papers laid the foundation for modern agroinfiltration technology. With decades of development, T-DNA binary vector systems are now one of the most widely tools used for plant genetic engineering.

As shown in Fig. 1-11, a typical binary vector system contains two plasmids: the T-DNA binary vector and a *vir* helper plasmid. A binary vector usually contains several features that are required for gene delivery: 1) the T-DNA left border (LB) and right border (RB), which flank the T-DNA region that will be delivered and integrated into the plant genome; 2) Two origins (*ori*) of replication, one each for the plasmid to replicate in *E. coli* and *Agrobacterium*. Two different origins can be inserted into the plasmid, or alternatively a single broad host range replication origin can be used. 3) Antibiotic resistance genes for screening for the presence of the T-DNA binary vector in *E. coli* or *Agrobacterium.* 4) A gene transfer selection marker, either an Ab^r or herbicide resistance gene, for successful plant transformation screening. 5) Multicloning sites which contain multiple restriction enzyme sites which can be used to clone genes of interest. Gateway technology has recently been introduced to simply

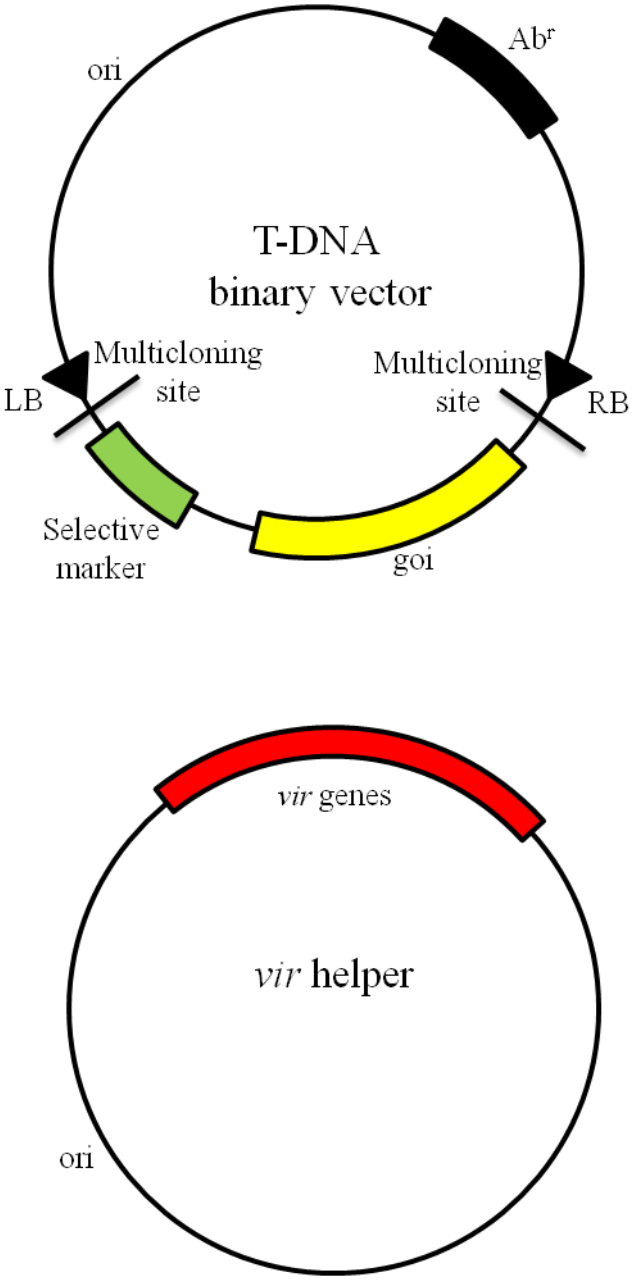

Fig.1-11 T-DNA binary vector system. LB: left border; RB: right border; goi: gene of interest; ori: Origin of replication; Ab^r, antibiotic-resistance gene used in screening for binary vector in E. coli; selection marker: antibiotic-resistance gene or herbicide resistance gene used in screening for successful plant transformation.

the insertion of foreign genes without the use of restriction enzymes (Curtis & Grossniklaus, 2003). T-DNA binary vectors containing genes of interest can be easily electroporated into disarmed agrobacteria strains and delivered into plant cell by agroinfiltration (Lee & Gelvin, 2008).

6. CHARACTERIZATION OF THE MOLECULAR BIOLOGY OF GVCV.

My dissertation is focused on further characterization of the badnavirus, GVCV, with the goal of eventually creating an infectious clone. This project has involved the identification of the major GVCV promoter, as well as the 5' and 3' ends of the terminally redundant GVCV transcript (Zhang *et al.*, 2011) Chapter 2). Out of necessity, we also used the caulimovirus, CaMV for development of essential tools for delivery of viruses into plant cells and for verification of the replication of an infectious clone (Chapter 3). Our progress towards the development of an infectious clone of GVCV is described in Chapter 4. Finally, our progress towards the identification of a potential vector for spread of GVCV in vineyards is described in Chapter 5.

REFERENCE

Abuodeh, R. O., Orbach, M. J., Mandel, M. A., Das, A. & Galgiani, J. N. (2000). Genetic transformation of Coccidioides immitis facilitated by Agvobactevium tumefaciens. *Journal of Infectious Diseases* **181**, 2106-2110.

Angel, C. A., Lutz, L., Yang, X., Rodriguez, A., Adair, A., Zhang, Y., Leisner, S. M., Nelson, R. S. & Schoelz, J. E. (2013). The P6 protein of *Cauliflower mosaic virus* interacts with CHUP1, a plant protein which moves chloroplasts on actin microfilaments. *Virology* **443**, 363-374.

Aparna, G. S., Kotakadi, V. S., Saigopal, D. & Reddy, M. (2012). Citrus yellow mosaic: a transmissible virus of citrus species in India. *The bioscan* **7**, 283-287.

Armour, S. L., Melcher, U., Pirone, T. P., Lyttle, D. & Essenberg, R. (1983). Helper component for aphid transmission encoded by region II of *Cauliflower mosaic virus* DNA. *Virology* **129**, 25-30.

Basso, J., Dallaire, P., Charest, P. J., Devantier, Y. & Laliberté, J.-F. (1994). Evidence for an internal ribosome entry site within the 5′ non-translated region of turnip mosaic potyvirus RNA. *Journal of general virology* **75**, 3157-3165.

Baughman, G. A., Jacobs, J. D. & Howell, S. H. (1988). *Cauliflower mosaic virus* gene VI produces a symptomatic phenotype in transgenic tobacco plants. *Proceedings of the National Academy of Sciences* **85**, 733-737.

Bhattacharyya‐Pakrasi, M., Peng, J., Elmer, J. S., Laco, G., Shen, P., Kaniewska, M. B., Kononowicz, H., Wen, F., Hodges, T. K. & Beachy, R. N. (1993). Specificity of a promoter from the rice tungro bacilliform virus for expression in phloem tissues. *The Plant Journal* **4**, 71-79.

Blanc, S., Hébrard, E., Drucker, M. & Froissart, R. (2001). Molecular basis of vector transmission: caulimoviruses. *Virus-Insect-Plant Interactions*, pp. 143-166. Edited by K. Harris, O. P. Smith & J. E. Duffus. San Diego, CA: Academic Press.

Blanc, S., Schmidt, I., Vantard, M., Scholthof, H. B., Kuhl, G., Esperandieu, P., Cerutti, M. & Louis, C. (1996). The aphid transmission factor of *Cauliflower*

mosaic virus forms a stable complex with microtubules in both insect and plant cells. *Proceedings of the National Academy of Sciences* **93**, 15158-15163.

Bonneville, J., Sanfaçon, H., Fütterer, J. & Hohn, T. (1989). Posttranscriptional trans-activation in *Cauliflower mosaic virus*. *Cell* **59**, 1135-1143.

Bundock, P., den Dulk-Ras, A., Beijersbergen, A. & Hooykaas, P. (1995). Trans-kingdom T-DNA transfer from Agrobacterium tumefaciens to Saccharomyces cerevisiae. *The EMBO journal* **14**, 3206-3214.

Cecchini, E., Gong, Z., Geri, C., Covey, S. N. & Milner, J. J. (1997). Transgenic Arabidopsis lines expressing gene VI from *Cauliflower mosaic virus* variants exhibit a range of symptom-like phenotypes and accumulate inclusion bodies. *Molecular plant-microbe interactions* **10**, 1094-1101.

Cheng, R., Olson, N. & Baker, T. (1992). *Cauliflower mosaic virus*: a 420 subunit (T= 7), multilayer structure. *Virology* **186**, 655-668.

Citovsky, V., Knorr, D. & Zambryski, P. (1991). Gene I, a potential cell-to-cell movement locus of *Cauliflower mosaic virus*, encodes an RNA-binding protein. *Proceedings of the National Academy of Sciences* **88**, 2476-2480.

Covey, S. N. & Hull, R. (1981). Transcription of *Cauliflower mosaic virus* DNA. Detection of transcripts, properties, and location of the gene encoding the virus inclusion body protein. *Virology* **111**, 463-474.

Curtis, M. D. & Grossniklaus, U. (2003). A gateway cloning vector set for high-throughput functional analysis of genes in planta. *Plant physiology* **133**, 462-469.

Dasgupta, I., Hull, R., Eastop, S., Poggi-Pollini, C., Blakebrough, M., Boulton, M. I. & Davies, J. W. (1991). Rice tungro bacilliform virus DNA independently infects rice after Agrobacterium-mediated transfer. *Journal of general virology* **72**, 1215-1221.

Daubert, S., Richins, R., Shepherd, R. & Gardner, R. C. (1982). Mapping of the coat protein gene of *Cauliflower mosaic virus* by its expression in a prokaryotic system. *Virology* **122**, 444-449.

Daubert, S., Schoelz, J., Debao, L. & Shepherd, R. (1983). Expression of disease symptoms in *Cauliflower mosaic virus* genomic hybrids. *Journal of molecular*

and applied genetics **2**, 537-547.

De Framond, A. J., Barton, K. A. & Chilton, M.-D. (1983). Mini–Ti: a new vector strategy for plant genetic engineering. *Nature Biotechnology* **1**, 262-269.

De La Riva, G. A., González-Cabrera, J., Vázquez-Padrón, R. & Ayra-Pardo, C. (1998). Agrobacterium tumefaciens: a natural tool for plant transformation. *Electronic Journal of Biotechnology* **1**, 24-25.

De Tapia, M., Himmelbach, A. & Hohn, T. (1993). Molecular dissection of the *Cauliflower mosaic virus* translation transactivator. *The EMBO journal* **12**, 3305-3314.

Dixon, L. K. & Hohn, T. (1984). Initiation of translation of the *Cauliflower mosaic virus* genome from a polycistronic mRNA: evidence from deletion mutagenesis. *The EMBO journal* **3**, 2731-2736.

Dongo, L. & Orisajo, S. (2007). Status of cocoa swollen shoot virus disease in Nigeria. *African Journal of Biotechnology* **6**, 2054-2061.

Dorokhov, Y. L., Skulachev, M. V., Ivanov, P. A., Zvereva, S. D., Tjulkina, L. G., Merits, A., Gleba, Y. Y., Hohn, T. & Atabekov, J. G. (2002). Polypurine (A)-rich sequences promote cross-kingdom conservation of internal ribosome entry. *Proceedings of the National Academy of Sciences* **99**, 5301-5306.

Escobar, M. A. & Dandekar, A. M. (2003). Agrobacterium tumefaciens as an agent of disease. *Trends in plant science* **8**, 380-386.

Fütterer, J., Gordon, K., Bonneville, J., Sanfaçon, H., Pisan, B., Penswick, J. & Hohn, T. (1988). The leading sequence of caulimovirus large RNA can be folded into a large stem-loop structure. *Nucleic acids research* **16**, 8377-8390.

Fütterer, J. & Hohn, T. (1991). Translation of a polycistronic mRNA in the presence of the *Cauliflower mosaic virus* transactivator protein. *The EMBO journal* **10**, 3887-3896.

Fütterer, J. & Hohn, T. (1992). Role of an upstream open reading frame in the translation of polycistronic mRNAs in plant cells. *Nucleic acids research* **20**, 3851-3857.

Franck, A., Guilley, H., Jonard, G., Richards, K. & Hirth, L. (1980). Nucleotide sequence of *Cauliflower mosaic virus* DNA. *Cell* **21**, 285-294.

Gardner, R. & Shepherd, R. (1980). A procedure for rapid isolation and analysis of *Cauliflower mosaic virus* DNA. *Virology* **106**, 159-161.

Gelvin, S. B. (2000). Agrobacterium and plant genes involved in T-DNA transfer and integration. *Annual review of plant biology* **51**, 223-256.

Giband, M., Mesnard, J.-M. & Lebeurier, G. (1986). The gene III product (P15) of *Cauliflower mosaic virus* is a DNA-binding protein while an immunologically related P11 polypeptide is associated with virions. *The EMBO journal* **5**, 2433-2438.

Glass, M. J., Jia, X.-Y. & Summers, D. F. (1993). Identification of the hepatitis A virus internal ribosome entry site: in vivo and in vitro analysis of bicistronic RNAs containing the HAV 5′ noncoding region. *Virology* **193**, 842-852.

Goldberg, K.-B., Kiernan, J. & Shepherd, R. J. (1991). A disease syndrome associated with expression of gene VI of caulimoviruses may be a nonhost reaction. *Mol Plant-Microbe Interact* **4**, 182-189.

Gowda, S., Wu, F. C., Scholthof, H. B. & Shepherd, R. J. (1989). Gene VI of Figwort mosaic virus (caulimovirus group) functions in posttranscriptional expression of genes on the full-length RNA transcript. *Proceedings of the National Academy of Sciences* **86**, 9203-9207.

Gray, N. K. & Hentze, M. W. (1994). Regulation of protein synthesis by mRNA structure. *Molecular biology reports* **19**, 195-200.

Grimsley, N., Hohn, T., Davies, J. W. & Hohn, B. (1987). Agrobacterium-mediated delivery of infectious maize streak virus into maize plants. *Nature* **325**, 177-179.

Guilley, H., Dudley, R. K., Jonard, G., Balàzs, E. & Richards, K. E. (1982). Transcription of *Cauliflower mosaic virus* DNA: detection of promoter sequences, and characterization of transcripts. *Cell* **30**, 763-773.

Guo, Q., Honesty, S., Xu, M. L., Zhang, Y., Schoelz, J. & Qiu, W. (2014). Genetic Diversity and Tissue and Host Specificity of *Grapevine vein clearing virus*. *Phytopathology* **104**, 539-547.

Haas, M., Bureau, M., Geldreich, A., Yot, P. & Keller, M. (2002). *Cauliflower mosaic virus*: still in the news. *Molecular plant pathology* **3**, 419-429.

Hahn, P. & Shepherd, R. J. (1982). Evidence for a 58-kilodalton polypeptide as precursor of the coat protein of *Cauliflower mosaic virus*. *Virology* **116**, 480-488.

Harries, P. A., Palanichelvam, K., Yu, W., Schoelz, J. E. & Nelson, R. S. (2009). The *Cauliflower mosaic virus* protein P6 forms motile inclusions that traffic along actin microfilaments and stabilize microtubules. *Plant physiology* **149**, 1005-1016.

Hearon, S. & Locke, J. (1984). Graft, pollen, and seed transmission of an agent associated with top spotting in Kalancho ë blossfeldiana. *Plant disease* **68**, 346-350.

Himmelback, A., Chapdelaine, Y. & Hohn, T. (1996). Interaction between *Cauliflower mosaic virus* inclusion body protein and capsid protein: implications for viral assembly. *Virology* **217**, 147-157.

Hoekema, A., Hirsch, P., Hooykaas, P. & Schilperoort, R. (1983). A binary plant vector strategy based on separation of vir-and T-region of the Agrobacterium tumefaciens Ti-plasmid. *Nature* **303**, 179-180.

Hohn, T., Hohn, B., Lesot, A. & Lebeurier, G. (1980). Restriction map of native and cloned *Cauliflower mosaic virus* DNA. *Gene* **11**, 21-31.

Hohn, T., Hohn, B. & Pfeiffer, P. (1985). Reverse transcription in CaMV. *Trends in biochemical Sciences* **10**, 205-209.

Hohn, T. (2013). Plant pararetroviruses: interactions of *Cauliflower mosaic virus* with plants and insects. *Current opinion in virology* **3**, 629-638.

Howarth, A., Gardner, R., Messing, J. & Shepherd, R. (1981). Nucleotide sequence of naturally occurring deletion mutants of *Cauliflower mosaic virus*. *Virology* **112**, 678-685.

Huang, Q. & Hartung, J. S. (2001). Cloning and sequence analysis of an infectious clone of Citrus yellow mosaic virus that can infect sweet orange via Agrobacterium-mediated inoculation. *Journal of General Virology* **82**, 2549-2558.

Huang, Z., Han, Y. & Howell, S. H. (2000). Formation of surface tubules and fluorescent foci in Arabidopsis thaliana protoplasts expressing a fusion

between the green fluorescent protein and the *Cauliflower mosaic virus* movement protein. *Virology* **271**, 58-64.

Hull, R., Covey, S. & Maule, A. (1987). Structure and replication of caulimovirus genomes. *Journal of Cell Science* **1987**, 213-229.

Hull, R., Lockart, B.E., Reddy, D.V.R. and Schoelz, J.E. (2005). Family *Caulimoviridae*. In: *Virus Taxonomy. Seventh Report of the International Committee on Taxonomy of Viruses* (Edited by van Regenmortel, M.V.H., Fauquet, C.M., Bishop, D.H.L., Carstens, E.B., Estes, M.K., Lemon, S.M., Maniloff, J., Mayo, M.A., McGeoch, D.J., Pringle, C.R. and Wickner, R.B.), pp335-347, Academic Press, San Diego.

Jang, S., Kräusslich, H., Nicklin, M., Duke, G., Palmenberg, A. & Wimmer, E. (1988). A segment of the 5'nontranslated region of encephalomyocarditis virus RNA directs internal entry of ribosomes during in vitro translation. *Journal of virology* **62**, 2636-2643.

Jones, A. T., McGavin, W. J., Geering, A. & Lockhart, B. (2002). Identification of Rubus yellow net virus as a distinct badnavirus and its detection by PCR in Rubus species and in aphids. *Annals of applied biology* **141**, 1-10.

Kasteel, D., Perbal, M.-C., Boyer, J.-C., Wellink, J., Goldbach, R., Maule, A. & Van Lent, J. (1996). The movement proteins of cowpea mosaic virus and *Cauliflower mosaic virus* induce tubular structures in plant and insect cells. *Journal of General Virology* **77**, 2857-2864.

Kozak, M. (1986). Point mutations define a sequence flanking the AUG initiator codon that modulates translation by eukaryotic ribosomes. *Cell* **44**, 283-292.

Kozak, M. (1987). Effects of intercistronic length on the efficiency of reinitiation by eukaryotic ribosomes. *Molecular and Cellular Biology* **7**, 3438-3445.

Kozak, M. (1989). The scanning model for translation: an update. *The Journal of cell biology* **108**, 229-241.

Kunik, T., Tzfira, T., Kapulnik, Y., Gafni, Y., Dingwall, C. & Citovsky, V. (2001). Genetic transformation of HeLa cells by Agrobacterium. *Proceedings of the National Academy of Sciences* **98**, 1871-1876.

Latz, A., Ivashikina, N., Fischer, S., Ache, P., Sano, T., Becker, D., Deeken, R. & Hedrich, R. (2007). In planta AKT2 subunits constitute a pH-and

Ca2+-sensitive inward rectifying K+ channel. *Planta* **225**, 1179-1191.

Lee, L.-Y. & Gelvin, S. B. (2008). T-DNA binary vectors and systems. *Plant physiology* **146**, 325-332.

Leh, V., Jacquot, E., Geldreich, A., Hermann, T., Leclerc, D., Cerutti, M., Yot, P., Keller, M. & Blanc, S. (1999). Aphid transmission of *Cauliflower mosaic virus* requires the viral PIII protein. *The EMBO journal* **18**, 7077-7085.

Leh, V., Yot, P. & Keller, M. (2000). The *Cauliflower mosaic virus* translational transactivator interacts with the 60S ribosomal subunit protein L18 of Arabidopsis thaliana. *Virology* **266**, 1-7.

Leh, V., Jacquot, E., Geldreich, A., Haas, M., Blanc, S., Keller, M. & Yot, P. (2001). Interaction between the open reading frame III product and the coat protein is required for transmission of *Cauliflower mosaic virus* by aphids. *Journal of virology* **75**, 100-106.

Leisner, S. M., Turgeon, R. & Howell, S. H. (1992). Long distance movement of *Cauliflower mosaic virus* in infected turnip plants. *Mol Plant-Microbe Interact* **5**, 41-47.

Linstead, P., Hills, G., Plaskitt, K., Wilson, I., Harker, C. & Maule, A. (1988). The subcellular location of the gene 1 product of *Cauliflower mosaic virus* is consistent with a function associated with virus spread. *Journal of General Virology* **69**, 1809-1818.

Liu, L., Zhang, Y., Tang, S., Zhao, Q., Zhang, Z., Zhang, H., Dong, L., Guo, H. & Xie, Q. (2010). An efficient system to detect protein ubiquitination by agroinfiltration in *Nicotiana benthamiana*. *The Plant Journal* **61**, 893-903.

Lockhart, B. & Autrey, L. (1991). Mealy bug transmission of sugarcane bacilliform and sugarcane clostero-like viruses. In: III International Society of Sugarcane Technologist Pathology Workshop, 17.

Lockhart, B. & Olszewski, N. (1996). Schefflera ringspot virus, a widely distributed mealybug-transmitted badnavirus occurring in Schefflera and Aralia. In *IX International Symposium on Virus Diseases of Ornamental Plants 432,* pp. 196-203.

Lockhart, B., Kiratiya-Angul, K., Jones, P., Eng, L., De Silva, P., Olszewski, N., Lockhart, N., Deema, N. & Sangalang, J. (1997). Identification of Piper

yellow mottle virus, a mealybug-transmitted badnavirus infecting Piper spp. in Southeast Asia. *European journal of plant pathology* **103**, 303-311.

Lockhart, B. & Geering, A. (2000). Partial characterization of two aphid-transmitted viruses associated with yellow leafspot of Spiraea. In *X International Symposium on Virus Diseases of Ornamental Plants 568*, pp. 163-168.

Loper, J. E. & Kado, C. I. (1979). Host range conferred by the virulence-specifying plasmid of Agrobacterium tumefaciens. *Journal of bacteriology* **139**, 591-596.

Love, A. J., Yun, B. W., Laval, V., Loake, G. J. & Milner, J. J. (2005). *Cauliflower mosaic virus*, a compatible pathogen of Arabidopsis, engages three distinct defense-signaling pathways and activates rapid systemic generation of reactive oxygen species. *Plant Physiology* **139**, 935-948.

Love, A. J., Laird, J., Holt, J., Hamilton, A. J., Sadanandom, A. & Milner, J. J. (2007). *Cauliflower mosaic virus* protein P6 is a suppressor of RNA silencing. *Journal of General Virology* **88**, 3439-3444.

Luis, L., Snapp, E. L., Denecke, J., Lippincott-Schwartz, J., Hawes, C. & Brandizzi, F. (2004). Endoplasmic reticulum export sites and Golgi bodies behave as single mobile secretory units in plant cells. *The Plant Cell* **16**, 1753-1771.

Lunden, S., Meng, B., Avery Jr, J. & Qiu, W. (2010). Association of Grapevine fanleaf virus, Tomato ringspot virus and Grapevine rupestris stem pitting-associated virus with a grapevine vein-clearing complex on var. Chardonnay. *European Journal of Plant Pathology* **126**, 135-144.

Lutz, L., Okenka, G., Schoelz, J. & Leisner, S. (2015). Mutations within A 35 amino acid region of P6 influence self-association, inclusion body formation, and Caulimovirus infectivity. *Virology* **476**, 26-36.

Macanawai, A. R., Ebenebe, A. A., Hunter, D., Devitt, L., Hafner, G. & Harding, R. (2005). Investigations into the seed and mealybug transmission of Taro bacilliform virus. *Australasian Plant Pathology* **34**, 73-76.

Kalischuk, M. L., Fusaro, A. F., Waterhouse, P. M., Pappu, H. R. & Kawchuk, L. M. (2013). Complete genomic sequence of a Rubus yellow net virus isolate and detection of genome-wide pararetrovirus-derived small RNAs. *Virus research* **178**, 306-313.

Matsuda, Y., Liang, G., Zhu, Y., Ma, F., Nelson, R. S. & Ding, B. (2002). The Commelina yellow mottle virus promoter drives companion-cell-specific gene expression in multiple organs of transgenic tobacco. *Protoplasma* **220**, 51-58.

McCullen, C. A. & Binns, A. N. (2006). Agrobacterium tumefaciens and plant cell interactions and activities required for interkingdom macromolecular transfer. *Annual Review of Cell and Developmental Biology* **22**, 101-127.

Medberry, S. L., Lockhart, B. & Olszewski, N. E. (1990). Properties of Commelina yellow mottle virus's complete DNA sequence, genomic discontinuities and transcript suggest that it is a pararetrovirus. *Nucleic Acids Research* **18**, 5505-5513.

Medberry, S. L., Lockhart, B. & Olszewski, N. E. (1992). The Commelina yellow mottle virus promoter is a strong promoter in vascular and reproductive tissues. *The Plant Cell Online* **4**, 185-192.

Menissier, J., Lebeuerier, G. & Hirth, L. (1982). Free *Cauliflower mosaic virus* supercoiled DNA in infected plants. *Virology* **117**, 322-328.

Mesnard, J.-M., Kirchherr, D., Wurch, T. & Lebeurier, G. (1990). The *Cauliflower mosaic virus* gene III product is a non-sequence-specific DNA binding protein. *Virology* **174**, 622-624.

Migliori, A. & Lastra, R. (1978). Study of viruses on Commelina diffusa Burm. in Guadeloupe. *Annales de Phytopathologie* **10**, 467-477.

Mougeot, J.-L., Guidasci, T., Wurch, T., Lebeurier, G. & Mesnard, J.-M. (1993). Identification of C-terminal amino acid residues of *Cauliflower mosaic virus* open reading frame III protein responsible for its DNA binding activity. *Proceedings of the National Academy of Sciences* **90**, 1470-1473.

Olszewski, N., Hagen, G. & Guilfoyle, T. J. (1982). A transcriptionally active, covalently closed minichromosome of *Cauliflower mosaic virus* DNA isolated from infected turnip leaves. *Cell* **29**, 395-402.

Özyiğit, İ. İ. (2012). Agrobacterium tumefaciens and its use in plant biotechnology. *Crop Production for Agricultural Improvement*, pp. 317-361. Edited by Ashraf M, Ozturk M, Ahmad MSA, and Aksoy A. Springer Science-Business Media, Heidelberg.

Palanichelvam, K., Cole, A. B., Shababi, M. & Schoelz, J. E. (2000).

Agroinfiltration of *Cauliflower mosaic virus* gene VI elicits hypersensitive response in Nicotiana species. *Molecular plant-microbe interactions* **13**, 1275-1279.

Park, H.-S., Himmelbach, A., Browning, K. S., Hohn, T. & Ryabova, L. A. (2001). A plant viral "reinitiation" factor interacts with the host translational machinery. *Cell* **106**, 723-733.

Pelletier, J. & Sonenberg, N. (1988). Internal initiation of translation of eukaryotic mRNA directed by a sequence derived from poliovirus RNA. *Nature* **334**, 320-325.

Perbal, M.-C., Thomas, C. & Maule, A. (1993). *Cauliflower mosaic virus* gene I product (P1) forms tubular structures which extend from the surface of infected protoplasts. *Virology* **195**, 281-285.

Pfeiffer, P. & Hohn, T. (1983). Involvement of reverse transcription in the replication of *Cauliflower mosaic virus*: a detailed model and test of some aspects. *Cell* **33**, 781-789.

Phillips, S., Briddon, R., Brunt, A. & Hull, R. (1999). The partial characterization of a badnavirus infecting the greater asiatic or water yam (Dioscorea alata). *Journal of Phytopathology* **147**, 265-269.

Pitzschke, A. & Hirt, H. (2010). New insights into an old story: Agrobacterium ‐ induced tumour formation in plants by plant transformation. *The EMBO Journal* **29**, 1021-1032.

Pooggin, M. M., Hohn, T. & Fütterer, J. (1998). Forced evolution reveals the importance of short open reading frame A and secondary structure in the *Cauliflower mosaic virus* 35S RNA leader. *Journal of virology* **72**, 4157-4169.

Pooggin, M. M., Hohn, T. & Fütterer, J. (2000). Role of a short open reading frame in ribosome shunt on the *Cauliflower mosaic virus* RNA leader. *Journal of Biological Chemistry* **275**, 17288-17296.

Pooggin, M. M., Fütterer, J., Skryabin, K. G. & Hohn, T. (2001). Ribosome shunt is essential for infectivity of *Cauliflower mosaic virus*. *Proceedings of the National Academy of Sciences* **98**, 886-891.

Powell, M. L. (2010). Translational termination–reinitiation in RNA viruses. *Biochemical Society Transactions* **38**, 1558-1564.

Qiu, S. G. & Schoelz, J. E. (1992). Three regions of *Cauliflower mosaic virus* strain W260 are involved in systemic infection of solanaceous hosts. *Virology* **190**, 773-782.

Qiu, W. & Lunden, S. (2007). Characterization of a severe virus-like disease in Chardonnay grapevines in Missouri. *Plant Health Progress*. doi: 10.1094/PHP-2007-1119-01-BR.

Qu, R., Bhattacharyya, M., Laco, G. S., De Kochko, A., Subba Rao, B., Kaniewska, M. B., Scott Elmer, J., Rochester, D. E., Smith, C. E. & Beachy, R. N. (1991). Characterization of the genome of rice tungro bacilliform virus: Comparison with Commelina yellow mottle virus and caulimoviruses. *Virology* **185**, 354-364.

Rodriguez, A., Angel, C. A., Lutz, L., Leisner, S. M., Nelson, R. S. & Schoelz, J. E. (2014). Association of the P6 Protein of *Cauliflower mosaic virus* with Plasmodesmata and Plasmodesmal Proteins. *Plant physiology* **166**, 1345-1358.

Ryabova, L. A. & Hohn, T. (2000). Ribosome shunting in the *Cauliflower mosaic virus* 35S RNA leader is a special case of reinitiation of translation functioning in plant and animal systems. *Genes & Development* **14**, 817-829.

Santos-Rosa, M., Poutaraud, A., Merdinoglu, D. & Mestre, P. (2008). Development of a transient expression system in grapevine via agro-infiltration. *Plant cell reports* **27**, 1053-1063.

Schöb, H., Kunz, C. & Meins Jr, F. (1997). Silencing of transgenes introduced into leaves by agroinfiltration: a simple, rapid method for investigating sequence requirements for gene silencing. *Molecular and General Genetics MGG* **256**, 581-585.

Schenk, P. M., Sagi, L., Remans, T., Dietzgen, R. G., Bernard, M. J., Graham, M. W. & Manners, J. M. (1999). A promoter from sugarcane bacilliform badnavirus drives transgene expression in banana and other monocot and dicot plants. *Plant molecular biology* **39**, 1221-1230.

Schenk, P. M., Remans, T., Sági, L., Elliott, A. R., Dietzgen, R. G., Swennen, R., Ebert, P. R., Grof, C. P. & Manners, J. M. (2001). Promoters for pregenomic RNA of banana streak badnavirus are active for transgene expression in monocot and dicot plants. *Plant molecular biology* **47**, 399-412.

Schoelz, J., Shepherd, R. J. & Daubert, S. (1986). Region VI of *Cauliflower mosaic virus* encodes a host range determinant. *Molecular and cellular biology* **6**, 2632-2637.

Schoelz, J. E. & Wintermantel, W. M. (1993). Expansion of viral host range through complementation and recombination in transgenic plants. *The Plant Cell* **5**, 1669-1679.

Schoelz, J. E., Harries, P. A. & Nelson, R. S. (2011). Intracellular transport of plant viruses: finding the door out of the cell. *Molecular plant* **4**, 813-831.

Schoelz, J. E., Angel, C. A., Nelson, R. S. & Leisner, S. M. (2015). A model for intracellular movement of *Cauliflower mosaic virus*: the concept of the mobile virion factory. *Journal of experimental botany* **67**, 2039-2048.

Sether, D., Melzer, M., Borth, W. & Hu, J. (2012). Pineapple bacilliform CO virus: diversity, detection, distribution, and transmission. *Plant Disease* **96**, 1798-1804.

Sha, Y., Broglio, E. P., Cannon, J. F. & Schoelz, J. E. (1995). Expression of a plant viral polycistronic mRNA in yeast, Saccharomyces cerevisiae, mediated by a plant virus translational transactivator. *Proceedings of the National Academy of Sciences* **92**, 8911-8915.

Shockey, M., Gardner, C., Melcher, U. & Essenberg, R. (1980). Polypeptides associated with inclusion bodies from leaves of turnip infected with *Cauliflower mosaic virus*. *Virology* **105**, 575-581.

Skulachev, M., Ivanov, P., Karpova, O., Korpela, T., Rodionova, N., Dorokhov, Y. L. & Atabekov, J. (1999). Internal initiation of translation directed by the 5′ -untranslated region of the tobamovirus subgenomic RNA I 2. *Virology* **263**, 139-154.

Stavolone, L., Villani, M. E., Leclerc, D. & Hohn, T. (2005). A coiled-coil interaction mediates *Cauliflower mosaic virus* cell-to-cell movement. *Proceedings of the National Academy of Sciences* **102**, 6219-6224.

Su, H.-J. (1998). First occurrence of banana streak badnavirus and studies on its vectorship in Taiwan. In: *Banana streak virus: a unique virus Musa interaction? Proceedings of a workshop of the Promusa Virology Working Group* (Edited by Frison, E.A. and Sharrock, S.L), Montpellier, France, pp. 20-25.

Takatsuji, H., Hirochika, H., Fukushi, T. & Ikeda, J.-E. (1986). Expression of *Cauliflower mosaic virus* reverse transcriptase in yeast. *Nature* **319**, 240-2443.

Takatsuji, H., Yamauchi, H., Watanabe, S., Kato, H. & Ikeda, J. (1992). *Cauliflower mosaic virus* reverse transcriptase. Activation by proteolytic processing and functional alteration by terminal deletion. *Journal of Biological Chemistry* **267**, 11579-11585.

Temp é, J. & Petit, A. (1982). Opine utilization by Agrobacterium. *Molecular biology of plant tumors*, 451-459.

Thomas, C., Perbal, C. & Maule, A. (1993). A mutation of *Cauliflower mosaic virus* gene I interferes with virus movement but not virus replication. *Virology* **192**, 415-421.

Thomashow, M., Panagopoulos, C., Gordon, M. & Nester, E. (1980). Host range of Agrobacterium tumefaciens is determined by the Ti plasmid. *Nature* **283**, 794-796.

Tidona, C. & Darai, G. (2011). *The Springer index of viruses*: Springer-Verlag, Berlin, Heidelberg, New York, 2011.

Toh, H., Hayashida, H. & Miyata, T. (1983). Sequence homology between retroviral reverse transcriptase and putative polymerases of hepatitis B virus and *Cauliflower mosaic virus*. *Nature* **305**, 827-829.

Tompkins, C. M. (1937). A transmissible mosaic disease of cauliflower. *Journal of Agricultural Research* **55**, 33-46.

Tsuge, S., Kobayashi, K., Nakayashiki, H., Mise, K. & Furusawa, I. (1999). *Cauliflower mosaic virus* ORF III product forms a tetramer in planta: its implication in viral DNA folding during encapsidation. *Microbiology and immunology* **43**, 773-780.

Tzafrir, I., Torbert, K. A., Lockhart, B. E., Somers, D. A. & Olszewski, N. E. (1998). The sugarcane bacilliform badnavirus promoter is active in both monocots and dicots. *Plant molecular biology* **38**, 347-356.

Weising, K., Schell, J. & Kahl, G. (1988). Foreign genes in plants: transfer, structure, expression, and applications. *Annual review of genetics* **22**, 421-477.

Winans, S. C. (1992). Two-way chemical signaling in Agrobacterium-plant interactions. *Microbiological reviews* **56**, 12-31.

Woolston, C. J., Covey, S. N., Penswick, J. R. & Davies, J. W. (1983). Aphid transmission and a polypeptide are specified by a defined region of the *Cauliflower mosaic virus* genome. *Gene* **23**, 15-23.

Wurch, T., Kirchherr, D., Mesnard, J.-M. & Lebeurier, G. (1990). The *Cauliflower mosaic virus* open reading frame VII product can be expressed in Saccharomyces cerevisiae but is not detected in infected plants. *Journal of virology* **64**, 2594-2598.

Yang, I. C., Iommarini, J., Becker, D. K., Hafner, G., Dale, J. L. & Harding, R. M. (2003). A promoter derived from taro bacilliform badnavirus drives strong expression in transgenic banana and tobacco plants. *Plant cell reports* **21**, 1199-1206.

Yang, Y., Li, R. & Qi, M. (2000). In vivo analysis of plant promoters and transcription factors by agroinfiltration of tobacco leaves. *The Plant Journal* **22**, 543-551.

Yu, W., Murfett, J. & Schoelz, J. E. (2003). Differential induction of symptoms in Arabidopsis by P6 of *Cauliflower mosaic virus*. *Molecular plant-microbe interactions* **16**, 35-42.

Zhang, Y., Singh, K., Kaur, R. & Qiu, W. (2011). Association of a novel DNA virus with the grapevine vein-clearing and vine decline syndrome. *Phytopathology* **101**, 1081-1090.

Zhang, Y., Angel, C., Valdes, S., Qiu, W. & Schoelz, J. (2015). Characterization of the promoter of *Grapevine vein clearing virus*. *Journal of General Virology* **96**, 165-169.

Zvereva, S., Ivanov, P., Skulachev, M., Klyushin, A., Dorokhov, Y. L. & Atabekov, J. (2004). Evidence for contribution of an internal ribosome entry site to intercellular transport of a tobamovirus. *Journal of general virology* **85**, 1739-1744.

CHAPTER 2: CHARACTERIZATION OF GRAPEVINE VEIN CLEARING VIRUS (GVCV) PROMOTER

Part of this chapter was published in *Journal of General Virology* **96**, (2015): 165-169.

ABSTRACT

Grapevine Vein Clearing Virus (GVCV) is a newly discovered DNA virus in grapevine that is closely associated with grapevine vein clearing syndrome observed in vineyards in Missouri and surrounding states. The genome sequence of GVCV indicates that it belongs to the *Caulimoviridae*, a family of viruses that replicate by reverse transcription of an RNA intermediate, and that is a species within the *Badnavirus* genus. The hallmarks of the *Caulimoviridae* include viruses with strong promoters, production of a terminally redundant RNA, and a viral RNA leader sequence capable of being folded into an intricate stem loop structure that facilitates a ribosomal shunt model for translation of the first true open reading frame (ORF1). To identify the GVCV promoter, we cloned portions of the GVCV large intergenic region in front of a GFP gene present in the *Agrobacterium tumefaciens* binary vector pKYLX7. GFP expression was assessed by ELISA three days after agroinfiltration of *Nicotiana benthamiana* leaves. We found that the GVCV DNA segment between nucleotides 7,332 and 7,672 directed expression of GFP that was stronger than the *Cauliflower mosaic virus* 35S promoter. 5' RACE revealed that transcription was initiated predominantly at nucleotide 7,571. This transcript initiation site was

confirmed in an analysis of GVCV-infected grapevine leaf tissues and a 3' RACE analysis of GVCV RNAs revealed that the GVCV RNA terminated at nucleotide 7,676. Additional transient expression analysis studies were supportive of a ribosomal shunt model for expression of ORF1 of GVCV.

1. INTRODUCTION

The badnaviruses are a genus of plant viruses that replicate by reverse transcription, have a genome that is composed of circular, double-stranded DNA, and form a bacilliform virion that has a diameter of 30 nm and a length of 120 to 150 nm (Tidona & Darai, 2011). The first badnavirus to be identified was *Commelina yellow mottle virus* (CoYMV) (Medberry *et al*., 1990; Migliori & Lastra, 1978)). Since that first discovery, many new badnavirus genomes have been found and characterized at the nucleotide sequence level. Much information can be inferred from the nucleotide sequences of these new badnaviruses. For example, it is generally accepted that all badnaviruses have a single promoter that drives transcription of a terminally redundant pregenomic RNA (Tidona & Darai, 2011). Less information is available concerning the precise map locations of the promoters and transcription start sites for the badnaviruses. In particular, the 5' and 3' ends of transcripts have only been mapped for CoYMV, *Rice tungro bacilliform virus* (RTBV), and several variants of *Banana streak virus* (BSV) (Medberry *et al*., 1990; Qu *et al*., 1991; Schenk *et al*., 2001). Information on promoters and transcripts is an important "next step" in the characterization of any badnavirus beyond the level of the nucleotide sequence. Furthermore, given the examples for how infectious clones of badnaviruses can be developed and inoculated, an understanding of the terminally redundant transcript of badnaviruses is important, if not essential. Generally, infectious clones for badnaviruses contain a longer than full-length genome copy, with duplicated promoter

regions on both ends of the insert (Dasgupta *et al*., 1991; Huang & Hartung, 2001; Medberry *et al.*, 1990).

Recently a badnavirus has been discovered in grapevines grown in the Midwest United States that is consistently associated with a new disease (Guo *et al*., 2014; Lunden, 2009; Qiu & Lunden, 2007; Zhang *et al*., 2011). The disease was first observed in *Vitis vinifera* vines in Missouri vineyards in 2004, and has since been found in Indiana, Illinois and Arkansas (Guo *et al*., 2014; Lunden, 2009; Qiu & Lunden, 2007). Typical symptoms of the disease include chlorosis in major or minor veins, especially in young shoots that emerge in early spring, short internodes that develop into a zigzag pattern, and small, crinkled leaves with a rolling back of leaf margins. The affected vines eventually become dwarfed, and bear smaller clusters with fewer fruits. In the most severe cases, the infection kills the vines (Guo *et al.*, 2014; Qiu & Lunden, 2007; Zhang *et al.*, 2011). The badnavirus, designated *Grapevine vein clearing virus* (GVCV), was identified through deep sequencing of siRNAs, and it was the first DNA virus shown to exist in grapevines (Zhang *et al*., 2011). The complete nucleotide sequence of GVCV was assembled from clones amplified through PCR, revealing a putative badnavirus genome composed of three open reading frames (ORFs). Within the *Badnavirus* genus, GVCV is most closely related to *Taro bacilliform virus* (Zhang *et al*., 2011). A survey was conducted in vineyards in Missouri, Illinois, and Indiana, and GVCV was amplified by PCR in symptomatic grapevines from cultivated grapevines in all three states (Zhang *et al.*,

2011). Although a final decisive proof is still lacking, GVCV is most likely the causal agent of grapevine vein clearing syndrome.

In this study, we used an agroinfiltration assay in *N. benthamiana* to identify the GVCV promoter and transcript initiation site. This information was subsequently used to confirm the 5' and 3' ends of the GVCV transcript in infected grape leaf tissue. An agroinfiltration assay also was used to evaluate the expression of ORF1 of GVCV and coupled with knowledge of the transcript initiation site, to suggest a ribosomal shunt model for translation of ORF1. Knowledge of the promoter and transcript initiation sites will be valuable for the development of an infectious clone and ultimately for completion of Koch's postulates.

2. RESULTS

2.1. The strength of the GVCV promoter is comparable to the CaMV 35S promoter

An analysis of the GVCV nucleotide sequence revealed two potential TATA boxes that could be used to initiate transcription of the GVCV pregenomic transcript: TATA1 (beginning at nt 7,539) and TATA2 (beginning at nt 7,131) (Fig. 2-1, Fig. 2-2). TATA1 is located within the large intergenic region, between ORF3 and the tRNA binding site, whereas TATA2 is found within GVCV ORF3 near its 3' end. Furthermore, the large intergenic region contains four short ORFs (sORFs) (Fig. 2-2). Multiple sORFs are found within the leader sequence of the pregenomic transcript of

6712 ATGGAAGGATGGGGAGGAATCTGCAAATGGAAGAACTCAAAGGGGGAGTC
6762 CAAAGGCAAGAATCTGAGCGGTGCTTACGCCAGCGGAAAATTCCCAACAG
6812 TCAAATCCACCATAGATGCTGAAATTTATGCAGTCATGGCATCCCTGGAG
6862 AATTTTAAGATTTACTATCTTGATAAGCGGGAAATCACCATTAGAACTGA
6912 CTGCCAGGCCATAATCAGCTTCTATGATAAGACGGCTATCAAGAAACCCA
6962 GCAGAGTTCGCTGGATTAATTTTTGTGATTACATCACTAACACAGGGATT
7012 AAAGTCCAGTTTGAACATATAAAAGGCCAAGATAATCAGCTTGCAGACCA
7062 GCTCTCAAGGCTTGCCCAGAATGTCTGCGCAATCCAGGTCATCCCTGAAT
7112 CAGCCCATGAAGCCCTCAG**TATAA**TTCTAGAACAAGACTGCACGGCCCAA
7162 GAATTAATGGCCCAGTTCAACTCTATGCTTCAGGCAAACCTCAGGCTCAA
7212 CCATGGAAGGCCCAACACTACTTGGTACTCAAGGACCAAGCCCAAGAAAT
7262 CCAAAGCCCGTAAGCAAGCCCAAGTCCAGCTACGCTTTGACGTAAGCAAT
7312 GACGACTAGGGATAATAATGGAGGAATCTTGTAAGGACAGCACATGGTCC
7362 TTCTTTCCTCTTTTCTTTTGTAATTTTTGTCTTCTTGTGTCGGCAACCGC
7412 TCCTTTTGTAAAGAGGAATCTGCTTTTGAGCTGTCGATGGGGCCCAATGT
7462 GTGTACCCGAGCTCTAAAAGTAACTTACCTCTAGTTGCTTTTGTAAACCT
7512 TAGTTAAGTTTGTTTTCCTTTCTCCCC**TATAAA**AGGGAGCCCCTCAGTTG
7562 TAAGAAGGCATCGAACAGAGCAATACCTCTGAGCGCTTCCTTCTCTCTAG
7612 ATTTCAAGTTTTCTTGTATCTTTCCAGTTCCAGTGTTCTTAATGCAATTT
7662 GAAGTCTTCATACTCTATGTCATTCTGTTCATAGTTCTTTTCCGCTACCT
7712 ATACTCTGTGATCCAAATTTTTAATTTGTGATCTGTTTAATCTGGTATCA
10 GAGCTCCAGTTTCAAATCTGGGAAATCTCTACAATTATTCCTTCAAGATT
60 ATGATGAGGAACTAACTCTCATAATCGTGTAGGGAATCGTTAGTAGGATC
110 TCAGAACAAGGTTCTTATCCCCTCATACTACTGATTCTGGTATATAGGCT
160 GGAAACACGACACTGTTACGATCCCACTTCTGTTGGAGTGGTAGTAGCCC
210 GTTGTGAGACAACGCCACGTACCATTTTCAGTTTTCCTAGCCCAAATCCC
260 CATGAACAGAACTCCCACGGTCAATAAGTTTCAACAGGATCCCTAGCCCA
310 ACAATACTGAAAGTCCTAGGACAGGCTGCGACGCGAAGTACCACCAGTTC
360 AGGCGATGCTGTTCCGCCGATTGTTTGTGGGAAAACTGCAGTAGGAGAGG
410 ACGGACAACTATTCAAGGGAACGGAACCTGGAGACACCGGCCGAGTTCTT
460 AGTAAGCGGTTCAAGGAAGGAGACTGATGCAAAGTATAGAACAACAACAG
510 TTTGAGGCGGAGATAGAA

Fig.2-1 GVCV sequences between nucleotides 6,712 and 527. Putative TATA boxes are highlighted in bold and underlined. The nucleotide sequences for sORF A, B, and C are in blue, purple, and red, respectively, whereas the tRNA primer binding site is in green. The beginning of the tRNA primer binding site, immediately after

nucleotide 7,762, corresponds to the beginning of the GVCV sequence. The sequence for ORF1, beginning at nucleotide 485, is underlined.

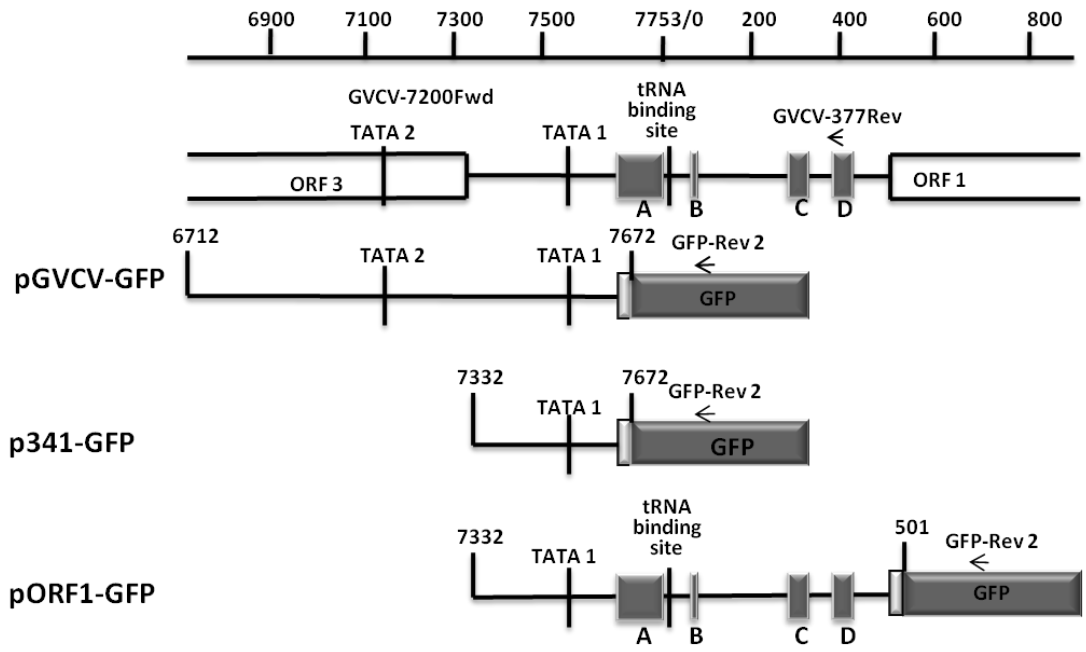

Fig.2-2 Genomic structure of GVCV, showing three opening reading frames and tRNA binding site. Top: The structure of GVCV intergenic region between ORF1 and ORF 3, showing two TATA boxes (TATA1, TATA2), four small open reading frames (sORFs) A, B, C, D, and T-RNA binding site. Bottom: Fragments cloned into plasmid pGVCV-GFP, p341-GFP, and pORF1-GFP, separately.

all of the caulimoviruses (Baughman & Howell, 1988; Fütterer *et al.*, 1988; Pooggin *et al.*, 2006). Consequently, to identify the putative GVCV promoter region, we amplified a GVCV segment that included both TATA1 and TATA2, as well as the start codon of sORF A, which was fused in-frame with GFP to form pGVCV-GFP (Fig. 2-2).

To determine whether the large intergenic region of GVCV contained promoter activity, we compared the strength of a putative GVCV promoter to the *Cauliflower mosaic virus* (CaMV) 35S promoter. The plasmids pGVCV-GFP and p35S-GFP (Angel *et al.*, 2011) were transformed into *Agrobacterium tumefaciens* strain AGL1 and agroinfiltrated into young leaves of *N. benthamiana*. To reduce leaf-to-leaf variation in response to agroinfiltration, all constructs were agroinfiltrated into leaf panels on a single leaf, and at least three leaves were included in each test. Leaves were collected at 3 days after infiltration (dai), and the expression level of GFP was assessed by illumination with a UV lamp and quantified by a GFP-specific ELISA. At 3 dai, illumination with the UV lamp indicated no visual difference between expression of GFP from pGVCV-GFP and p35S-GFP infiltrated leaves (Fig. 2-3A). However, ELISA data showed that the strength of the GVCV full-length promoter was significantly higher than the 35S promoter (Fig. 2-3B), $n = 3$, $p<0.01$). The agroinfiltration assay and quantification of GFP by ELISA was repeated in two additional tests and in each case the GVCV promoter was significantly stronger than the 35S promoter.

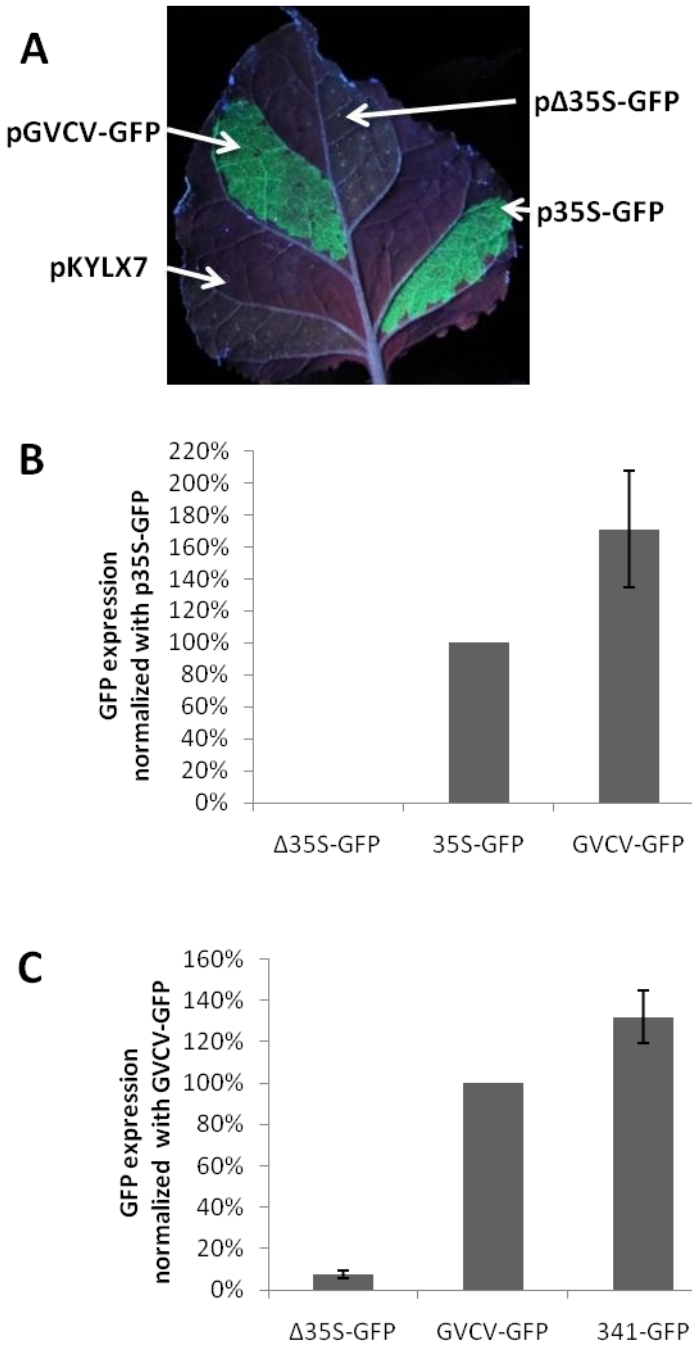

Fig.2-3 GFP expression reveals the activity of promoters. (A) One representative picture taken 3 days after infiltration showing GFP fluorescence under UV light. (B) GFP ELISA comparing the strength of GVCV full length promoter and **CaMV** 35S promoter. GFP expression was normalized with p35S-GFP (C) GFP

ELISA comparing strength of GVCV full length promoter and GVCV 341 promoter. GFP expression was normalized with pGVCV-GFP.

To further define the GVCV promoter, a second recombinant plasmid was made that contained only the TATA1 box (Fig. 2-2, p341-GFP) and its expression was compared to pGVCV-GFP. As in the previous test, both constructs along with a negative control were agroinfiltrated into separate leaf panels on the same leaf and multiple leaves were evaluated in each test. This experiment showed that the TATA1 box was sufficient to drive expression of GFP and that GFP expression of GFP from p341-GFP was significantly higher than that from pGVCV-GFP (Fig. 2-3C, n=3, $p<0.01$). This test was repeated three times and results were confirmed. Given the strength of this promoter element and its position in the GVCV genome sequence relative to other caulimoviruses, we concluded that TATA1 constituted the major promoter for GVCV.

2.2. Identification of the initiation and termination sites for the major GVCV transcript present in infected grape tissues

All caulimoviruses produce a terminally redundant RNA that has a dual role for expression of viral proteins and for replication during reverse transcription. To further characterize the transcription and replication strategies of GVCV, we sought to identify the initiation and termination sites of the transcript generated from the GVCV promoter.

To identify the 5' end of the transcript expressed from the GVCV promoter, pGVCV-GFP was infiltrated into *N. benthamiana* leaves and total RNA was isolated

at 3 dai, which was then used as a template for a 5'RACE reaction. The 5' RACE RT-PCR was performed with a reverse primer that corresponded to a sequence within GFP (Fig. 2-2, primer GFP-Rev2) and a forward primer containing an adaptor sequence that was supplied by the RACE kit. A single PCR product of approximately 400 bp was generated from the 5' RACE reaction (data not shown) and the DNA band was cloned into the *E. coli* vector pGEM-T Easy. Fourteen clones were sequenced to determine the transcript initiation site. The sequencing results revealed that transcription in *N. benthamiana* was initiated in eight of fourteen clones at nucleotide 7,571, which placed the initiation site 27 nucleotides downstream from the TATA box (Fig. 2-5). In the remaining six clones, the transcript was initiated at nucleotide 7,568 (in two clones), at nucleotide7,574 (in three clones), and at 7,578 (in one clone). We concluded that the preferred transcript initiation site was at nucleotide 7,751.

To investigate whether the same transcript initiation site was used in GVCV-infected grape tissue as in the transient expression assay in *N. benthamiana*, a second 5' RACE reaction was performed on total RNA isolated from GVCV-infected grape leaves. In this reaction we used the reverse primer GVCV-377Rev. (Fig. 2-2), and a single PCR product was generated that had an approximate size of 610 bp (Fig. 2-4A). In an analysis of three clones, the transcript was initiated at 7,571 in two and 7,574 in one, confirming that the same transcript initiation sites were used in GVCV infected grape as in the transient expression assays in *N. benthamiana*.

To identify the 3' end of the major GVCV present in GVCV-infected grape

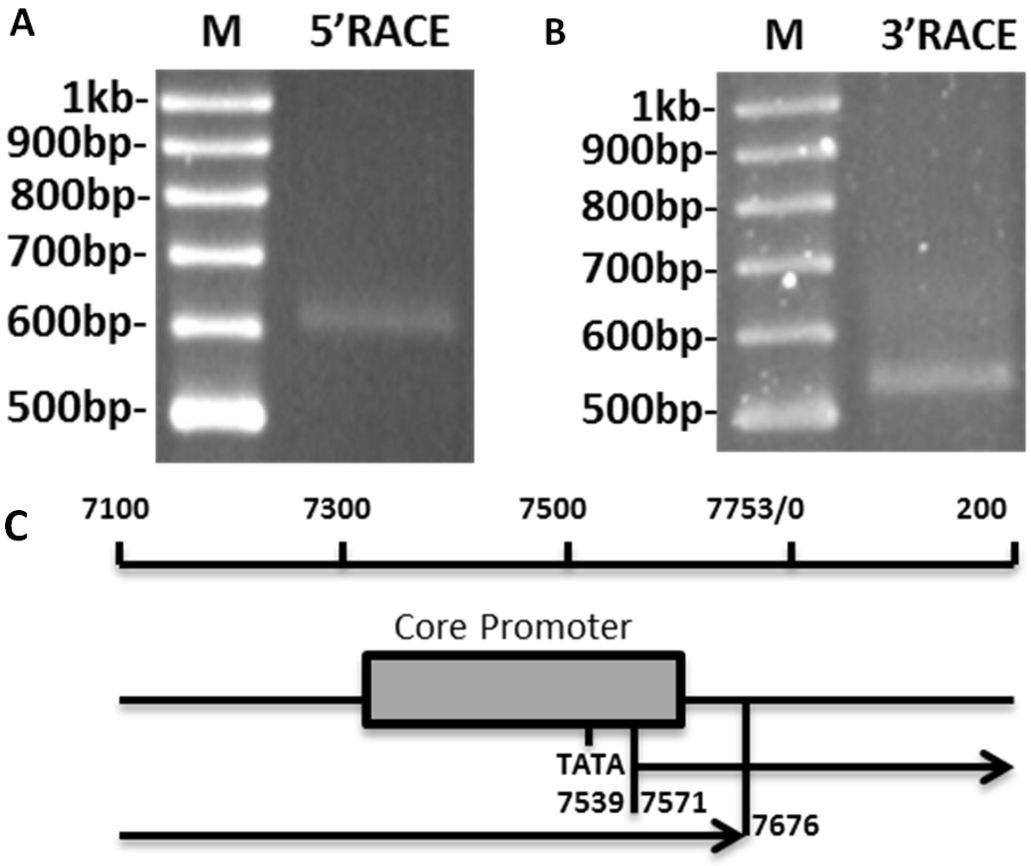

Fig.2-4 5' RACE and 3' RACE PCR for GVCV- infected grapevine. (A) 5' RACE PCR for GVCV- infected grapevine using universal primer mix (UPM) and GVCV-specific primer GVCV-377Rev. (B) 3' RACE PCR for GVCV- infected grapevine using UPM and GVCV 7200Fwd. M:100bp marker (Invitrogen). (C) Diagram illustrating the position of the core promoter, TATA box, transcript initiation site at 7571 and transcript termination site at 7676. Arrows indicate direction of transcription.

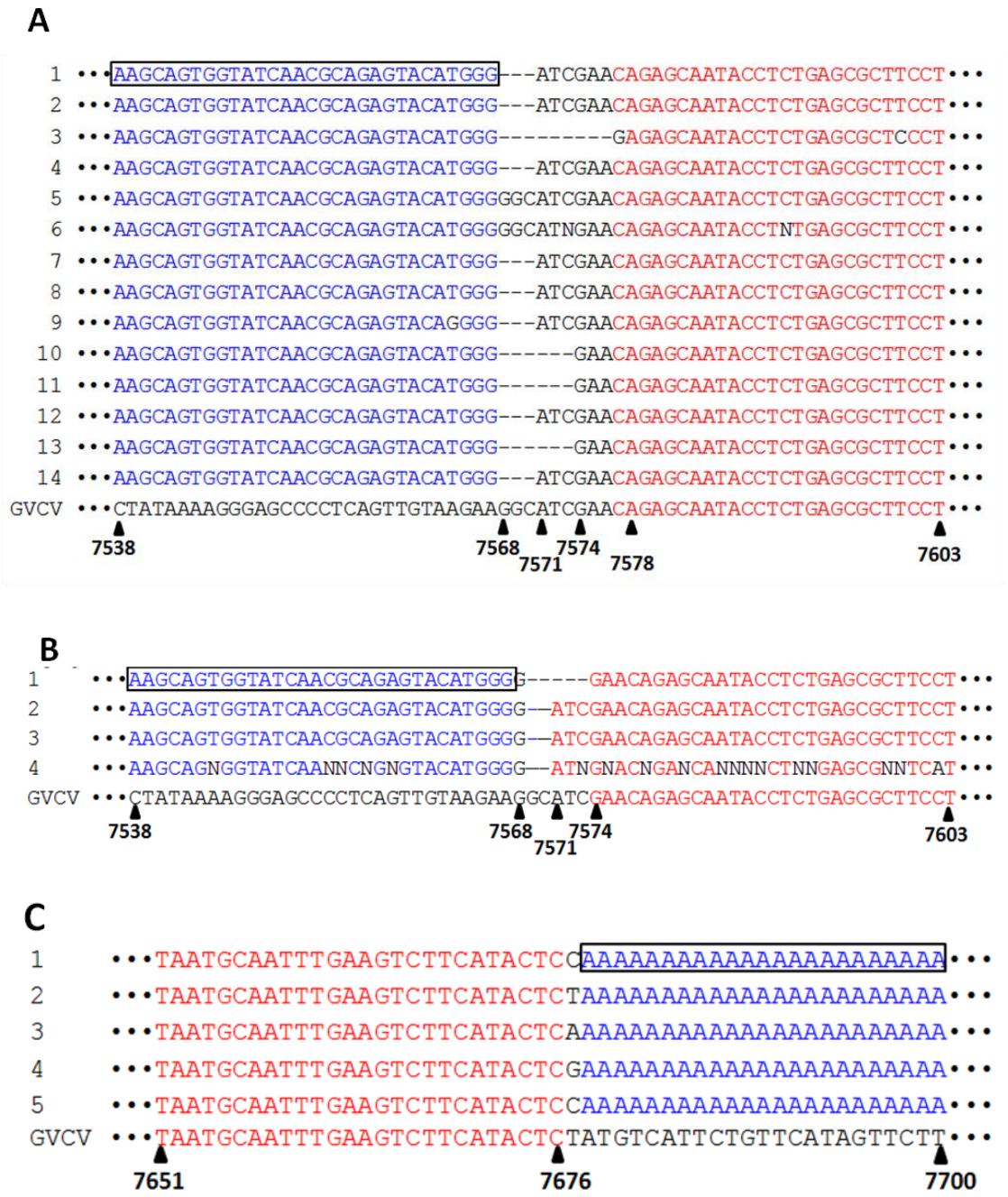

Fig.2-5 Sequence alignment. (A) Sequencing data for 5'RACE performed in pGVCV-GFP infiltrated *N. benthamiana* leaves. 14 clones were sequenced individually. Box indicates 5' adaptor. (B) Sequencing data for 5'RACE performed in GVCV infected grapevine leaves. Box indicates 5' adaptor. (C) Sequencing data for 3'

RACE performed in GVCV infected grapevine leaves. Box indicates polyA tail. Blue indicates sequences from RACE linker or poly A tail, red indicates sequences from GVCV transcripts, and black indicates unmatched or unknown sequences.

leaves, 3’ RACE was performed only on total RNA isolated from GVCV infected grapevine. For the 3' RACE reaction, the forward primer corresponded to the GVCV sequence at nucleotides 7,200-7,227, and this reaction generated a band approximately 550bp in size (Fig. 2-4B). This PCR band was cloned into pGEM-T Easy and five clones were sequenced to determine the 3' termination site. Nucleotide sequencing showed that the GVCV transcript was terminated at 7,676 bp in all four clones. Taken together, the transcript initiation at 7,571 and termination at 7,676 would yield a terminal redundancy of 105 nucleotides in the GVCV mRNA (Fig. 2-4C).

2.3. Influence of sORFs in the leader sequence on expression of ORF1

Our studies showed that transcription from the major GVCV promoter is initiated at or near nucleotide 7,571. The transcript initiated at this site would contain four sORFs in its leader sequence with predicted sizes of 5 to 30 codons (Fig. 2-1, Fig. 2-2). As with other caulimoviruses, it is expected that these sORFs would have an inhibitory effect on translation of the ORF1 product (Baughman & Howell, 1988; Futterer *et al.*, 1989; Pooggin *et al.*, 2006).

To examine the effect of the sORFs in the leader sequence on expression of ORF1, we fused the GFP coding sequence in frame to the third codon of ORF1 to create the construct, pORF1-GFP (Fig. 2-2) and compared the level of GFP protein transiently expressed from pORF1-GFP to p341-GFP.Both of these constructs were

agroinfiltrated into leaf panels of the same *N. benthamiana* leaf and GFP expression was assessed by illumination with a UV lamp and quantified by GFP ELISA. At 3 dai, expression of GFP from pORF1-GFP was clearly less intense than GFP expression from p341-GFP (Fig. 2-6A), and the GFP ELISA showed that expression of GFP in pORF1-GFP was approximately one fifth that of GFP expressed from p341-GFP (Fig. 2-6B).

Translation of the ORF1-GFP fusion protein might originate from an unspliced transcript, as occurs with CaMV (Fütterer *et al*., 1993), or it might be translated from a spliced mRNA. To investigate whether splicing occurs within sequences upstream of ORF1, we agroinfiltrated the construct pORF1-GFP into *N. benthamiana* leaves, isolated total RNA, and utilized a 5' RACE to analyze GVCV transcripts. The primer used in the 5'RACE was GVCV-377 Rev, and the assay yielded PCR bands that 947 bp and approximately 1,200 bp (Fig. 2-6C). We cloned the 947 bp band into pGEM-T Easy, determined its sequence, and confirmed that it represented the full-length transcript; no splicing event was detected. Although we tried several times, we were unable to clone the 1200 bp band. However, since it was larger than the 947 bp full-length transcript, we considered that it was unlikely to represent a spliced product.

The leader sequence of the pregenomic RNA caulimoviruses is able to fold into an elaborate stem-loop structure, which allows ribosomes that enter at the 5' end of the RNA to bypass most of the leader and the sORFs to gain access to ORF1. This

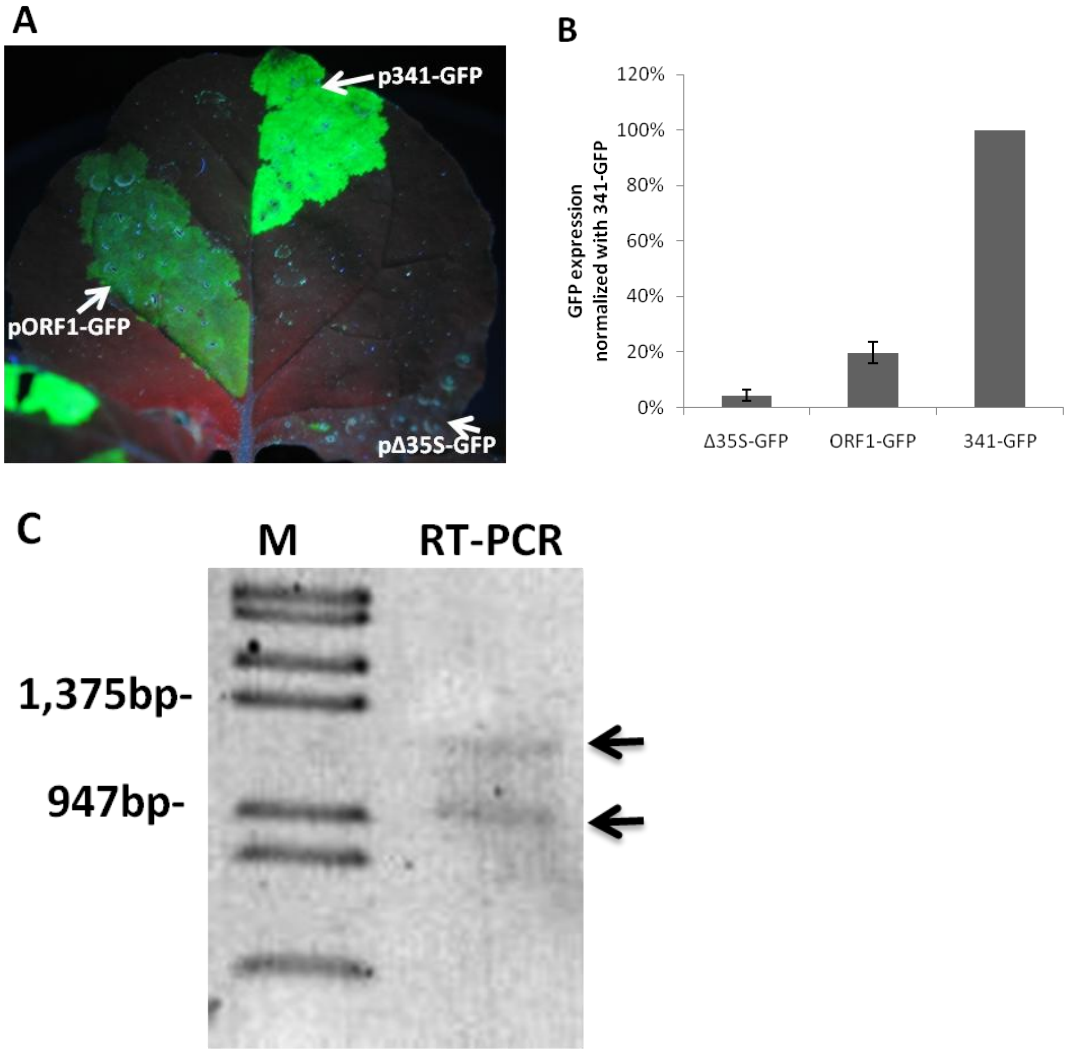

Fig.2-6 Effects of sORFs in downstream ORF expression. (A) Expression of GFP, taken 3 days after infiltration. (B) GFP ELISA comparing GFP expression of pORF1-GFP and p341-GFP. Bars illustrate average and standard deviation. GFP expression was normalized with p341-GFP. (C) 5' RACE of pORF1-GFP infiltrated benthamiana. Arrows indicate two weak bands.

mechanism of translation has been described as a ribosomal shunt (Fütterer *et al.*, 1988; Fütterer *et al.*, 1993). A comparison of the leader sequences of present in the pregenomic RNAs of fourteen caulimoviruses revealed that in each case, the stem loop structure led to the juxtaposition of the first sORF and the first long ORF (Pooggin *et al.*, 1999). To determine whether the GVCV leader sequence was able to form into a stem loop structure, we utilized the RNA folding computer program mFold. The input sequence consisted of the GVCV nucleotide sequences present in transcript of pORF1-GFP, from the mRNA initiation site at 7,571 through the start codon and the first five codons of ORF1, ending at nucleotide 502.

The pregenomic RNA of GVCV was folded into a stable stem look structure with four stem-loop structures (Fig. 2-7, stems 1-4). Stem 1was formed upstream from the start codon of sORF1. This stem loop was also predicted to occur when GFP was fused to sORF1 (i.e. p341-GFP, data not show), but it clearly did not have an inhibitory effect on the expression of GFP fused to sORF1. We considered that the branched, stem-loop structure that contains stems 2, 3, and 4 forms a very stable structure that could allow for a shunt mechanism. In this structure, ribosomes would terminate translation of sORF1, traverse 14 nucleotides to the base of the stem-loop structure and be shunted to the start codon of ORF1.

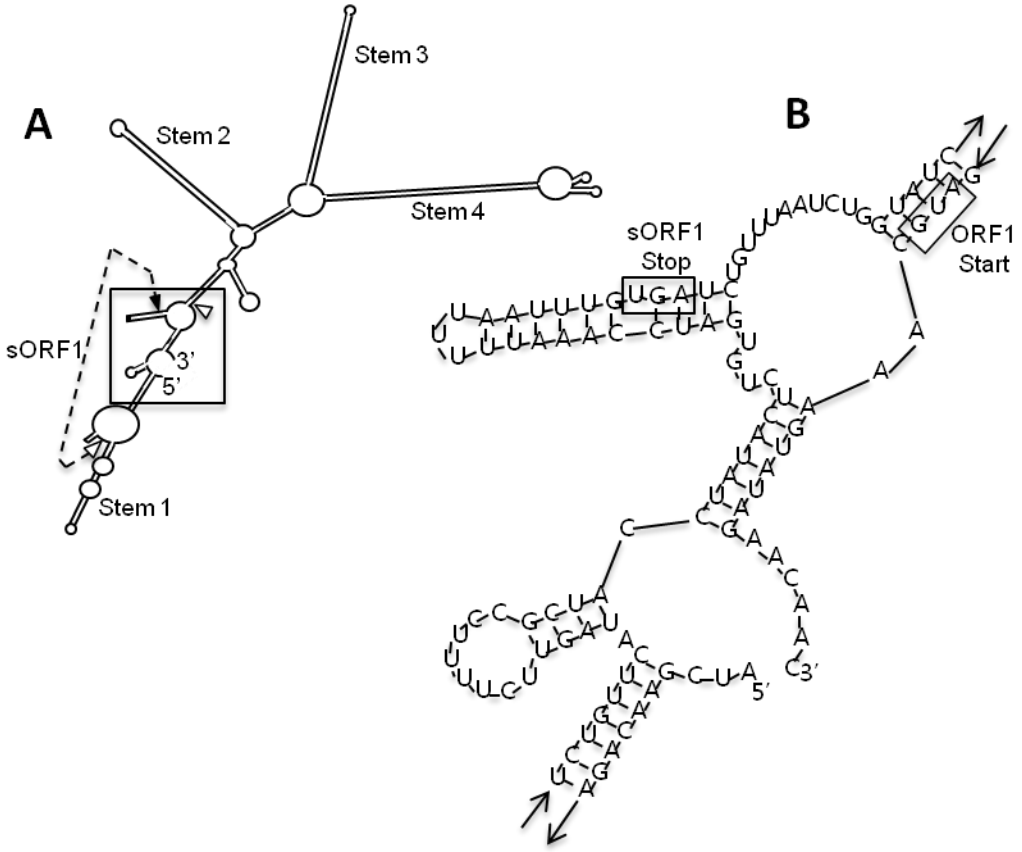

Fig.2-7 Predicted structure of leader RNA using the program mFold. Sequences between the transcription initiation site (5,771) and the first five codons of ORF1, (ending at nucleotide 502) were submitted to the mFold server. (**http://mfold.rna.albany.edu/?q=mfold**)(Zuker, 2003)

3. DISCUSSION

An inspection of the nucleotide sequence immediately upstream from the transcript terminus indicated that GVCV does not contain a canonical mRNA polyadenylation poly(A) signal (5'AAUAAA3') (Fig. 2-8). The poly(A) signal is highly conserved in mammals, but is much less prevalent in plants. A survey of transcripts of Arabidopsis revealed that only approximately 10% of the transcripts contained a poly(A) signal in the predicted location (Loke *et al.*, 2005). Amongst the caulimoviruses, the poly(A) signal is much more common; a well-defined poly(A) signal can be found in many of the sequences of the *Caulimoviridae*, including CaMV and CoYMV, the type species for the genera *Caulimovirus* and *Badnavirus*, respectively (Medberry *et al.*, 1990; Sanfaçon *et al.*, 1991). Furthermore, the presence of a poly(A) signal has been used to approximate the position of the 3' end of a number of caulimovirus sequences in the absence of experimental evidence for the 3' end (Pooggin *et al.*, 1999). However, even with caulimoviruses the poly(A) signal cannot always be identified. For example, a poly(A) signal cannot be located in the sequence of BSV GF, even though it is found in BSV OL (Fig. 2-8). Therefore, it may not be surprising that GVCV lacks a clear poly (A) signal.

Next Generation sequencing techniques have greatly facilitated the discovery and characterization of new plant virus genomes at the nucleotide sequencing level. For example, GVCV was identified through deep sequencing of siRNAs and its genomic sequence was completed through amplification of its viral DNA by PCR and

cloning into bacterial plasmids (Zhang *et al*., 2011). PCR has also been used to characterize GVCV populations in infected grapevines from several Midwest states in the U.S (Zhang *et al*., 2011). New badnavirus genomic sequences that have been characterized in the past few years include *Sweet potato badnavirus B* (Kreuze *et al*., 2009), *Sweet potato badnavirus A* (Mbanzibwa *et al*., 2011), *Gooseberry vein banding virus* (Xu *et al*., 2011), *Fig badnavirus 1* (Laney *et al*., 2012), *Rubus yellow net virus* (Kalischuk *et al*., 2013), and *Piper yellow mottle virus* (Hany *et al*., 2014), as well as GVCV (Zhang *et al*., 2011). However, little is known about the genome organization of these viruses beyond the positioning of the open reading frames. To further annotate the genome structure of GVCV, we have delimited the boundaries of the major promoter, identified the 5' and 3' ends of the GVCV pregenomic transcript, and quantified the effect of the leader sequence of the pregenomic transcript on expression of GVCV ORF1.

We used agroinfiltration of *N. benthamiana* to identify the GVCV promoter, as well as the 5' and 3' ends of the GVCV pregenomic transcript. Although *N. benthamiana* does not appear to be a host for GVCV, there are strong precedents for the use of nonhosts for the characterization of caulimovirus promoters. For example, CoYMV infects the monocot *Commelina diffusa*, yet its promoter was initially characterized in *N. tabacum* and maize (Medberry *et al*., 1992). Similarly, the CaMV 35S promoter was characterized in *N. tabacum* (Odell *et al*., 1985), which cannot support infections of CaMV. It is also important to note that the transcript initiation

sites for the GVCV promoter were identical in agroinfiltrated *N. benthamiana* leaves and GVCV-infected grape leaves, a demonstration that the host transcriptional machinery in these two plant species recognizes the same elements.

We found that the GVCV promoter was significantly stronger than the CaMV 35S promoter. This is intriguing because GVCV appears to be a low titer virus and limited bacilliform virions were observed under electron microscope (Schoelz and Qiu, unpublished). By contrast, CaMV virions are easily detected in infected plant tissues (Cecchini *et al*., 1997; Fujisawa *et al*., 1967; Rubio *et al*., 1968; Shalla & Petersen, 1980). Some Badnavirus promoters have been shown to exhibit tissue specificity. For example, the promoter of CoYMV is specific to vascular and reproductive tissues, even though it is comparable in strength to the CaMV 35S promoter (Medberry *et al*., 1992). The promoter of *Rice tungro baciliform virus* (RTBV) is phloem-specific (Bhattacharyya-Pakrasi *et al*., 1993). The *Sugarcane bacilliform badnavirus* (SCBV) promoter functions in both monocots and dicots, and it has different tissue-specificity in oat, barley, and wheat (Al-Saady *et al*., 2004; Braithwaite *et al*., 2004; Schenk *et al*., 1999; Tzafrir *et al*., 1998). Given that the expression pattern for the GVCV promoter was similar to the CaMV 35S promoter (Fig. 2-2), the GVCV promoter does not appear to exhibit tissue specificity. It may be that the potential secondary structures formed by the viral pregenomic RNA are an attractive target for posttranscriptional gene silencing, which might directly limit the accumulation of the products of reverse transcription and ultimately, the virions in

plant tissues.

With the identification of the 5' end of the pregenomic RNA, it also became possible to predict the stable stem-loop structure that is an essential element of the ribosomal shunt mechanism. Pooggin and coworkers (2006) have suggested that the shunt mechanism involves the translation of the first sORF in the leader sequence; ribosomes terminate translation of the sORF a few nucleotides upstream from the base of a stable stem-loop structure and bypass the remaining sORFs present in the stem-loop structure to initiate translation at ORF1. An inspection of the stem-loop structure formed by the pregenomic RNA of GVCV demonstrates that these elements are conserved in the leader sequence of the GVCV pregenomic RNA. Fig. 2-7 illustrates the juxtaposition of the stop codon of GVCV sORF1 with the start codon of GVCV ORF1. Although the formation of a stable stem-loop structure has been predicted to be conserved in all plant pararetroviruses (Pooggin *et al.*, 1999), the expression of the first true open reading frame in the viral genome has only been thoroughly examined for CaMV and RTBV (Fütterer *et al*., 1993; Fütterer *et al*., 1996; Pooggin *et al*., 2001; Pooggin *et al*., 1999; Pooggin *et al*., 2000; Pooggin *et al*., 2006). In the case of GVCV we showed that an ORF1-GFP fusion was expressed in agroinfiltration assay at approximately 20% of the level found for the sORF1-GFP fusion, a demonstration that ORF1 can be efficiently translated from the GVCV pregenomic RNA. Our study also illustrates the versatility of the agroinfiltration assay for characterization of caulimovirus promoters, transcripts and expression of ORFs.

4. METHODS

4.1. Plasmid Construction

To identify the GVCV promoter and the expression strategy for ORF1, we created four plasmids: pGVCV-GFP, p341-GFP, pORF1-GFP, and pΔ35S-GFP. In each case, we utilized the plasmid GVCV 6192-1935 as a template for amplification of GVCV sequences (Zhang *et al*., 2011). PCR primers used for each plasmid are listed in Table 2-1. Amplified fragments were ligated with pGEM-T Easy vector (pGEM®-T Easy Vector System I, Promega, Madison, WI) according to the manufacturer's instructions. Once cloned in pGEM-T Easy, the GVCV nucleotide sequences were determined to verify that the sequence matched the published sequence (Zhang *et al*., 2011) and that no mutations had occurred during the PCR procedure. The GVCV sequences were subsequently excised from pGEM-T Easy with the restriction enzymes EcoRI and HindIII and moved into plasmid p35S-GFP (Angel *et al*., 2011). This step replaced the 35S promoter of pKYLX7 with the putative GVCV promoter sequences. p35S-GFP was derived from the Agrobacterium tumefaciens binary vector pKYLX7 (Schardl *et al*., 1987), with insertion of GFP into the XhoI and SacI sites (Angel *et al*., 2011). To make the clone pΔ35S-GFP, p35S-GFP was digested by EcoRI and HindIII and then re-circularized by ligation. All clones were mobilized into A. tumefaciens strain AGL1 (Lazo *et al*., 1991) by electroporation. Transformants were selected on Luria Bertani (LB) medium

supplemented with kanamycin (50μg/ml).

4.2. Agroinfiltration

The agroinfiltration procedure has been described in Angel *et al*. (2011). Briefly, Agrobacterium cultures were grown in 20ml LB liquid media to stationary phase, then collected by low speed centrifugation and resuspended in 10 ml agroinfiltration media (for 100 ml infiltration media, 0.39g MES-hydrate, 2g sucrose, and 1g glucose, pH adjusted to 5.4 with KOH). To induce T-DNA transfer, 100ul 0.2M acetosyringone (solvent: N-dimethyformamide) was added and the culture incubated at 28℃ for an additional 12 hours. Before agroinfiltration, the OD600 was adjusted to 1.5. GFP expression in *N. benthamiana* leaves was examined in a darkroom at 3 dai with a Blak Ray Long Wave Ultraviolet Lamp (Upland CA).

4.3. GFP ELISA

N. benthamiana leaf tissue agroinfiltrated with GVCV promoter constructs and controls was collected and weighed at 3 dai. Tissues were ground with 0.05M sodium phosphate buffer (pH=7) (10μl buffer per 10mg tissue) to release proteins and the concentration of total proteins was assessed by a Bradford assay (Bio Rad, Hercules CA). The ELISA was performed using GFP ELISA kit (Cell Biolabs Inc, San Diego, CA) following the manufacturer's instructions. Total protein concentrations were initially adjusted to 1μg/ml, and then further diluted 1,000 times, 5,000 times, or

50,000 times for the absorbance values to fall within the GFP standard curve that ranged from 15.6 to 1,000 pg/ml. GFP protein values for the GVCV promoters were normalized against the GFP expression level obtained with the 35S-GFP control. Figures were generated by Microsoft Excel.

4.4. 5' and 3' RACE

Total RNA was isolated from pGVCV-GFP and pORF1-GFP infiltrated *N. benthamiana* leaves (3dai) using the RNeasy Mini Kit (Qiagen, Germantown MD) following the manufacturer's instructions. For RNA isolation from grape leaves, we used the RNA isolation protocol described in Reid *et al*. (2006), which included CTAB to counteract the high content of secondary metabolites. 5'RACE and 3'RACE were performed using the SMARTer^{TM} RACE cDNA Amplification Kit (Clontech, Mountain View, CA) using a combination of GVCV-specific primers (Fig. 2-5) and the Universal Primer A Mix (provided by the kit). DNA products amplified in the RACE reactions were cloned into pGEM-T Easy and the nucleotide sequences of the inserts were determined in the DNA Core Facility at the University of Missouri-Columbia.

4.5. mFold

RNA structured was predicted by the mFold Web Server (http://mfold.rna.albany.edu/?q=mfold) (Zuker, 2003). GVCV sequences included in

the folding program began at the GVCV 5' transcription initiation site and ended at the fifth codon of ORF 1. Eleven predicted folding structures were downloaded from mFold Web Server, and a representative structure is presented in Fig. 2-7.

REFERENCE

Al-Saady, N. A., Torbert, K. A., Smith, L., Makarevitch, I., Baldridge, G., Zeyen, R. J., Muehlbauer, G. J., Olszewski, N. E. & Somers, D. A. (2004). Tissue specificity of the sugarcane bacilliform virus promoter in oat, barley and wheat. *Molecular breeding* **14**, 331-338.

Angel, C. A., Hsieh, Y. C. & Schoelz, J. E. (2011). Comparative analysis of the capacity of tombusvirus P22 and P19 proteins to function as avirulence determinants in *Nicotiana* species. *Molecular Plant-Microbe Interactions* **24**, 91-99.

Baughman, G. & Howell, S. H. (1988). *Cauliflower mosaic virus* 35 S RNA leader region inhibits translation of downstream genes. *Virology* **167**, 125-135.

Bhattacharyya-Pakrasi, M., Peng, J., Elmer, J. S., Laco, G., Shen, P., Kaniewska, M. B., Kononowicz, H., Wen, F., Hodges, T. K. & Beachy, R. N. (1993). Specificity of a promoter from the rice tungro bacilliform virus for expression in phloem tissues. *The Plant Journal* **4**, 71-79.

Braithwaite, K. S., Geijskes, R. J. & Smith, G. R. (2004). A variable region of the *Sugarcane bacilliform virus* (SCBV) genome can be used to generate promoters for transgene expression in sugarcane. *Plant cell reports* **23**, 319-326.

Cecchini, E., Gong, Z., Geri, C., Covey, S. N. & Milner, J. J. (1997). Transgenic Arabidopsis lines expressing gene VI from *Cauliflower mosaic virus* variants exhibit a range of symptom-like phenotypes and accumulate inclusion bodies. *Molecular plant-microbe interactions* **10**, 1094-1101.

Dasgupta, I., Hull, R., Eastop, S., Poggi-Pollini, C., Blakebrough, M., Boulton, M. I. & Davies, J. W. (1991). *Rice tungro bacilliform virus* DNA independently infects rice after Agrobacterium-mediated transfer. *Journal of General Virology* **72**, 1215-1221.

Fütterer, J., Gordon, K., Bonneville, J., Sanfaçon, H., Pisan, B., Penswick, J. & Hohn, T. (1988). The leading sequence of caulimovirus large RNA can be folded into a large stem-loop structure. *Nucleic acids research* **16**, 8377-8390.

Fütterer, J., Gordon, K., Pfeiffer, P., Sanfacon, H., Pisan, B., Bonneville, J. M. &

Hohn, T. (1989). Differential inhibition of downstream gene expression by the *Cauliflower mosaic virus* 35S RNA leader. *Virus genes* **3**, 45-55.

Fütterer, J., Kiss-László, Z. & Hohn, T. (1993). Nonlinear ribosome migration on *Cauliflower mosaic virus* 35S RNA. *Cell* **73**, 789-802.

Fütterer, J., Potrykus, I., Bao, Y., Li, L., Burns, T. M., Hull, R. & Hohn, T. (1996). Position-dependent ATT initiation during plant pararetrovirus *Rice tungro bacilliform virus* translation. *Journal of Virology* **70**, 2999-3010.

Fujisawa, I., M, R., Matsui, C. & A, Y. (1967). Intracellular appearance of *Cauliflower mosaic virus* particles. *Phytopathology* **57**, 1130-&.

Guo, Q., Honesty, S., Xu, M. L., Zhang, Y., Schoelz, J. & Qiu, W. (2014). Genetic Diversity and Tissue and Host Specificity of *Grapevine vein clearing virus*. *Phytopathology* **104**, 539-547.

Hany, U., Adams, I., Glover, R., Bhat, A. & Boonham, N. (2014). The complete genome sequence of *Piper yellow mottle virus* (PYMoV). *Archives of Virology* **159**, 385-388.

Huang, Q. & Hartung, J. S. (2001). Cloning and sequence analysis of an infectious clone of *Citrus yellow mosaic virus* that can infect sweet orange via Agrobacterium-mediated inoculation. *Journal of General Virology* **82**, 2549-2558.

Kalischuk, M. L., Fusaro, A. F., Waterhouse, P. M., Pappu, H. R. & Kawchuk, L. M. (2013). Complete genomic sequence of a *Rubus yellow net virus* isolate and detection of genome-wide pararetrovirus-derived small RNAs. *Virus research* **178**, 306-313.

Kreuze, J. F., Perez, A., Untiveros, M., Quispe, D., Fuentes, S., Barker, I. & Simon, R. (2009). Complete viral genome sequence and discovery of novel viruses by deep sequencing of small RNAs: a generic method for diagnosis, discovery and sequencing of viruses. *Virology* **388**, 1-7.

Laney, A. G., Hassan, M. & Tzanetakis, I. E. (2012). An integrated badnavirus is prevalent in fig germplasm. *Phytopathology* **102**, 1182-1189.

Lazo, G. R., Stein, P. A. & Ludwig, R. A. (1991). A DNA transformation–competent Arabidopsis genomic library in Agrobacterium. *Nature Biotechnology* **9**, 963-967.

Loke, J. C., Stahlberg, E. A., Strenski, D. G., Haas, B. J., Wood, P. C. & Li, Q. Q. (2005). Compilation of mRNA polyadenylation signals in Arabidopsis revealed a new signal element and potential secondary structures. *Plant physiology* **138**, 1457-1468.

Lunden, S., Meng, B., Avery, J. & Qiu, W. (2009). Characterization of a grapevine vein-clearing complex on Chardonnay. *Eur J of Plant Pathol*. **126**, 135-144.

Mbanzibwa, D., Tairo, F., Wandu, G., Kullaya, A. & Valkonen, J. (2011). First report of *Sweet potato symptomless mastrevirus 1* and *Sweet potato badnavirus A* in sweet potatoes in Tanzania. *Plant Disease* **95**, 225.

Medberry, S. L., Lockhart, B. & Olszewski, N. E. (1990). Properties of Commelina yellow mottle virus's complete DNA sequence, genomic discontinuities and transcript suggest that it is a pararetrovirus. *Nucleic Acids Research* **18**, 5505-5513.

Medberry, S. L., Lockhart, B. & Olszewski, N. E. (1992). The Commelina yellow mottle virus promoter is a strong promoter in vascular and reproductive tissues. *The Plant Cell* **4**, 185-192.

Migliori, A. & Lastra, R. (1978). Study of viruses on Commelina diffusa Burm. in Guadeloupe. *Annual Phytopathology* **10**, 467-477.

Odell, J., Nagy, F. & Chua, N. (1985). Identification of DNA sequences required for activity of the *Cauliflower mosaic virus* 35S promoter. *Nature* **313**, 810-812.

Pooggin, M. M., Fütterer, J., Skryabin, K. G. & Hohn, T. (2001). Ribosome shunt is essential for infectivity of *Cauliflower mosaic virus*. *Proceedings of the National Academy of Sciences* **98**, 886-891.

Pooggin, M. M., Futterer, J., Skryabin, K. G. & Hohn, T. (1999). A short open reading frame terminating in front of a stable hairpin is the conserved feature in pregenomic RNA leaders of plant pararetroviruses. *The Journal of general virology* **80**, 2217-2228.

Pooggin, M. M., Hohn, T. & Fütterer, J. (2000). Role of a short open reading frame in ribosome shunt on the *Cauliflower mosaic virus* RNA leader. *Journal of Biological Chemistry* **275**, 17288-17296.

Pooggin, M. M., Ryabova, L. A., He, X., Fütterer, J. & Hohn, T. (2006).

Mechanism of ribosome shunting in *Rice tungro bacilliform pararetrovirus*. *RNA* **12**, 841-850.

Qiu, W. & Lunden, S. (2007). Characterization of a severevirus-like disease in Chardonnay grapevines in Missouri. *Plant Health Progress*. doi:10.1094/PHP-2007-1119-01-BR

Qu, R., Bhattacharyya, M., Laco, G. S., De Kochko, A., Subba Rao, B., Kaniewska, M. B., Scott Elmer, J., Rochester, D. E., Smith, C. E. & Beachy, R. N. (1991). Characterization of the genome of *Rice tungro bacilliform virus*: Comparison with *Commelina yellow mottle virus* and caulimoviruses. *Virology* **185**, 354-364.

Reid, K. E., Olsson, N., Schlosser, J., Peng, F. & Lund, S. T. (2006). An optimized grapevine RNA isolation procedure and statistical determination of reference genes for real-time RT-PCR during berry development. *BMC plant biology* **6**, 27-37.

Rubio, M., Matsui, C., Yamaguch, A. & Kamei, T. (1968). Electron microscopy of X-body formation in cells of cabbage infected with *Brassica virus 3*. *Phytopathology* **58**, 548-549.

Sanfaçon, H., Brodmann, P. & Hohn, T. (1991). A dissection of the *Cauliflower mosaic virus* polyadenylation signal. *Genes development* **5**, 141-149.

Schardl, C. L., Byrd, A. D., Benzion, G., Altschuler, M. A., Hildebrand, D. F. & Hunt, A. G. (1987). Design and construction of a versatile system for the expression of foreign genes in plants. *Gene* **61**, 1-11.

Schenk, P. M., Remans, T., Sági, L., Elliott, A. R., Dietzgen, R. G., Swennen, R., Ebert, P. R., Grof, C. P. & Manners, J. M. (2001). Promoters for pregenomic RNA of *Banana streak badnavirus* are active for transgene expression in monocot and dicot plants. *Plant molecular biology* **47**, 399-412.

Schenk, P. M., Sagi, L., Remans, T., Dietzgen, R. G., Bernard, M. J., Graham, M. W. & Manners, J. M. (1999). A promoter from sugarcane bacilliform badnavirus drives transgene expression in banana and other monocot and dicot plants. *Plant molecular biology* **39**, 1221-1230.

Shalla, T. & Petersen, L. (1980). Comparative cytology of nine isolates of *Cauliflower mosaic virus*. *Virology* **102**, 381-388.

Tidona, C. & Darai, G. (2011). *The Springer index of viruses*: Springer. Berlin, Heidelberg, New York, 2011.

Tzafrir, I., Torbert, K. A., Lockhart, B. E., Somers, D. A. & Olszewski, N. E. (1998). The *Sugarcane bacilliform badnavirus* promoter is active in both monocots and dicots. *Plant molecular biology* **38**, 347-356.

Xu, D., Mock, R., Kinard, G. & Li, R. (2011). Molecular analysis of the complete genomic sequences of four isolates of *Gooseberry vein banding associated virus*. *Virus genes* **43**, 130-137.

Zhang, Y., Singh, K., Kaur, R. & Qiu, W. (2011). Association of a novel DNA virus with the grapevine vein-clearing and vine decline syndrome. *Phytopathology* **101**, 1081-1090.

Zuker, M. (2003). Mfold web server for nucleic acid folding and hybridization prediction. *Nucleic Acids Research* **31**, 3406-3415.

CHAPTER 3: A *NICOTIANA BENTHAMIANA* SYSTEM TO TEST INFECTIVITY OF INFECTIOUS CLONES

ABSTRACT

The P6 protein of *Cauliflower mosaic virus* (CaMV) is a multifunctional protein. It has been shown to be the major component of CaMV inclusion bodies (IB), hypersensitive response elicitor, translational transactivator, host range and chlorosis system determinant, silencing suppressor, and salicylic acid and jasomonic acid defense regulator. In addition, P6 also interacts with multiple host proteins and microfilaments and plays a key role in intracellular movement of CaMV virions. The recently proposed "mobile virion factory" model for P6 IBs suggests that CaMV virions are produced and assembled inside of the P6 IB, and P6 IB traffics along microfilaments towards plasmodesmata, where CaMV virions will be delivered for transit to the adjacent cell. However, most evidences which supported this "mobile virion factory" model involve utilization of P6 tagged with green fluorescent protein (GFP); as a result, it is essential to prove that P6-GFP or GFP-P6 can support the replication of the virus. In this chapter, P6 and P6-GFP were examined for the ability to complement a defect CaMV isolate that contains a lethal mutation in its P6 coding region. P6-GFP was able to perform all the functions of P6 and support coat protein expression and virion assembly.

1. INTRODUCTION

The P6 protein of *Cauliflower mosaic virus* (CaMV) is a multifunctional protein (Schoelz *et al.*, 2015). It was initially identified as the major protein component of the CaMV amorphous inclusion bodies (IBs) (Covey & Hull, 1981; Shockey *et al.*, 1980), and was subsequently shown to be elicitor of the hypersensitive response (HR) in resistant hosts and a chlorosis symptom determinant in susceptible hosts (Daubert *et al.*, 1983; Schoelz *et al.*, 1986). Other studies showed that P6 is a translational transactivator (TAV), modifying host ribosomes for translation of the CaMV polycistronic 35S RNA (Bonneville *et al.*, 1989), and P6 also has been shown to modify host defenses, suppressing the RNA silencing machinery (Haas *et al.*, 2008; Love *et al.*, 2007a; Shivaprasad *et al.*, 2008), suppressing the salicylic acid defenses, and activating the jasomonic acid defense pathway (Love *et al.*, 2012; Love *et al.*, 2007b; Love *et al.*, 2005).

Recently, evidence has accumulated for the role of CaMV P6 in intracellular movement for delivery of virions to plasmodesmata (Schoelz *et al.*, 2015). To visualize the P6 protein and to examine its subcellular distribution, P6 was fused with green fluorescent protein (GFP) either at its C-terminus. Harries *et al* (2009a) reported that P6 IBs associate with microfilaments, microtubules, and the ER, and that P6 IBs are capable of moving along microfilaments. When microfilaments were disrupted by latrunculin B, the movement of P6 IBs, as well as the development of CaMV local lesion in the CaMV host *N. edwardsonii*, was abolished, indicating that

microfilaments had an essential role in CaMV infections (Harries *et al.*, 2009a). P6 also interacts with several host proteins that interact with either microfilaments or are themselves localized to plasmodesmata, such as CHUP1 (for Chloroplast Unusual Positioning protein) (Angel *et al.*, 2013), PDLP1 (for Plasmodesmatal-Located Protein 1) and AtSRC2.2 (for Soybean Response to Cold) , as well as the CaMV movement protein (MP) (Rodriguez *et al.*, 2014). Schoelz and co-workers recently proposed that IBs function as a mobile CaMV virion factory; CaMV virions are produced and assembled inside of the P6 IB, and P6 IB traffics along microfilaments towards plasmodesmata, where CaMV virions will be delivered for transit to the adjacent cell (Schoelz *et al.*, 2015).

In any study in which a plant or pathogen protein is tagged with a fluorescent protein such as GFP, it is important to show that the GFP fusion does not affect the function of the protein. For example, the development of the model for intracellular movement of P6 is dependent on the subcellular localization studies of P6-GFP. Similarly, Haas and coworkers (2005) fused GFP to the N-terminus of P6 to show that P6 is capable of both nuclear import and export. Although it was essential to tag P6 with GFP, little is known about the effect of GFP on the varied functions of P6. In fact, the only study that examined any function associated with P6-GFP was Harries *et al.* (2009a). They showed that the TAV function of P6-GFP was comparable to wild type P6. However, it has not yet been proven that the P6-GFP or GFP-P6 proteins can support the replication of the virus, so it remains a possibility that the localization

studies may not represent what happens in a virus infection.

In this chapter, we have examined the ability of P6 and P6-GFP to complement a CaMV isolate that contains a lethal mutation in its P6 coding sequence for replication and encapsidation. This complementation study serves an additional purpose beyond examining the functionality of P6-GFP. It also has allowed us to develop and validate a system for evaluating the infectivity of a *Grapevine vein clearing virus* (GVCV) clone.

2. RESULTS

2.1. CaMV viral DNA was detected from JS215+P6 and JS215+P6-GFP co-infiltration

To investigate whether transient co-expression of either the P6 or P6-GFP genes with a CaMV replicon would support the formation of the "virion factory" in plant cells, we utilized a defective version of CaMV that could be agroinfiltrated into plant tissues. This clone was designed to contain an 11 bp frameshift deletion near the 5'-terminus of the P6 gene (Fig. 3-1) (Yu *et al.*, 2003). The virus was unable to infect wild type *Arabidopsis* and turnips, but could be complemented for development of a systemic infection in stably transformed Arabidopsis that expressed the wild type P6 protein (Yu *et al.*, 2003). Although the original mutation in the viral DNA was supposed to comprise an 11 bp deletion, a subsequent nucleotide sequence analysis of JS215 revealed that it was actually more complex, consisting of the 11 bp deletion but

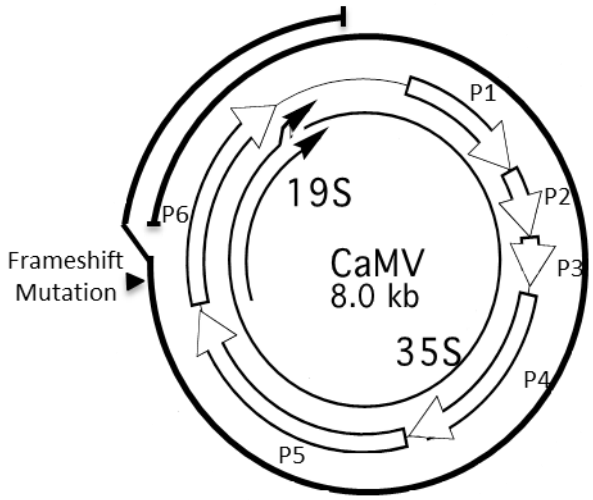

Fig. 3-1 Structure of the defective CaMV isolate JS215**.** The outer arrow illustrates the composition of the terminally redundant CaMV sequences cloned into the T-DNA of the Agrobacterium binary vector. The position of the frameshift mutation within P6 is indicated by the arrowhead. The circular, open arrows illustrate the positions of the six genes proven to encode functional proteins. P1- encodes a movement protein, P2 - an aphid transmission factor, P3 – a virion-associated protein that interacts with P2 for aphid transmission and P1 for cell-to-cell movement, P4 – the capsid protein, P5 – the reverse transcriptase, P6 – the multifunctional TAV/viroplasmin protein. The inner, solid arrows illustrate the positions of the 19S and 35S RNAs.

also a 33 bp insertion with a reiteration of a *Sac*I restriction enzyme site (Fig. 3-2).

The first question we asked is, can ectopic co-expression of P6 or P6-GFP with JS215 support the CaMV life cycle through replication and encapsidation? A co-infiltration assay was developed to address this question (Fig. 3-3). One hallmark of CaMV completing its life cycle is the formation of virions that contains viral DNA; only when CaMV is replicating and encapsidation proceeds normally would the replicated viral DNA be packaged within the virion and protected by the coat protein from DNases. The underlying principle for this assay is that the DNase treatment degrades all free, unencapsidated DNA including the input DNA from agroinfiltration, whereas if the CaMV virions are present, encapsidated viral DNA is protected by the coat protein and from the DNaseI treatment (Gardner & Shepherd, 1980). Consequently, viral DNA recovered from virions could be recovered from virions and amplified by PCR.

In our procedure, approximately 20 grams of *N. benthamiana* leaf tissue were agroinfiltrated with JS215 + P6, JS215 + P6-GFP, or JS215 alone. At seven days post-infiltration (dpi), the leaves were subjected to the standard CaMV virion purification procedure (Gardner *et al.*, 1981) and all unencapsidated viral DNA and host chromosomal DNA were eliminated through a 30 minute treatment with DNaseI. To isolate the encapsidated viral DNA, the virion preparation was treated with Proteinase K for 30 minutes and the viral DNA was concentrated by ethanol precipitation, followed by PCR amplification of CaMV DNA with forward and

```
   Codon
    1                    13
W260   ATG GAG AAC ATA GAA AAA CTC CTC ATG CAA GAG AAA ATA
JS215  ATG GAG AAC ATA GAA AAA CTC CTC ATG CAA GAG AAA AGA

    14                   19
W260   CTA ATG CTA GAG CTC --- --- --- --- --- --- --- GAT
JS215  GCT CGG TAC CGA CAG TAC AGC ATG GCG ATC GGA GCT CGA

       20                    32
W260   CTA GTA AGA GCA AAA ATA AGC TTA GCA AGA GCT AAC GGC
JS215  TCT AGT AAG AGC AAA AAT AAG CTT AGC AAG AGC TAA CGG
```

Fig. 3-2 Rearrangements in the nucleotide sequence of JS215 result in frameshift mutations in the P6 coding sequence**.** An 11 bp deletion (highlighted in aqua in the W260 P6 sequence) was introduced into the P6 coding sequence of JS215 directly upstream of a *Sac*I restriction enzyme site (*Sac*I sites highlighted in green). However, nucleotide sequencing of the JS215 clone revealed an extra *Sac*I site and a 33 bp insertion of unknown origin (underlined in the JS215 sequence). Consequently, an intended frameshift in the P6 coding sequence, as observed at codon 13 of the W260 sequence, was coupled with a second frameshift beginning at codon 19 (highlighted in red). Codon numbers are related to the W260 sequence.

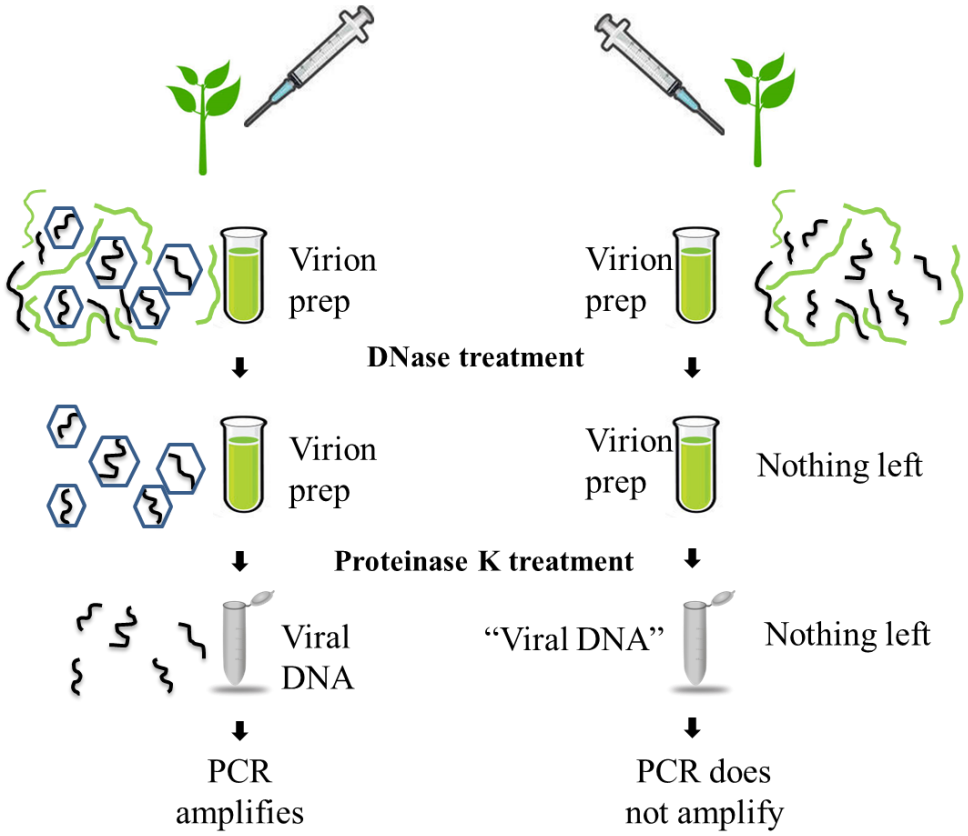

Fig. 3-3 Experimental design to detect virion. Constructs were infiltrated *in N. benthamiana* leaves for six days, infiltrated leaves were then collected and processed with a standard viral DNA purification protocol. PCR was performed using these putative viral DNA as templates. Only if viral DNA is protected by coat protein, it survives the treatment of DNase treatment and proteinase K treatment; otherwise it would be degraded by DNase and PCR does not amplify any band.

reverse primers specific to the P6 gene. As shown in Fig 3-4, CaMV DNA corresponding to the P6 gene was amplified from virion DNA isolated from plants co-infiltrated with JS215 and either P6 or P6-GFP, indicating both versions of P6 could complement JS215 for replication and viral DNA encapsidation. No band was amplified when JS215 was infiltrated alone, suggesting that the DNaseI treatment was sufficient to degrade all non-encapsidated DNA (Fig. 3-3).

2.2. The infectivity of JS215+P6 and JS215+P6-GFP co-infiltration is due to complementation instead of recombination.

Previous studies have shown that CaMV viral DNA is able to recombine with and acquire a gene VI transgene during replication of the virus in transgenic plants (Gal *et al.*, 1992; Schoelz & Wintermantel, 1993). Consequently, it was important to investigate whether the infections that resulted from co-agroinfiltration of JS215 and P6 or P6-GFP were the result of complementation, recombination with the separate P6 or P6-GFP construct, or due to restoration of gene VI function due to a second-site mutation. To investigate these possibilities, the P6 PCR products amplified from plants inoculated with JS215 and P6 were cloned and two clones were sequenced. An analysis of the first 300 nucleotides of gene VI confirmed the presence of the rearrangements that distinguished JS215 from CM1841 (Fig. 3-5). The retention of the deletion and insertions within gene VI of the encapsidated viral DNA showed that the JS215 virus was complemented in trans for expression of the reverse transcriptase

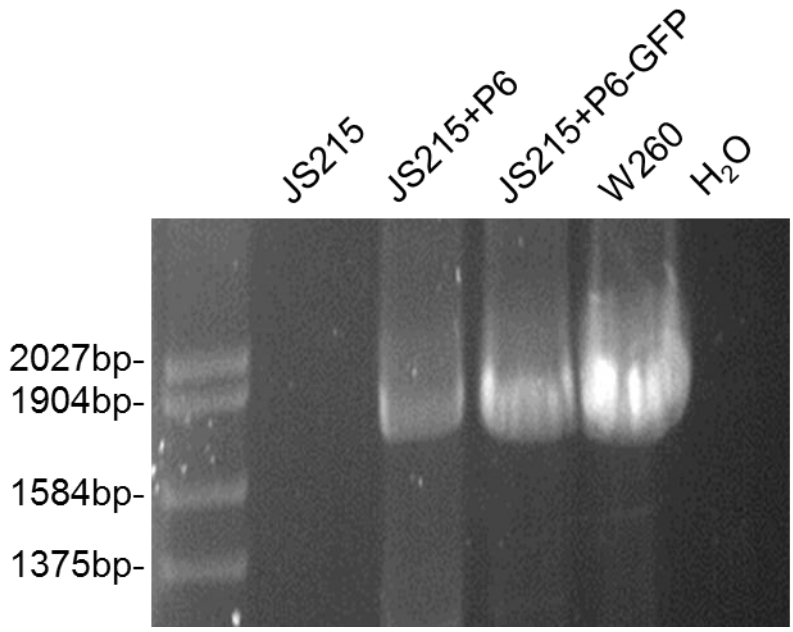

Fig. 3-4 P6 and P6GFP complement JS215 in CaMV virion production. Constructs were infiltrated in *N. benthamiana* leaves (listed on top) for six days, infiltrated leaves were then collected and processed with a standard viral DNA purification protocol. PCR was performed using these putative viral DNA as templates. P6 protein coding region was amplified. Viral DNA was diluted 100 fold before added into PCR system. CaMV W260 full length clone plasmid was used as a positive control.

```
    1
CM1841ATGGAGAACATAGAAAAACTCCTCATGCAAGAGAAAATACTAATGCTAGA
JS215 ATGGAGAACATAGAAAAACTCCTCATGCAAGAGAAAA----------GA

    51
CM1841GCTC------------------------------GATCTAGTAAGAG
JS215 GCTCGGTACCGACAGTACAGCATGGCGATCGGAGCTCGATCTAGTAAGAG
P6-1  GCTCGGTACCGACAGTACAGCATGGCGATCGGAGCTCGATCTAGTAAGAG
P6-3  GCTCGGTACCGACAGTACAGCATGGCGATCGGAGCTCGATCTAGTAAGAG

    151
CM1841CAAAAATAAGCTTAGCAAGAGCTAACGGCTCTTCGCAACAAGGAGACCTC
JS215 CAAAAATAAGCTTAGCAAGAGCTAACGGCTCTTCGCAACAAGGAGACCTC
P6-1  CAAAAATAAGCTTAGCAAGAGCTAACGGCTCTTCGCAACAAGGAGACCTC
P6-3  CAAAAATAAGCTTAGCAAGAGCTAACGGCTCTTCGCAACAAGGAGACCTC

    201
CM1841CCTCTCCACCGTGAAACACCGGTAAAAGAAGAAGCAGTTCACTCTGCACT
JS215 CCTCCCCACCGTGAAACACCGGTAAAAGAAGAAGCAGTTCACTCTGCACT
P6-1  CCTCCCCACCGTGAAACACCGGTAAAAGAAGAAGCAGTTCACTCTGCACT
P6-3  CCTCCCCACCGTGAAACACCGGTAAAAGAAGAAGCAGTTCACTCTGCACT

    251
CM1841GGCTACTTTTACGCCATCTCAAGTAAAAGCTATTCCAGAGCAAACGGCTC
JS215 GGCTACTTTTACGCCAACTCAAGTAAAGGCTATTCCAGAGCAAACGGCTC
P6-1  GGCTACTTTTACGCCAACTCAAGTAAAGGCTATTCCAGAGCAAACGGCTC
P6-3  GGCTACTTTTACGCCAACTCAAGTAAAGGCTATTCCAGAGCAAACGGCTC
```

Fig. 3-5 CaMV DNA recovered from the complementation experiment is derived from JS215. PCR products amplified from CaMV DNA were cloned and two clones sequenced. Each clone retained the 11 bp deletion, the 33 bp insertion, and five point mutations, matching the nucleotide sequence of JS215 and distinguishing the sequence from the P6 of CaMV strain W260. Sequences unique to P6 of W260 (designated as W260) are shown in aqua; sequences unique to JS215 are shown in red.

by transient expression of a functional P6 protein.

2.3. Both P6 and P6-GFP support the expression of CaMV coat protein and virion assembly

The next question we asked is if both P6 and P6-GFP were capable of supporting the translation of CaMV proteins and the assembly of the CaMV virion to a level that could be detected in a western blot. One of the main function of P6 as the translational transactivator (TAV) is to reprogram ribosomes for expression of the CaMV polycistronic 35S mRNA. The TAV function of P6 facilitates the reinitiation of translation of downstream ORFs. To test whether the fusion of GFP to the C-terminus of the P6 protein inhibits its ability to translate the coat protein (CP) cistron, a western blot was performed to examine the CaMV virion preparation for the CaMV CP. The CaMV CP is the fourth cistron in the 35S RNA (Fig. 3-1). As shown in Fig. 3-6, the CaMV CP was not produced in *N. benthamiana* agroinfiltrated with JS215 alone, but was produced in *N. benthamiana* co-agroinfiltrated with JS215 and P6-GFP, as well as in leaves co-agroinfiltrated with JS215 and P6. This study shows that the P6-GFP protein was capable of directing ribosomes to translate detectable levels of CaMV CP.

2.4. CaMV virions form upon co-agroinfiltration of JS215 with P6 or P6-GFP into *N. benthamiana* leaves

The PCR assay and western blots indicated that co-expression of P6 or P6-GFP

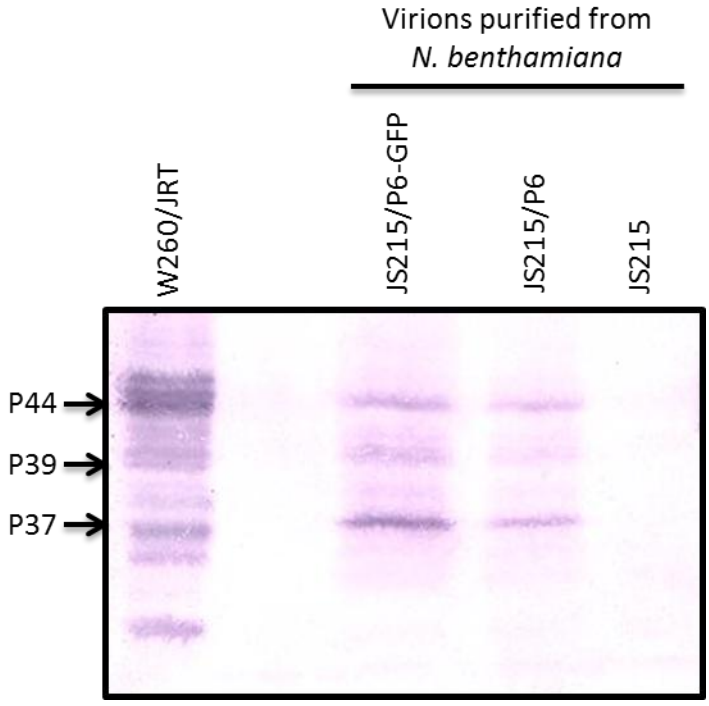

Fig. 3-6 Western blot for CaMV coat protein. *N. benthamiana* leaves were co-agroinfiltrated with JS215 and either P6 or P6-GFP, or agroinfiltrated with JS215 alone. CaMV virions were purified from 20 g of agroinfiltrated leaves at 7 dpi. Each lane contains approximately XX µg of protein recovered from a CaMV virion preparation. The multiple CP bands detected represent the full-length CP and processed CP forms.

with JS215 supported the synthesis of the CaMV CP in *N. benthamiana*. To visually confirm the presence of CaMV virions, I used a Transmission Election Microscope to examine the virion preparations recovered from leaves co-agroinfiltration JS215 + P6, JS215 + P6-GFP, and JS215 agroinfiltrated by itself. CaMV virions were visualized in purified virions preparations from JS215 + P6-GFP (Fig. 3-7) and from JS215 + P6 (data not shown), but not in JS215 alone (date not shown). The visualization of CaMV virions proves definitively that P6 and P6-GFP can complement JS215 to support the full expression of all viral proteins, resulting in replication and encapsidation of CaMV DNA into virions.

2.5. JS215+P6 co-infiltration system can be used in other *Nicotiana* species in addition to *N. benthamiana*

A commonly used method to determine virus host range is to inoculate viruses onto potential host plants and observe them for the appearance of local lesions and systemic infections (Schoelz *et al.*, 1986; Schoelz & Shepherd, 1988; Schoelz & Wintermantel, 1993). However, it is generally accepted that virus host ranges may extend beyond the development of local lesions and systemic symptoms. Viruses may be able to replicate in individual plant cells but may not move intercellularly. These infections would not be detected at the whole plant level, because symptom development is contingent on cell-to-cell movement. With JS215+P6 co-infiltration, we are able to test whether CaMV is able to replicate in individual plant cells in a

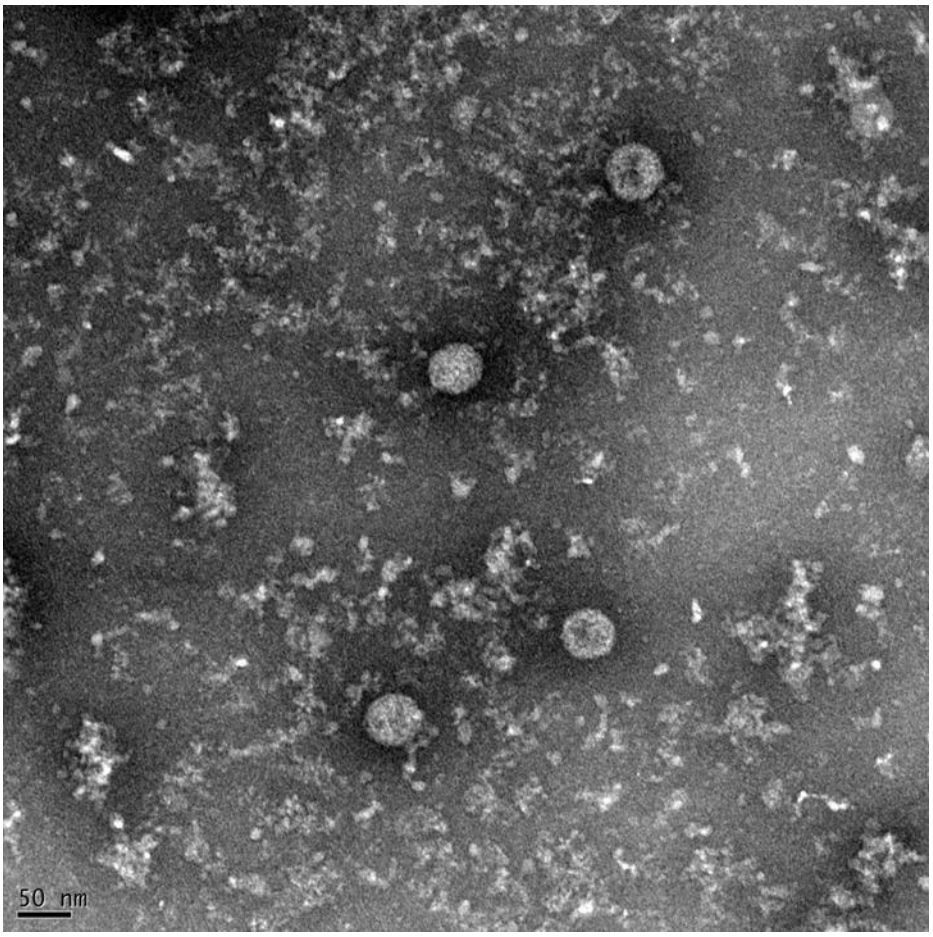

Fig.3-7 CaMV virions purified from JS215+P6-GFP co-infiltrated *N. benthamiana.*

sensitive and less time-consuming manner.

To re-evaluate the host range of CaMV, JS215 and P6 of CaMV strain D4 were co-infiltrated into six *Nicotiana* species. The D4 version of P6 was used in this experiment rather than P6 of strain W260, because P6 of W260 has been shown to trigger a hypersensitive response in some *Nicotiana* species (Palanichelvam *et al.*, 2000). In addition, P19 of TBSV was co-infiltrated as well to assist in suppression of any potential gene silencing response of the host. Infiltrated leaves were collected at 7 dpi for virion purification and DNaseI treatment, followed by viral DNA isolation and PCR with P6 primers to detect CaMV viral DNA. *N. edwardsonii* was included as a positive control in the test, as it was shown previously to support systemic movement of CaMV (Schoelz *et al.*, 1986). None of the other five *Nicotiana* species had previously been reported to be susceptible to CaMV. This test was conducted twice; a *Nicotiana* species was considered a host for CaMV only when CaMV DNA was amplified in both tests. The results are shown in Table 3-1. Of the five *Nicotiana* species, only *N. repanda* was able to support CaMV replication and encapsidation in both tests. *N langsdorffii* supported replication and encapsidation of JS215 in one test, but JS215 was not detected in the second test. Further testing will be necessary to determine if the divergent results obtained with *N. langsdorffii* are related to age of the plants, environmental conditions, or some other factor. By contrast, *N. rustica*, *N. tabacum*, and *N. sylvestris* were all negative for replication of CaMV in both tests and are not considered CaMV hosts.

	N. edwardsonii	*N. rustica*	*N. tabacum*	*N. langsdorffii*	*N. repanda*	*N. sylvestris*
First replicate	+	-	-	+	+	-
Second replicate	+	-	-	-	+	-

Table 3-1 Evaluation of Nicotiana species as hosts for CaMV host test. A positive (+) reaction indicates that CaMV gene VI could be amplified from a CaMV virion preparation, whereas in a negative (-) reaction, no CaMV DNA was amplified.

3. DISCUSSION

Over the past several years, several studies have examined the subcellular localization of P6 by tagging the protein with GFP (Angel *et al.*, 2013; Haas *et al.*, 2008; Haas *et al.*, 2005; Harries *et al.*, 2009a; Rodriguez *et al.*, 2014). These investigations have led to models for intracellular movement of P6 for delivery of virions to the plasmodesmata, as well as entry of P6 into the nucleus to function as a suppressor of gene silencing (reviewed in Schoelz *et al.*, 2015). However, the P6 protein is exceedingly complex, interacting with several host proteins to facilitate the infection process (Schoelz *et al.*, 2015). To examine whether a fusion of GFP to P6 might affect its function, we developed a complementation assay and proved that P6-GFP could support the replication cycle of CaMV in initially infected cells.

GFP was discovered by Shimomura and coworkers (1962), and it is widely used as a reporter gene, cell marker, fusion tag, and active indicator (Tsien, 1998). The most successful application of GFP has been as a genetic fusion partner to host proteins to monitor their localization and fate. In an ideal situation, GFP gene is fused in frame with the coding region of a host protein, and the fusion protein maintains its normal function and localization but is now fluorescent. However, this may not be true in all cases. As a consequence, it is very important to confirm that the function of the fusion protein is retained in any experiments involving GFP fusions.

Although numerous virus proteins have been tagged with GFP or some other fluorescent protein for subcellular localization studies, in only a few cases has it been

possible to validate the localization studies by incorporating the fusion protein into an infectious virus clone. For example, GFP was fused to the C-terminus of the 30 KDa movement protein of Tobacco mosaic virus (TMV) and reintroduced into an infectious clone to show that the TMV movement protein associates with microtubules and accumulates at in plasmodesmata (Epel *et al.*, 1996; Heinlein *et al.*, 1995; Padgett *et al.*, 1996). By contrast, it has not been possible to introduce a 126 KDa-GFP fusion into the TMV infectious clone and retain infectivity. Such an experiment would be valuable to validate the role of the 126 KDa protein bodies in intracellular movement in association with microfilaments (Harries *et al.*, 2009b; Liu *et al.*, 2005). Other viral proteins that have been tagged with GFP and successfully integrated back into an infectious virus clone include the $6K_2$ protein of Turnip mosaic virus (Cotton *et al.*, 2009) and TGBp2 of Potato virus X (Ju *et al.*, 2005). With both viruses the incorporation of virus protein-GFP fusions into an infectious clone has been invaluable for understanding the role of those viral proteins in movement of the viral genome.

Unlike the 30 KDa movement protein of TMV, the $6K_2$ protein of Turnip mosaic virus and the TGBp2 protein of Potato virus X, it was not possible to integrate a P6-GFP fusion into an infectious CaMV clone, for at least two reasons. First, the genome of CaMV can only tolerate small insertions, likely due to packaging limitations within the icosahedral virion of CaMV (Brisson *et al.*, 1984; Gronenborn *et al.*, 1981). A more important reason is that the complete 35S promoter has been

shown to extend into the 3' end of the P6 coding sequence (Fang *et al.*, 1989; Odell *et al.*, 1985). Consequently a fusion of the GFP gene to the 3' end of the P6 gene would disrupt the 35S promoter. For these reasons we chose to develop a complementation system, essentially turning the CaMV genome into a two-component virus.

Earlier studies indicated that a complementation approach would likely be successful. For example, Harries *et al* (2009a) developed an agroinfiltration system to compare the TAV functions of P6 versus P6-GFP. They developed a transient expression assay to examine the capacity of P6 to facilitate translation of a GUS gene present as the second cistron of a bicistronic reporter plasmid. They found that GUS expression of the reporter plasmid alone was 1.6% of the level of the monocistronic GUS control construct. By contrast, GUS expression was increased more than five-fold when the bicistronic reporter plasmid was con-agroinfiltrated with either P6 or P6-GFP. This study showed that the fusion of GFP to the C-terminus of P6 did not affect the TAV function of P6 protein. However, it remained to be proven that P6-GFP would support a complete replication cycle in inoculated leaves. The JS215+P6-GFP co-infiltration experiment in this chapter showed that P6-GFP is in fact able to support CaMV replication and encapsidation, indicating that GFP does not interfere with any function of P6 involved in these processes.

JS215 was created by Yu *et al* (2003). They had intended to make an 11 bp deletion within the P6 coding sequence present in a full-length clone of CaMV strain CM1841. The deletion was introduced into a *Sal*I (nucleotide 4,833) to *Sac*I (5,822)

DNA segment of CaMV, and the deletion was confirmed by sequencing the cloned *Sal*I – *Sac*I DNA segment, before cloning the DNA segment back into the full-length viral clone. However, we found that the P6 DNA sequence contained not only this 11 bp deletion, but also a 33 bp insertion between nucleotides 5,827 and 5,828. A BLAST analysis did not detect any significant similarity of the 33 bp insertion (data not shown), so the origin of this sequence is unclear. Since Yu *et al* (2003) did not confirm sequences downstream of nucleotide 5,822, it is not clear if this insertion was inserted by mistake during the creation of JS215, or JS215 has undergone recombination. The 33 bp insertion did not restore JS215 P6 function since the reading frame was still altered comparing to the functional P6 gene.

The viral DNA isolated from CaMV virion preparation could not be used immediately in the P6 PCR (date not shown). On the contrary, it had to be diluted before P6 could be amplified. This may be due to inhibitors of the PCR reaction present in the viral DNA preparation; dilution of inhibitors resulted in successful amplification of the P6 gene. CaMV viral DNA was diluted 10, 100, 1000, and 10000 fold to identify an ideal dilution for P6 amplification, and we found that the 100 fold dilution of CaMV viral DNA could be used as a template in the PCR, as illustrated in Fig. 3-4.

In addition to demonstrating the functionality of the P6-GFP construct, our co-agroinfiltration assay of *N. benthamiana* can also be used to evaluate the infectivity of an infectious clone of *Grapevine vein clearing virus* (GVCV). Due to

the low titer of GVCV, an infectious clone is the best method to complete Kohl's postulates and determine if GVCV is the causal agent of the grapevine vein clearing disease observed in Midwest. However, grapevine, as the natural host of GVCV, is not so compatible with agroinfiltration, and it presents challenges for inoculation of viruses. By contrast, *N. benthamiana* is the most widely used experimental host in plant virology because of the large number of diverse plant viruses that can successfully infect it (Goodin *et al.*, 2008). As a result, the same assay was performed with a GVCV infectious clone to test its infectivity, and this will be discussed in Chapter 4.

4. MATERIAL AND METHODS

4.1. Plasmids

Clones used in this paper are listed in Table 3-2. In particular, the plasmid JS215 is a full-length, terminally redundant CaMV clone inserted into the agrobacterium binary vector pOCA28 and was previously transformed into *A. tumefaciens* strain GV2260 (Yu *et al.*, 2003). *Agrobacterium* containing pJS215 was grown on LB media supplemented with spectinomycin (100 μg/ml). Agrobacteria containing all other plasmids were grown on LB media supplemented with Kanamycin (100 μg/ml).

4.2. Growth and maintenance of plants

Seven species of *Nicotiana*, *N. benthamiana*, *N. edwardsonii*, *N. rustica*,

Name	Description	vector	Cell	Reference
JS215	P6-defected clone of CaMV, with deletion in P6 protein coding region.	pOCA28	*A. tumefaciens* GV2260	(Yu *et al*., 2003)
P6	CaMV strain W260 P6 protein cloned into binary vector	pKYLX7	*A. tumefaciens* GV2260	(Palanichelvam *et al*., 2000)
P6-D4	CaMV strain D4 P6 protein cloned into binary vector	pKYLX7	*A. Tumefaciens* GV2260	(Palanichelvam *et al*., 2000)
P6-GFP	CaMV P6 protein fused with GFP and cloned into binary vector	pKYLX7	*A. tumefaciens* AGL1	(Harries *et al*., 2009)
P19	TBSV P19 protein (silencing suppressor) cloned into binary vector	pLYLX7	*A. tumefaciens* AGL1	(Angel *et al*., 2011)

Table 3-2 List of constructs

N. tabacum, *N. langsdorffii*, *N. repanda*, and *N. sylvestris* were grown under greenhouse conditions, with sufficient water and controlled-release fertilizers. Plants were grown for at least two months before being agroinfiltrated.

4.3. Agroinfiltration

For each agroinfiltration experiment, cells were grown at 28℃ for two days in LB media (1.6% Tryptone, 1% yeast extract, 0.5% NaCl). *Agrobacterium* cells were pelleted by centrifugation at 17,000 x g for 10 min, and the pellet was resuspended in agroinfiltration media (0.39% MES, 2% sucrose, 1% glucose, pH adjusted to 5.4 with KOH). Acetosyringone stock (dissolved in N-dimethylformamide) was added to a final concentration of 0.2 mM to induce T-DNA transfer. Cell density was adjusted to an OD_{600} of 1.5 prior to agroinfiltration. For co-infiltration of plasmids, agrobacteria carrying different plasmids were mixed at a 1:1 ratio.

4.4. Purification of CaMV virions and viral DNA

To assess replication of CaMV through PCR analysis or protein gel electrophoresis, *N. benthamiana* leaves were agroinfiltrated with the appropriate constructs and tissues were collected at 6-7 days post-agroinfiltration (dai). Twenty grams of agroinfiltrated leaves were homogenized in 1X grinding buffer (200 mM Tris pH 7.0-7.4, 20 mM EDTA, 1.5 M urea) at 6 ml buffer per gram, and triton-X100 was subsequently added to a final concentration of 2%. The solution was stirred

overnight to release virions from inclusion bodies, followed by centrifugation at 15,000 x g for 10 min. The supernatant was poured through one layer of miracloth (Calbiochem, San Diego CA) to remove plant debris and the virions were pelleted through centrifugation at 190,000 x g for 75 min at 8℃. Putative virion pellets were rinsed with dH_2O for three times before resuspension in 1.5 ml of dH_2O overnight with stirring.

For viral DNA isolation, the putative virion preparations were treated with DNase I followed by proteinase K treatment. One ml of the putative virion preparation was added to 2.6 ml water, as well as 0.4 ml 1M Tris (pH 7.4-7.8), 20 µl of 1M $MgCl_2$, and 25 µl of a 1 mg/ml DNase I stock solution. This mixture was incubated at 37℃ for 30 min to degrade any unencapsidated DNA. EDTA was added to a final concentration of 1 mM to terminate the DNase I treatment. SDS and proteinase K were added to 1% and 0.1 mg/ml, respectively, followed by a 30 min incubation at 37℃ to release the viral DNA from the capsid. Viral DNA was purified by phenol extraction and concentrated through ethanol precipitation. The DNA pellet was resuspended in 100 µl of dH_2O.

4.5. PCR

PCR was performed to amplify the full-length P6 gene using primer P6Fwd (5'- ATAAGATTCCCACACACTTGT-3', CaMV strain W260 nts 5,680-5,700 - accession number JF809616.1) and P6Rev (5'- CCAAATGAAATGAACTTCCTT-3',

CaMV strain W260 nts 7,423-7,403). The PCR program was: 95℃ for 10 min for initial denaturation, followed by 35 cycles of 95℃ for 30 s, 48℃ for 30 s and 72℃ for 90 s, and then 72℃ for another 10 min for a final extension. PCR products were analyzed in a 1% agrose gel and DNA bands were visualized using the Fotodyne™ FOTO/Analyst™ Investigator Eclipse UV Workstation photodocumentation system (Fotodyne, Hartland WI).

4.6. Western blotting

The total protein concentration of the putative virion preparations was measured by a Bio-Rad Protein Assay following the manufacturer's instructions (Bio-Rad Laboratory, Hercules, CA). Total protein concentration was normalized to the putative virion preparation which has the lowest protein concentration.

Western blots ere completed as described in Angel *et al.* (2013), but key details are discussed here. The putative virion preparations were mixed with a 2X loading buffer at a 1:1 ratio, and the mixture was boiled for 10 min to denature CaMV coat protein. Denatured samples were run in a 10% SDS-PAGE gel and transferred to 0.45 µm nitrocellulose membrane. The membrane was incubated in blocking buffer (3% non-fat milk in PBS) overnight at 4℃. Western blot analyses were performed incubating the blocked membrane with rabbit-anti-CaMV CP (Anderson *et al.*, 1992) antibodies at a 1:100 dilution in 10 ml of blocking buffer at room temperature for 1.5 h. Following several washes, 2 µl of Anti-Rabbit IgG (Fc) AP conjugate (Promega,

Madison, WI) were added to 10 ml of blocking buffer as the secondary antibody, and it was incubated at room temperature for an addition 1.5 h. Finally, the blots were exposed to 10 ml of AP development solution (100 mm Tris-HCl, pH 9.0, 150 mm NaCl, 1 mm MgCl2, 66 µl of nitroblue tetrazolium, and 33 µl of 5-bromo-4-chloro3-indolyl phosphate, Promega, Madison WI).

4.7. Electron microscopy

Transmission Electron Microscopy (TEM) was utilized at the University of Missouri Electron Microscopy Core to visualize CaMV virions. The conditions visualizing the virions were according to standard core protocols. Briefly, for carbon coated grids were glow discharged to make them hydrophilic before loading samples. The sample was negative stained with Nano-W (methylamine tungstate) for 5 min before visualization under TEM (Williams & Carter, 1996).

REFERENCES

Anderson, E. J., Trese, A. T., Sehgal, O. P. & Schoelz, J. E. (1992). Characterization of a chimeric *Cauliflower mosaic virus* isolate that is more severe and accumulates to higher concentrations than either of the strains from which it was derived. *Molecular Plant-Microbe Interact* **5**, 48-54.

Angel, C. A., Hsieh, Y.-C. & Schoelz, J. E. (2011). Comparative analysis of the capacity of tombusvirus P22 and P19 proteins to function as avirulence determinants in Nicotiana species. *Molecular plant-microbe interactions* **24**, 91-99.

Angel, C. A., Lutz, L., Yang, X., Rodriguez, A., Adair, A., Zhang, Y., Leisner, S. M., Nelson, R. S. & Schoelz, J. E. (2013). The P6 protein of *Cauliflower mosaic virus* interacts with CHUP1, a plant protein which moves chloroplasts on actin microfilaments. *Virology* **443**, 363-374.

Bonneville, J., Sanfaçon, H., Fütterer, J. & Hohn, T. (1989). Posttranscriptional trans-activation in *Cauliflower mosaic virus*. *Cell* **59**, 1135-1143.

Brisson, N., Paszkowski, J., Penswick, J., Gronenborn, B., Potrykus, I. & Hohn, T. (1984). Expression of a bacterial gene in plants by using a viral vector. *Nature* **310**, 511-514.

Cotton, S., Grangeon, R., Thivierge, K., Mathieu, I., Ide, C., Wei, T., Wang, A. & Laliberté, J.-F. (2009). Turnip mosaic virus RNA replication complex vesicles are mobile, align with microfilaments, and are each derived from a single viral genome. *Journal of virology* **83**, 10460-10471.

Covey, S. N. & Hull, R. (1981). Transcription of *Cauliflower mosaic virus* DNA. Detection of transcripts, properties, and location of the gene encoding the virus inclusion body protein. *Virology* **111**, 463-474.

Daubert, S., Schoelz, J., Debao, L. & Shepherd, R. (1983). Expression of disease symptoms in *Cauliflower mosaic virus* genomic hybrids. *Journal of molecular and applied genetics* **2**, 537-547.

Epel, B. L., Padgett, H. S., Heinlein, M. & Beachy, R. N. (1996). Plant virus movement protein dynamics probed with a GFP-protein fusion. *Gene* **173**, 75-79.

Fang, R.-X., Nagy, F., Sivasubramaniam, S. & Chua, N.-H. (1989). Multiple cis regulatory elements for maximal expression of the *Cauliflower mosaic virus* 35S promoter in transgenic plants. *The Plant Cell* **1**, 141-150.

Gal, S., Pisan, B., Hohn, T., Grimsley, N. & Hohn, B. (1992). Agroinfection of transgenic plants leads to viable *Cauliflower mosaic virus* by intermolecular recombination. *Virology* **187**, 525-533.

Gardner, R. & Shepherd, R. (1980). A procedure for rapid isolation and analysis of *Cauliflower mosaic virus* DNA. *Virology* **106**, 159-161.

Gardner, R. C., Howarth, A. J., Hahn, P., Brown-Luedi, M., Shepherd, R. J. & Messing, J. (1981). The complete nucleotide sequence of an infectious clone of *Cauliflower mosaic virus* by M13mp7 shotgun sequencing. *Nucleic acids research* **9**, 2871-2888.

Goodin, M. M., Zaitlin, D., Naidu, R. A. & Lommel, S. A. (2008). *Nicotiana benthamiana*: its history and future as a model for plant-pathogen interactions. *Molecular Plant-Microbe Interactions* **21**, 1015-1026.

Gronenborn, B., Gardner, R. C., Schaefer, S. & Shepherd, R. J. (1981). Propagation of foreign DNA in plants using *Cauliflower mosaic virus* as vector. *Nature* **294**, 773-776.

Haas, G., Azevedo, J., Moissiard, G., Geldreich, A., Himber, C., Bureau, M., Fukuhara, T., Keller, M. & Voinnet, O. (2008). Nuclear import of CaMV P6 is required for infection and suppression of the RNA silencing factor DRB4. *The EMBO Journal* **27**, 2102-2112.

Haas, M., Geldreich, A., Bureau, M., Dupuis, L., Leh, V., Vetter, G., Kobayashi, K., Hohn, T., Ryabova, L. & Yot, P. (2005). The open reading frame VI product of *Cauliflower mosaic virus* is a nucleocytoplasmic protein: its N terminus mediates its nuclear export and formation of electron-dense viroplasms. *The Plant Cell* **17**, 927-943.

Harries, P. A., Palanichelvam, K., Yu, W., Schoelz, J. E. & Nelson, R. S. (2009a). The *Cauliflower mosaic virus* protein P6 forms motile inclusions that traffic along actin microfilaments and stabilize microtubules. *Plant physiology* **149**, 1005-1016.

Harries, P. A., Park, J.-W., Sasaki, N., Ballard, K. D., Maule, A. J. & Nelson, R. S. (2009b). Differing requirements for actin and myosin by plant viruses for

sustained intercellular movement. *Proceedings of the National Academy of Sciences* **106**, 17594-17599.

Heinlein, M., Epel, B. L., Padgett, H. S. & Beachy, R. N. (1995). Interaction of tobamovirus movement proteins with the plant cytoskeleton. *Science* **270**, 1983-1985.

Ju, H.-J., Samuels, T. D., Wang, Y.-S., Blancaflor, E., Payton, M., Mitra, R., Krishnamurthy, K., Nelson, R. S. & Verchot-Lubicz, J. (2005). The potato virus X TGBp2 movement protein associates with endoplasmic reticulum-derived vesicles during virus infection. *Plant physiology* **138**, 1877-1895.

Liu, J.-Z., Blancaflor, E. B. & Nelson, R. S. (2005). The tobacco mosaic virus 126-kilodalton protein, a constituent of the virus replication complex, alone or within the complex aligns with and traffics along microfilaments. *Plant Physiology* **138**, 1853-1865.

Love, A. J., Geri, C., Laird, J., Carr, C., Yun, B.-W., Loake, G. J., Tada, Y., Sadanandom, A. & Milner, J. J. (2012). *Cauliflower mosaic virus* protein P6 inhibits signaling responses to salicylic acid and regulates innate immunity. *PLoS One* **7**, e47535.

Love, A. J., Laird, J., Holt, J., Hamilton, A. J., Sadanandom, A. & Milner, J. J. (2007a). *Cauliflower mosaic virus* protein P6 is a suppressor of RNA silencing. *Journal of General Virology* **88**, 3439-3444.

Love, A. J., Laval, V., Geri, C., Laird, J., Tomos, A. D., Hooks, M. A. & Milner, J. J. (2007b). Components of Arabidopsis defense-and ethylene-signaling pathways regulate susceptibility to *Cauliflower mosaic virus* by restricting long-distance movement. *Molecular plant-microbe interactions* **20**, 659-670.

Love, A. J., Yun, B. W., Laval, V., Loake, G. J. & Milner, J. J. (2005). *Cauliflower mosaic virus*, a compatible pathogen of Arabidopsis, engages three distinct defense-signaling pathways and activates rapid systemic generation of reactive oxygen species. *Plant physiology* **139**, 935-948.

Odell, J. T., Nagy, F. & Chua, N.-H. (1985). Identification of DNA sequences required for activity of the *Cauliflower mosaic virus* 35S promoter. *Nature* **313**, 810-812.

Padgett, H. S., Epel, B. L., Kahn, T. W., Heinlein, M., Watanabe, Y. & Beachy, R.

N. (1996). Distribution of tobamovirus movement protein in infected cells and implications for cell-to-cell spread of infection. *The Plant Journal* **10**, 1079-1088.

Palanichelvam, K., Cole, A. B., Shababi, M. & Schoelz, J. E. (2000). Agroinfiltration of *Cauliflower mosaic virus* gene VI elicits hypersensitive response in Nicotiana species. *Molecular plant-microbe interactions* **13**, 1275-1279.

Rodriguez, A., Angel, C. A., Lutz, L., Leisner, S. M., Nelson, R. S. & Schoelz, J. E. (2014). Association of the P6 Protein of *Cauliflower mosaic virus* with Plasmodesmata and Plasmodesmal Proteins. *Plant physiology* **166**, 1345-1358.

Schoelz, J., Shepherd, R. J. & Daubert, S. (1986). Region VI of *Cauliflower mosaic virus* encodes a host range determinant. *Molecular and cellular biology* **6**, 2632-2637.

Schoelz, J. E., Angel, C. A., Nelson, R. S. & Leisner, S. M. (2015). A model for intracellular movement of *Cauliflower mosaic virus*: the concept of the mobile virion factory. *Journal of experimental botany* **67**, 2039-2048.

Schoelz, J. E. & Shepherd, R. J. (1988). Host range control of *Cauliflower mosaic virus*. *Virology* **162**, 30-37.

Schoelz, J. E. & Wintermantel, W. M. (1993). Expansion of viral host range through complementation and recombination in transgenic plants. *The Plant Cell* **5**, 1669-1679.

Shimomura, O., Johnson, F. H. & Saiga, Y. (1962). Extraction, purification and properties of aequorin, a bioluminescent protein from the luminous hydromedusan, Aequorea. *Journal of cellular and comparative physiology* **59**, 223-239.

Shivaprasad, P. V., Rajeswaran, R., Blevins, T., Schoelz, J., Meins, F., Hohn, T. & Pooggin, M. M. (2008). The CaMV transactivator/viroplasmin interferes with RDR6-dependent trans-acting and secondary siRNA pathways in Arabidopsis. *Nucleic acids research* **36**, 5896-5909.

Shockey, M., Gardner, C., Melcher, U. & Essenberg, R. (1980). Polypeptides associated with inclusion bodies from leaves of turnip infected with *Cauliflower mosaic virus*. *Virology* **105**, 575-581.

Tsien, R. Y. (1998). The green fluorescent protein. *Annual review of biochemistry* **67**, 509-544.

Williams, D. B. & Carter, C. B. (1996). The transmission electron microscope. In *Transmission electron microscopy*, Springer. New York: Plenum Press, pp. 3-17.

Yu, W., Murfett, J. & Schoelz, J. E. (2003). Differential induction of symptoms in Arabidopsis by P6 of *Cauliflower mosaic virus*. *Molecular plant-microbe interactions* **16**, 35-42.

CHAPTER 4: DEVELOPMENT OF A *GRAPEVINE VEIN CLEARING VIRUS* INFECTIOUS CLONE AND ANALSYSIS OF PUTATIVE VIRIONS

ABSTRACT

Grapevine vein clearing virus (GVCV) is closely associated with a grapevine vein clearing syndrome observed in Missouri and surrounding states. The virus was initially characterized through deep sequencing of small RNAs isolated from symptomatic grape tissue. To further characterize the virus, I created a terminally redundant clone for agroinoculation to plants. The GVCV genome was assembled three overlapping DNA fragments amplified from GVCV-infected tissues and the terminally redundant clone, designated pGVCV-1, was inserted into an Agrobacterium binary vector for delivery into plant cells. pGVCV-1 was infiltrated into *Nicotiana benthamiana* leaves, and leaves were collected at 7 dpi for purification of virions and subsequently viral DNA isolation. A PCR-based assay indicated that pGVCV-1 was capable of replication and encapsidation. Furthermore, a systemic veinal chlorosis symptom was observed in several of the *N. benthamiana* plants agroinoculated with pGVCV-1, further evidence that the virus clone was infectious. To analyze the virions produced in *N. benthamiana* by pGVCV-1 and produced in symptomatic grape leaves, putative virions were purified by ultracentrifugation. In contrast to the expected bacilliform virions, a flexuous rod structure was isolated from *N. benthamiana*

agroinoculated with pGVCV-1 that had a 15nm diameter and varied in length from 83 to 930 nm. The same virion purification procedure was applied to GVCV-infected grape leaves showing typical vein clearing symptoms and two types of virions were observed in a single virion preparation; a flexuous rod that had a width of 15nm and a length up to 8,025 nm, as well as the typical bacilliform virion that had a diameter of 30 nm and a length of 160 nm. Healthy *N. benthamiana* leaves and healthy grape leaves subjected to the same virion isolation procedure also revealed the presence of a limited number of flexuous rods with a diameter of 15 nm. Further research is planned to characterize the nature of the flexuous rods in these plants.

1. INTRODUCTION

The discovery of *Grapevine vein clearing virus* (GVCV) and the close association between GVCV and the vein clearing symptoms were described in chapter 2. However, Koch's postulates have never been completed and GVCV has never been formally proven to be the causal agent of grapevine vein clearing diseases observed in Midwest vineyards. In order to complete Koch's postulates, plant virus virions need to be purified from symptomatic plant tissue and re-inoculated to healthy plant. However, grapevines pose a special challenge to this technique, because it is difficult if not impossible to mechanically inoculate virions of any grape virus to grape leaves. Furthermore, GVCV virions have not yet been purified and characterized from infected grape leaf tissues, even after attempts over several years (Schoelz, unpublished).

One alternative approach for the completion of Koch's postulates is to create an infectious clone of a virus and to inoculate this form to plants. This was first demonstrated with *Cauliflower mosaic virus* (CaMV) in 1980 (Hohn *et al.*, 1980). However, as with inoculation of virions, grape leaves would not be amenable to inoculations of naked viral DNA. An alternative is to use agrobacterium to deliver a virus genome into plant leaves in which the infection can be initiated. This was first demonstrated with CaMV in 1987 (Grimsley *et al.*, 1987). In this instance, a full-length or a greater-than-full-length clone can be inserted into an Agrobacterium binary vector and delivered into plant cells by the agrobacteria. The virus mRNA

would be transcribed and individual plant proteins translated, leading to the generation and assembly of virions. Agroinfiltration of grape leaves is feasible, but the success of the technique in grape tissue is dependent on the cultivar and the age of the plants (reviewed by Jelly *et al*., 2014). Typically, young, newly emerged grape leaves are more amenable to the technique.

Since the creation of the first plant virus infection clone in 1980, the generation of infectious clones of DNA or RNA plant viruses has become a standard laboratory technique and an important "first step" in the characterization of a plant virus. An infectious clone offers the possibility to study the functions of individual plant virus proteins in the context of the virus life cycle and to examine other aspects of virus-plant interactions. In particular, an infectious clone of GVCV would be the best solution for completion of Koch's postulates. Furthermore, a successful infection of GVCV to the plant species *Nicotiana benthamiana* might also offer improvements for purification of virions over the same techniques in grapevine leaves.

GVCV belongs to genus *Badnavirus*, family *Caulimoviridae (Zhang et al., 2011)*. The GVCV genome consists of circular, double-stranded DNA that has a size of 7753 bp. An analysis of the GVCV promoter in *N. benthamiana* revealed that the region between nucleotides (nt) 7,332 and 7,672 is efficient to direct transcription (Chapter 2, (Zhang *et al.*, 2015). Furthermore, the GVCV promoter was comparable in strength to the 35S promoter of CaMV. The GVCV transcript initiation site was mapped to nt 7,531 and the termination site was mapped to nt 7,676, generating a 105

bp terminal redundancy the full-length GVCV genomic RNA (chapter 2, Zhang *et al.*, 2015). The promoter and transcript analysis provided a guide for the design of an infectious GVCV clone. In addition, a protocol to test the infectivity of an infectious caulimovirus clone in agroinfiltrated *N. benthamiana* leaves was optimized and validated for CaMV in Chapter 3.

In this chapter, I describe the development of an infectious clone of GVCV, as well as attempts to purify GVCV virions from agroinfiltrated *N. benthamiana* leaves and symptomatic grape leaves collected from the field and greenhouse. *N. benthamiana* was chosen as the initial host for GVCV because grape leaf tissue is not as receptive to agroinfiltration, and there was some concern that potentially low titers of GVCV virions in grape leaves would complicate their purification from that host. Although we obtained evidence that GVCV can infect *N. benthamiana*, the attempts to purify GVCV virions from *N. benthamiana* yielded flexuous rods rather than the expected bacilliform virions. I found that the virion purification techniques developed with pGVCV-1 and *N. benthamiana* could be adapted for purification of GVCV from symptomatic grape leaves. With this host we observed both bacilliform virions typical of a badnavirus as well as flexuous rods. The atypical virion morphology has introduced questions regarding the GVCV infectious clone, as well as questions regarding the nature of the GVCV virions present in *N. benthamiana* and grape leaves.

2. RESULTS

2.1. Construction of a terminally redundant GVCV clone

To create an infectious clone of a caulimovirus, the cloned region has to contain the promoter region and the coding region corresponding to the full-length transcript, as well as the signals for transcript termination; to accommodate these requirements, it means that the clone will be terminally redundant. In Chapter 2 I showed that the region between nt 7,332 and 7,672 contains the promoter of the major GVCV transcript (Fig. 4-1) and also showed that the transcript starts at nt 7,571 and ends at nt 7,676 (Fig. 4-2) (Zhang *et al.*, 2015). With this information, I designed a strategy to create a terminally redundant GVCV clone by assembling three separate GVCV DNA segments.

Three GVCV DNA segments (Segment 7,185-2,049, Segment 1,945-4,663, and Segment 4,628-30) were amplified from total DNA isolated from symptomatic grape leaves (Fig. 4-3). The DNA segment from 7,185 to 2,049 (indicated in red in Fig. 4-3) contains the whole intergenic region, and a *Cla*I restriction enzyme site was added to the 5'-end by adding the *Cla*I recognition sequences to the forward primer 7185F-ClaI (Table 4-1). This amplified DNA segment also contains a *Spe*I site close to the 3'end, a restriction enzyme recognition sequence that appears only once in the GVCV genomic sequence (Zhang *et al.*, 2011). The GVCV DNA segment from 1,945 to 4,663 (indicated in green in Fig. 4-3) was amplified using primers 1945F and 4663R (Fig. 4-3, Table 4-1). A *Spe*I recognition sequence is close to the 5'-end of the

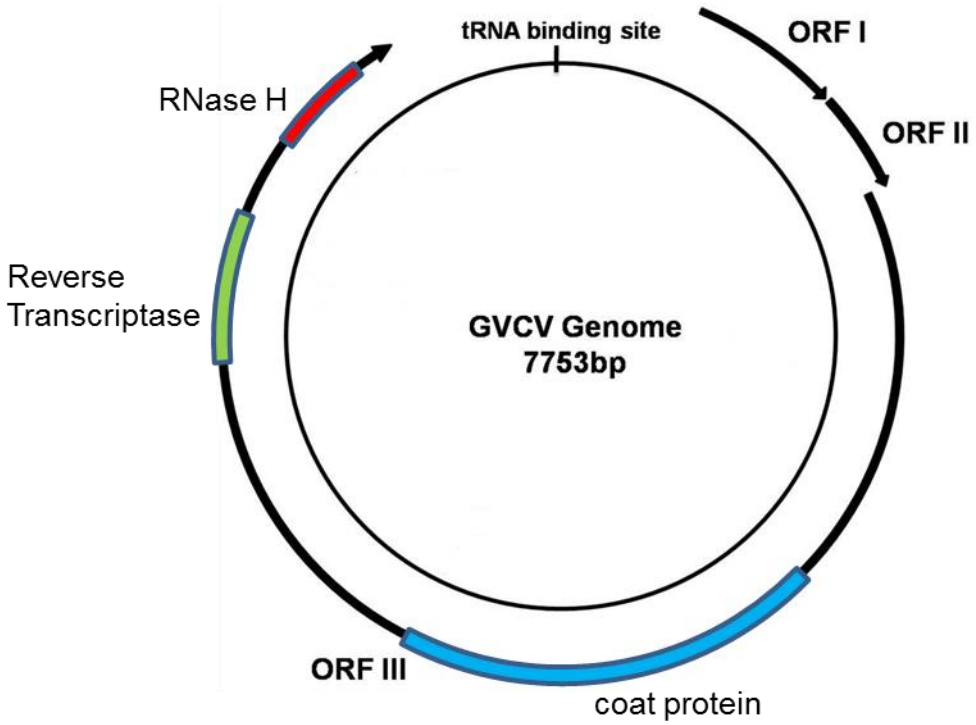

Fig. 4-1 genomic structure of *Grapevine vein clearing virus* (GVCV)

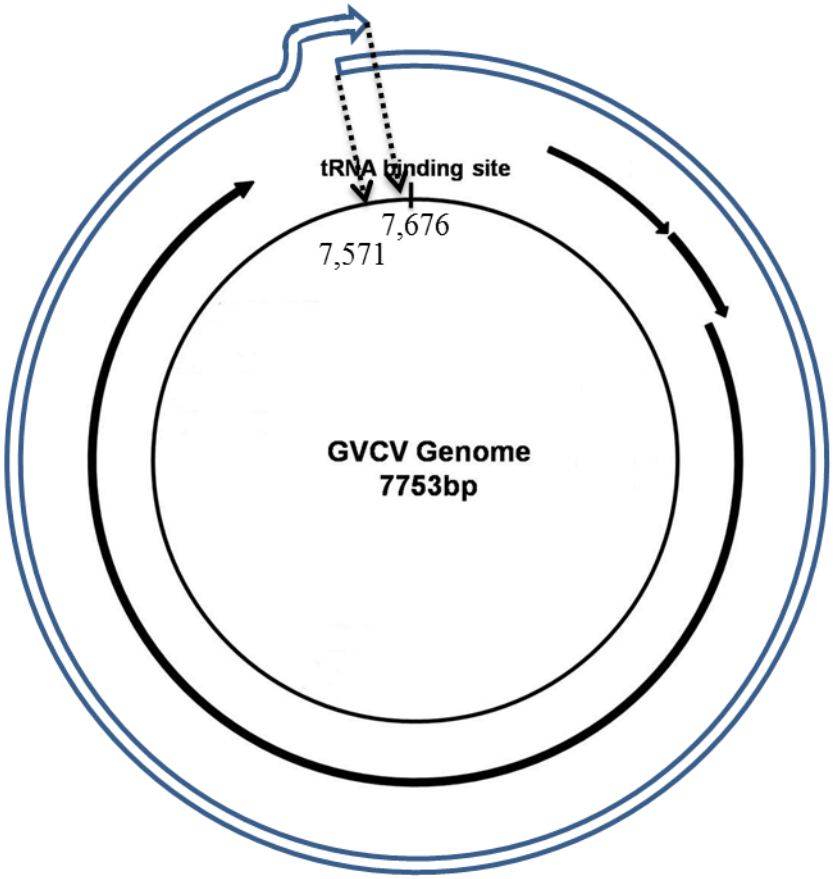

Fig. 4-2 The major transcript of GVCV starts at nt 7,571 and terminates at nt 7,676, generating a 105 bp terminal repeat.

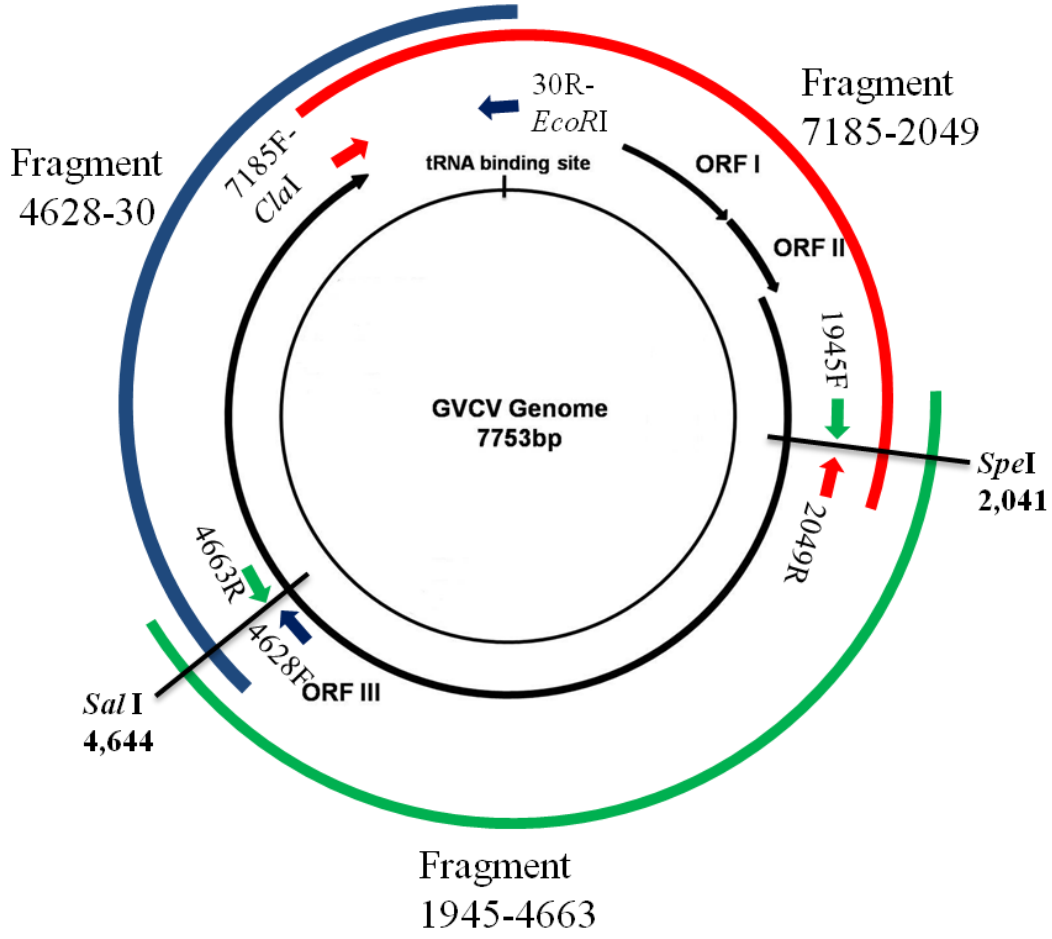

Fig. 4-3 Construction of GVCV infectious clone. Three fragments of GVCV were cloned.

Primer	5’-3’ sequences
GVCV7185F-ClaI	ATCGAT TATGCTTCAGGCAAACCTCAGGCTC
GVCV2049R	GTAGACTAGTTGTGCCCCTCTGGCC
GVCV1945F	GGAATTAGCGCCATGATCGTGTTCC
GVCV4663R	GGGTGCAAGTAGCACGTCGACCAAG
GVCV4628F	CCATCACTGTACTTGGTCGACGTGC
GVCV30R-EcoRI	GAATTC CCCAGATTTGAAACTGGAGCTCTGATACC
Polylinker F2	GGGG GAATTC GAGCTC GGTACC GGATCC GTCGAC CTGTAG ACTAGT GCATGC ATCGAT AAGCTT CCCC
Polylinker R2	GGGG AAGCTT ATCGAT GCATGC ACTAGT CTACAG GTCGAC GGATCC GGTACC GAGCTC GAATTC CCCC

Table 4-1 primer sequences

amplified DN segment, and a *Sal*I recognition site is located near the 3'-end. As with *Spe*I, the *Sal*I recognition sequence is found only once in the GVCV genomic sequence. The GVCV DNA segment from nt 4,628 through the sequence origin to nt 30 (indicated in blue in Fig. 4-3) also contains the *Sal*I site, but close to its 5'end, whereas the reverse primer 30R-*Eco*RI contained an added *Eco*RI site on its 3'end. These four restriction enzymes, *Cla*I, *Spe*I, *Sal*I, and *Eco*RI, were used to clone the three fragments into the intermediate vector pUC18 (red cloned into *Cla*I and *Spe*I, green into *Spe*I and *Sal*I, and blue into *Sal*I and *Eco*RI).

To deliver the GVCV sequences into plant cells, I modified the binary Agrobacterium vector pKYLX7 by removing the 35S promoter sequence with *Eco*RI and *Hind*III double digestion and replacing it with polylinker dimer. The restriction enzymes *Cla*I and *Eco*RI within polylinker were subsequently used to clone the assembled, terminally redundant GVCV clone into the modified binary vector pKYLX7.

The assembled GVCV terminally redundant clone starts at GVCV nt 7,185 and terminates at nt 30, resulting a 599 bp terminally redundant DNA segment at each end (Fig. 4-4). This clone was designated pGVCV-1. A negative control, designated pGVCV-N, was also constructed by assembling only DNA segments 7,185-2041 and 1,945-4,663 (Fig. 4-5) into the modified binary vector pKYLX7. pGVCV-N has the full GVCV promoter, which would facilitate translation, but lacks the reverse transcriptase and RNaseH regions. Thus, pGVCV-N would be expected to produce a

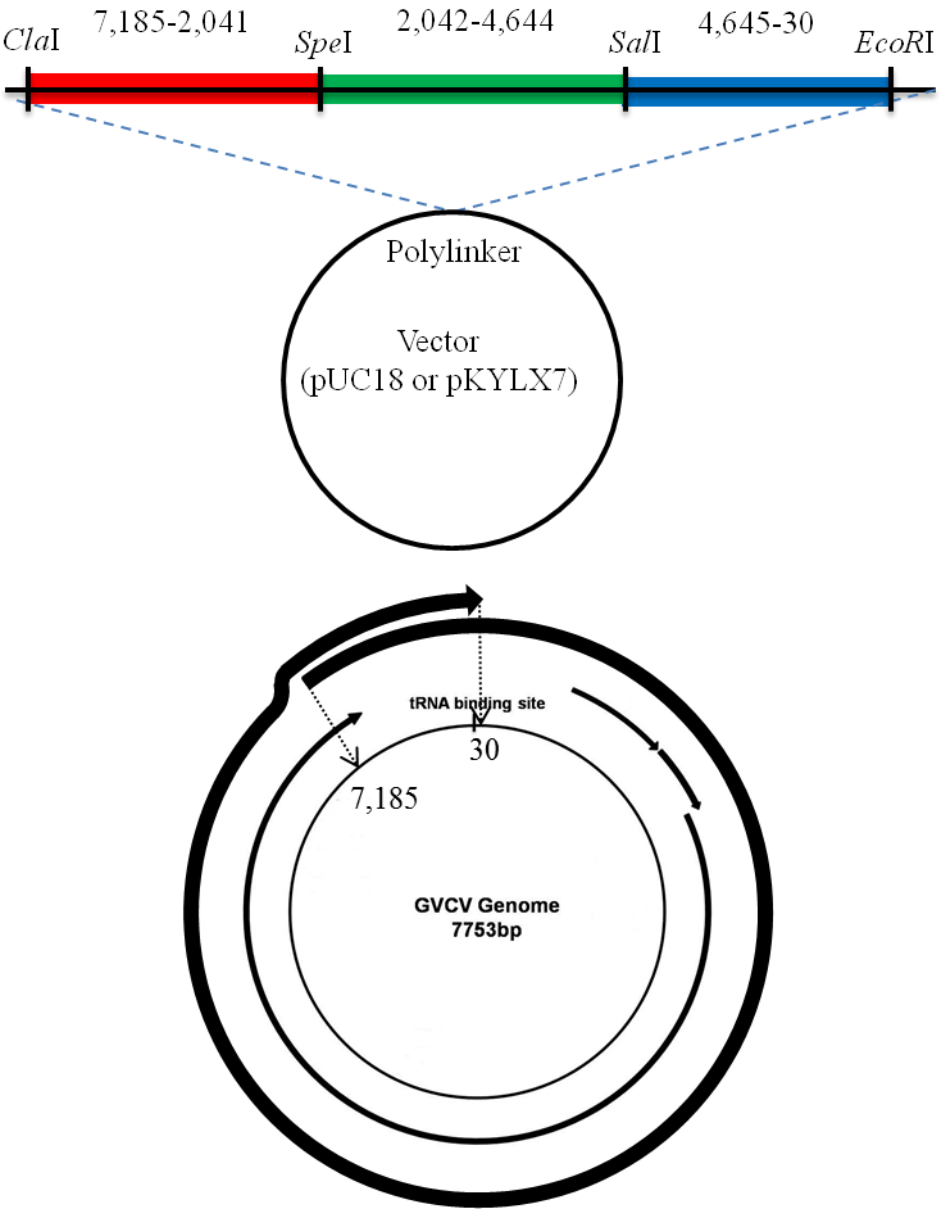

Fig. 4-4 Assemble of GVCV infectious clone

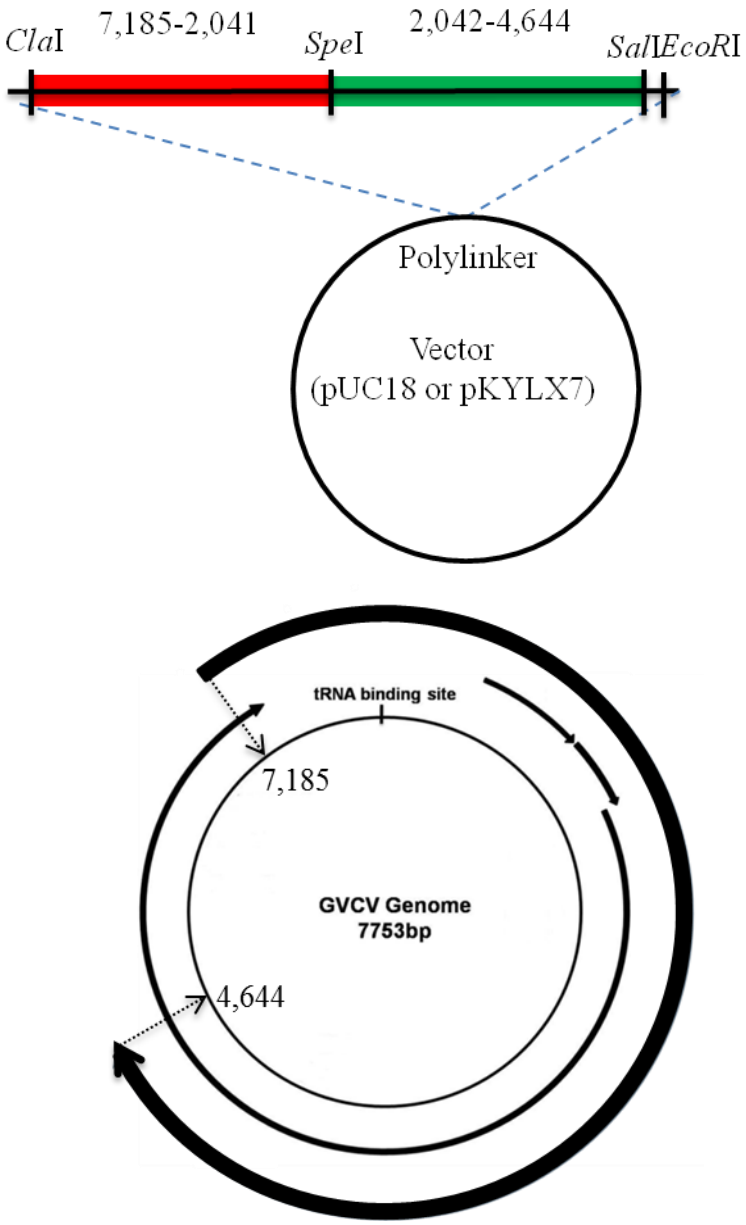

Fig. 4-5 Assemble of GVCV infectious clone negative control plasmid

truncated transcript, but would not be expected to be reverse transcribed into DNA and encapsidated.

Nucleotide sequencing of the amplified GVCV DNA segments showed that there were several single nucleotide differences within pGVCV-1 compared to the published GVCV nucleotide sequence (Isolate LBC0903, accession number JF301669, Zhang *et al*., 2011). In comparing the putative amino acid sequences of the three proteins of pGVCV-1 to LBC0903, the P1 amino acid sequences were identical, whereas the amino acid sequence of the pGVCV-1 P2 protein differed from LBC0903 at only amino acid 80 (as substitution of a valine in pGVCV-1 for an isoleucine in LBC0903. There were three amino acid differences that distinguished the P3 polyprotein of pGVCV-1 from LBC0903. The 144th amino acid of the pGVCV-1 P3 protein was methionine instead of valine, and the 1032-1033rd amino acids of pGVCV-1 were valine-proline instead of alanine-leucine. There was also one significant difference in the large intergenic region that distinguished pGVCV-1 from LBC0903. pGVCV-1 contained a 16 bp deletion at nucleotides 7397-7413 relative to the nucleotide sequence of LBC0903 (Fig. 4-6). This deletion was 126 nucleotides upstream from the TATAT box of the GVCV promoter (Zhang *et al*., 2015). Because pGVCV-1 was amplified from total DNA isolated from a GVCV-infected grapevine, it is not clear whether the nucleotide differences between pGVCV-1 and LBC0903 represent the diversity of the GVCV population in an infected plant or if the differences might be associated with PCR error.

```
        7301                    7350
LBC0903 …ACGTAAGCAATGACGACTAGGGATAATAATGGAGGAATCTTGTAAGGACA
Fragment
4628-30 …NNGTAN-CAATGACGACTAGGGATAATAATGGAGGAATCTCGTAAGGACA
        7351                    7400
LBC0903 GCACATGGTCCTTCTTTCCTCTTTTCTTTTGTAATTTTTGTCTTCTTGTG
Fragment
4628-30 GCACATGGTCCTTCTTTCCTCTTTTCTTTTGTACTTTTTGTCTTCTT---
        7401                    7450
LBC0903 TCGGCAACCGCTCCTTTTGTAAAGAGGAATCTGCTTTTGAGCTGTCGATG
Fragment
4628-30 ----------CTTTTGTAAAGAGGAATCTGCTTTTGAGCTGTCGATG
        7451                    7500
LBC0903 GGGCCCAATGTGTGTACCCGAGCTCTAAAAGTAACTTACCTCTAGTTGCT…
Fragment
4628-30 GGGCCCAATGTGTGTACCCGAGCTCTAAAAGTAACTTACCTCTAGTTGCT…
```

Fig. 4-6 16 bp deletion within the intergenic region of fragment 4628-30. Text highlighted in red indicates the 3’ end of ORF III.

2.2. Encapsidated GVCV DNA was detected from *Nicotiana benthamiana* leaves infiltrated with pGVCV-1 and some plants develop systemic symptoms

In Chapter 3, I validated an assay that linked agroinfiltration, virion purification, and PCR to distinguish a replicating form of *Cauliflower mosaic virus* (CaMV) from a nonreplicating form. The assay was based on the observation that encapsidated CaMV DNA is protected from DNaseI treatment, and in fact the DNaseI treatment of virions is a standard step in the isolation of CaMV DNA from plants (Gardner *et al.*, 1981). Consequently, only viral DNA isolated from purified virions, viral DNA that in itself would be a product of reverse transcription, would be available for a subsequent PCR assay.

To examine whether pGVCV-1 was capable of replication, pGVCV-1 and pGVCV-N were agroinfiltrated into young *N. benthamiana* leaves, and 20 g of leaves were collected at 7 days post-infiltration (dpi). The leaves were homogenized in CaMV virion grinding buffer, and each preparation was subjected to 75 minutes of centrifugation at 190,000 x g to pellet any virions formed in the leaves. The pellets were resuspended in H_20 and treated with DNaseI to eliminate unencapsidated DNA, followed by isolation of the encapsidated viral DNA as described for CaMV (Gardner *et al.*, 1981). To detect GVCV viral DNA, PCR was performed using primers 4628F and 30R (Table 4-1). As shown in Fig. 4-7, GVCV viral DNA was amplified successfully from leaves agroinfiltrated with pGVCV-1, but not from leaves

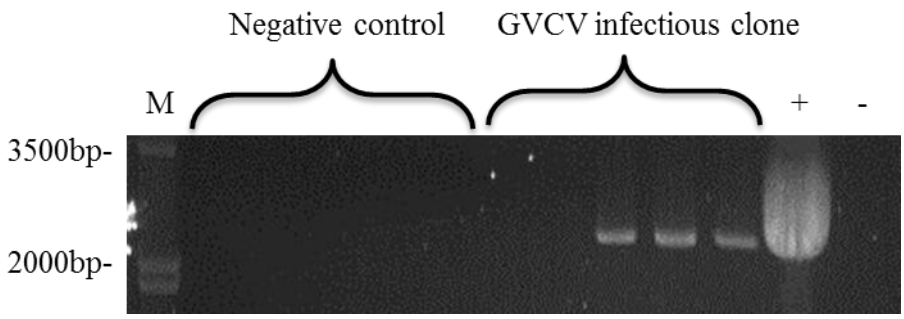

Fig. 4-7 PCR result that shows GVCV infectious clone is able to replicate and produce GVCV virions within *N. benthamiana* leaves. DNA was series diluted before PCR, numbers above the gel indicate different dilution factors.

agroinfiltrated with pGVCV-N. This assay suggested that pGVCV-1 is able to generate viral DNA that can be encapsidated into a GVCV nucleocapsid within the agroinfiltrated leaves.

Systemic vein clearing was observed in some *N. benthamiana* plants infiltrated with GVCV-1. Typically, a vein-clearing symptom that resembles the symptoms in GVCV-infected grape leaves was observed in the basal portion of upper, noninoculated *N. benthamiana* leaves (Fig. 4-8A). The symptoms appeared at 7 dpi, and became very obvious at 10 dpi. To verify that the systemic symptoms were truly caused by GVCV-1, total DNA was purified from symptomatic upper, non-inoculated leaves and screened for the presence of GVCV DNA using primer pair 4628F and 30R-*Eco*RI. An expected 3,162 bp DNA band was amplified successfully by PCR from multiple leaves that exhibited vein-clearing symptoms (Fig. 4-8B). The amplified DNA fragment was cloned into the *E. coli* plasmid pGEM-Teasy and submitted for sequencing at the University of Missouri DNA Sequencing Core Facility. A sequence analysis showed that the amplified DNA was derived from GVCV-1, as it contained the 16 bp deletion present at nucleotides 7398-7413 within the GVCV-1 clone (Fig. 4-9). This experiment showed that not only was GVCV-1 capable of replication and encapsidation, GVCV-1 was also capable of intercellular movement within leaves and systemic movement to young healthy leaves.

Interestingly, not all *N. benthamiana* plants infiltrated with GVCV-1 developed systemic vein clearing symptoms. Systemic movement of GVCV-1 was confirmed by

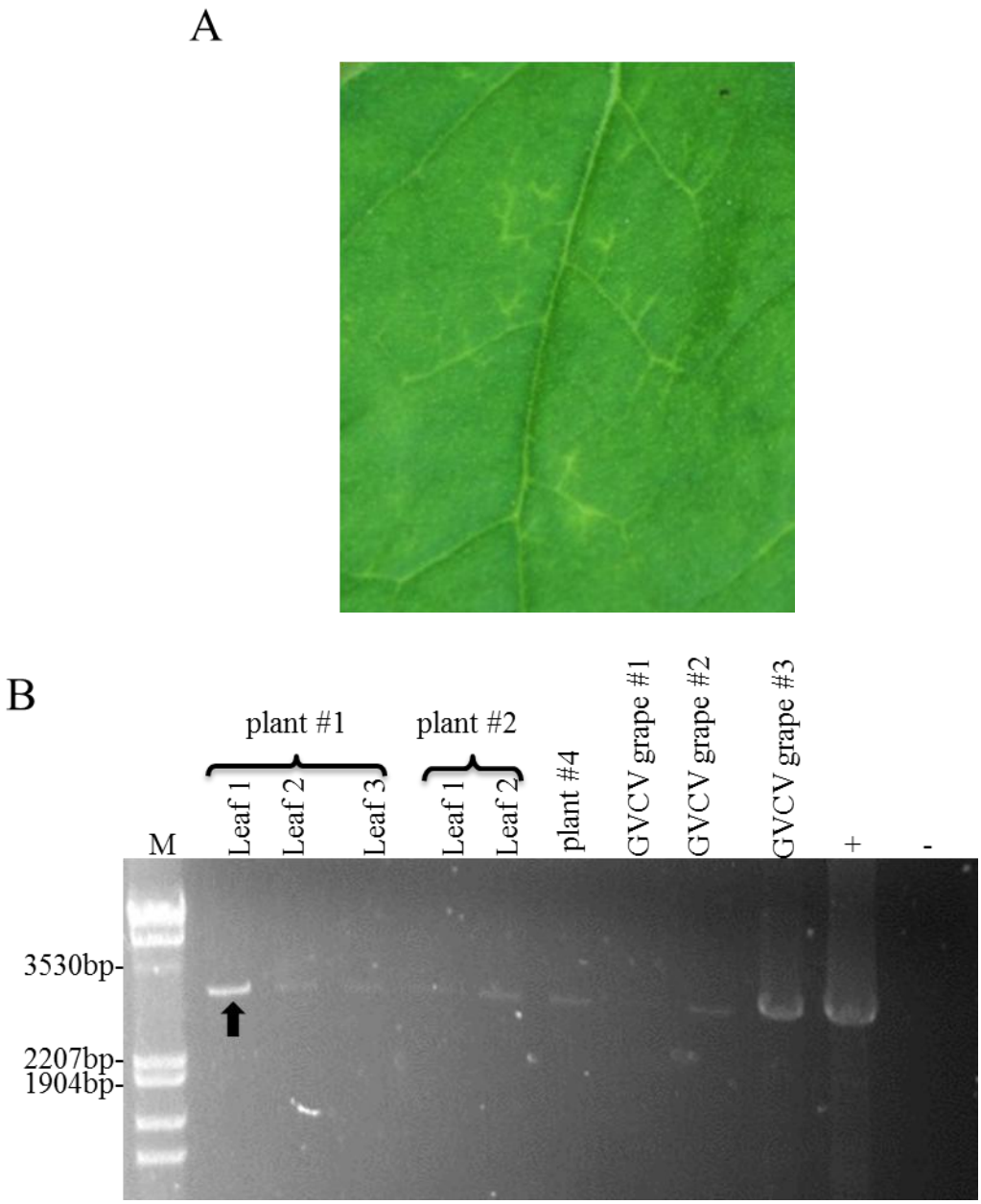

Fig. 4-8 Systematic infection of *N. benthamiana* caused by pGVCV-1 agroinfiltration. (A) Putative vein clearing symptoms observed on uninfiltrated newly grown *N. benthamiana* leaves caused by GVCV infectious clone, indicating systemic infection. (B) PCR using primer 4628F and 30R-EcoR I detected GVCV DNA from those leaves. Plant #1, #2 and #4 are three *N. benthamiana* showed putative vein clearing symptoms, GVCV grape #1, #2, and #3 are GVCV infected grapevine leaves.

```
           7301
LBC0903    …ACGTAAGCAATGACGACTAGGGATAATAATGGAGGAATCTTGTAAGGACA
GVCV-N.b   …NNGTAN-CAATGACGACTAGGGATAATAATGGAGGAATCTCGTAAGGACA

           7351
LBC0903    GCACATGGTCCTTCTTTCCTCTTTTCTTTTGTAATTTTTGTCTTCTTGTG
GVCV-N.b   GCACATGGTCCTTCTTTCCTCTTTTCTTTTGTACTTTTTGTCTTCTT---

           7401
LBC0903    TCGGCAACCGCTCCTTTTGTAAAGAGGAATCTGCTTTTGAGCTGTCGATG
GVCV-N.b   ----------CTTTTGTAAAGAGGAATCTGCTTTTGAGCTGTCGATG

           7451
LBC0903    GGGCCCATTGTGTGTACCCGAGCTCTAAAAGTAACTTACCTCTAGTTGCT…
GVCV-N.b   GGGCCCAATGTGTGTACCCGAGCTCTAAAAGTAACTTACCTCTAGTTGCT…
```

Fig. 4-9 DNA sequences recovered from symptomatic *N. benthamiana* contains the 16 bp deletion. Mutations are highlighted in red.

visual inspection and PCR in only three of six agroinfiltration tests (Table 4-2). In each test, 20 to 30 plants were agroinfiltrated with pGVCV-1, and even when systemic movement was confirmed, it was only seen in 1 to 3 plants per test. Furthermore, the symptoms were confined to only a few of the upper, non-inoculated leaves. Consequently, I concluded that pGVCV-1 is capable of limited systemic movement in *N. benthamiana*; however, further work needs to be done to identify the exact conditions that foster systemic infections, whether plants must be agroinoculated at a specific stage, a specific tissue type must be targeted, or specific environmental conditions must be identified.

2.3. Attempts to isolate GVCV viral particles from *N. benthamiana* leaves agroinfiltrated with pGVCV-1

The previous PCR results showed that pGVCV-1 could replicate and form a nucleocapsid in inoculated *N. benthamiana* leaves. To further demonstrate that pGVCV-1 was capable of forming virions, we utilized a standard purification scheme for purification of caulimovirus virions to isolate GVCV virions and observe them under an electron microscope.

pGVCV-1 was agroinfiltrated into *N. benthamiana* leaf tissue that had an approximate weight of 200 g and agroinfiltrated leaves were collected at 7 dpi. Virions were purified according to the procedure described in Chapter 3 and the preparation was examined for virus particles with an electron microscope.

Date	Number of *N. benthamiana* infiltrated with GVCV infectious clone	PCR positive for upper non-inoculated leaves*	Sequencing
7/21/15	20	1/1	N/A
8/21/15	20	2/2	Confirmed
9/6/15	30	3/4	N/A
9/25/15	20	0/3	N/A
10/10/15	20	0/5	N/A
3/18/16	20	0/2	N/A

***** Numbers indicates: number of upper non-inoculated leaves that are proved to be GVCV positive by PCR/numbers of upper non-inoculated showing putative vein clearing symptoms. PCR was performed with primers GVCV 4628F and GVCV 30R-EcoR I.

Table 4-2 Replication of GVCV infectious clone infiltration in young *N. benthamiana*.

Badnaviruses are known to form bacilliform virions that have an average width of 30 nm and a length of 120-150 nm (Tidona & Darai, 2011); however instead of bacilliform virions, I found only long flexuous rods that had a diameter of 15 nm and varying lengths (Fig. 4-10).

Ninety-three flexuous rod particles were observed from four individual virion preparations (Fig. 4-11). The average length of all 93 virions was 390 nm, but the lengths of individual virions varied dramatically from 80 nm to 900 nm (Table 4-3). Interestingly, a hook-like structure can be observed on some of the flexuous particles (Fig. 4-10, panel C and panel E), but the nature and function of this hook structure is unknown. In addition, the ends of some flexuous particles seemed to be broken, indicating these flexuous particles might have been longer and the centrifugation might have broken them down into shorter particles (Fig. 4-10, panels A-E, and panel K). No bacilliform virions were observed in any of these four tests.

To investigate the possibility that these flexuous particles might be present in healthy *N. benthamiana* genome, 200 grams of healthy *N. benthamiana* leaf tissue were collected and the same virion purification protocol was applied. Surprisingly, the same flexuous particles were also observed, but with a much lower frequency. Eleven flexuous particles were observed from three individual preparations of healthy *N. benthamiana*. At this moment it is unable to tell if these flexuous particles are found in healthy *N. benthamiana*, or if perhaps the healthy preparation was contaminated with virions from the earlier isolations conducted with pGVCV.

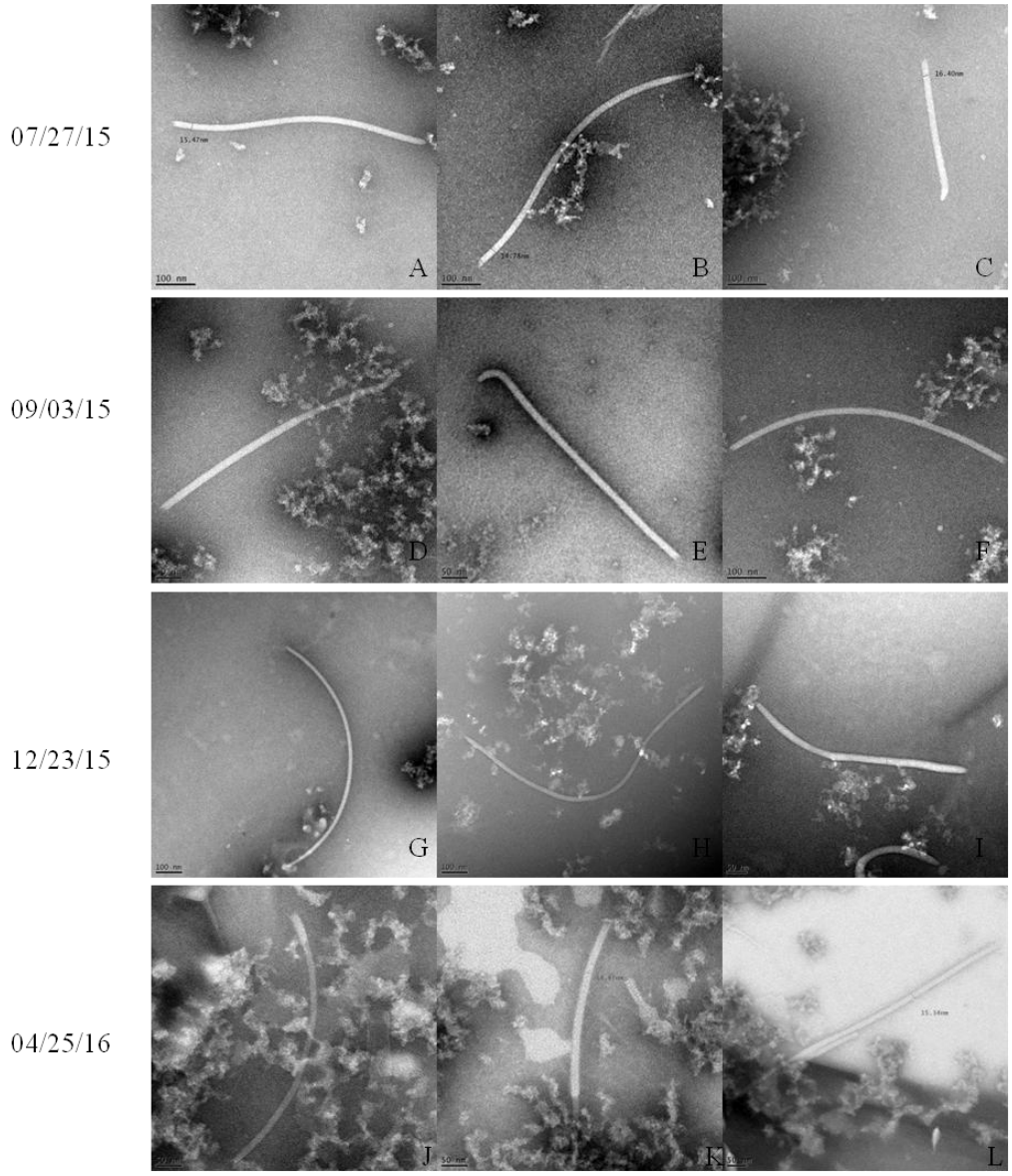

Fig. 4-10 Filamentous structure observed from *N. benthamiana* infiltrated with GVCV infectious clone. Dates indicate replications of infiltration and virion replication.

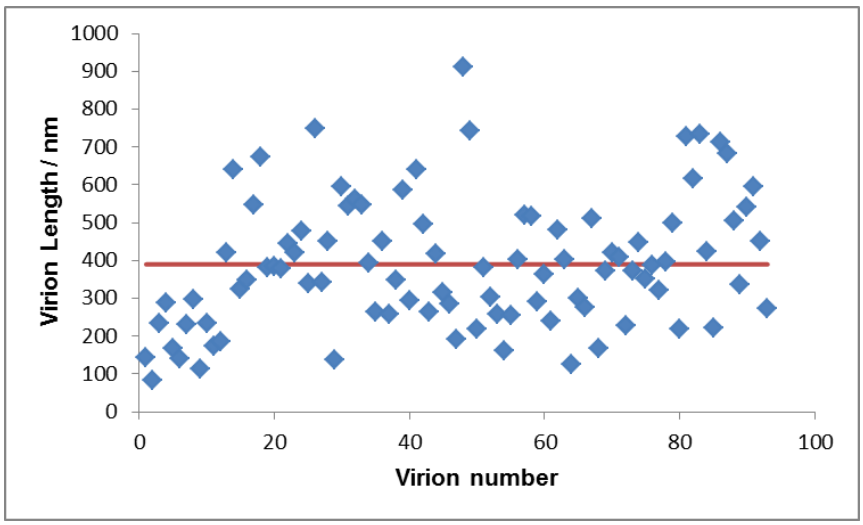

Fig. 4-11 Lengths of virions purified from *N. benthamiana* infiltrated with GVCV infectious clone vary dramatically. 93 measurements indicated. Red line indicates the average length.

	Number of observation	Width (nm)	Length (nm)
Flexuous virions from *N. benthamiana*	93	15	Average 390
Flexuous virions from grape	32	15	Average 3400
Bacilliform virions from *N. benthamiana*	0	N/A	N/A
Bacilliform virions from grape	17	30	160

Table 4-3 Two types of particles observed in *N. benthamiana* infiltrated with GVCV infectious clone and grape leaves showing vein clearing symptoms

2.4. Isolation of flexuous rods and bacilliform viral particles from GVCV infected grape leaves

Although the flexuous rods observed in the *N. benthamiana* virion preparation were unexpected, it did give us some insight in how to purify GVCV virions from symptomatic grape leaves. In particular, I recognized that I would need to start with more infected leaf material than would be necessary for CaMV, and that a sucrose gradient would be necessary to remove any plant debris for visualization of any particles with the electron microscope. Dr. Wenping Qiu (Missouri State University) provided 200 grams of symptomatic grape leaves and I also collected the same amount of tissue from Les Bourgeois vineyard. The virion purification procedure was the same as described for GVCV-1 purification from *N. benthamiana*.

Similar to the results with *N. benthamiana* and pGVCV-1, flexuous particles were observed in both samples of grape leaves. The diameter of the flexuous rods isolated from grape leaves was 15 nm; however, the length of the flexuous particles purified from grape leaves was much longer than ones purified from *N. benthamiana* (Fig. 4-12 and Fig. 4-13). Thirty-two flexuous particles were observed and measured. The average length was 3,400 nm while the longest particle observed was 8,250 nm (Fig. 4-12, panel B, and Table 4-3).

Interestingly, bacilliform particles were also observed in preparations from the grape leaves provided by Wenping Qiu, in addition to the flexuous rods. Seventeen bacilliform particles were measured, with a width of approximately 30 nm and an

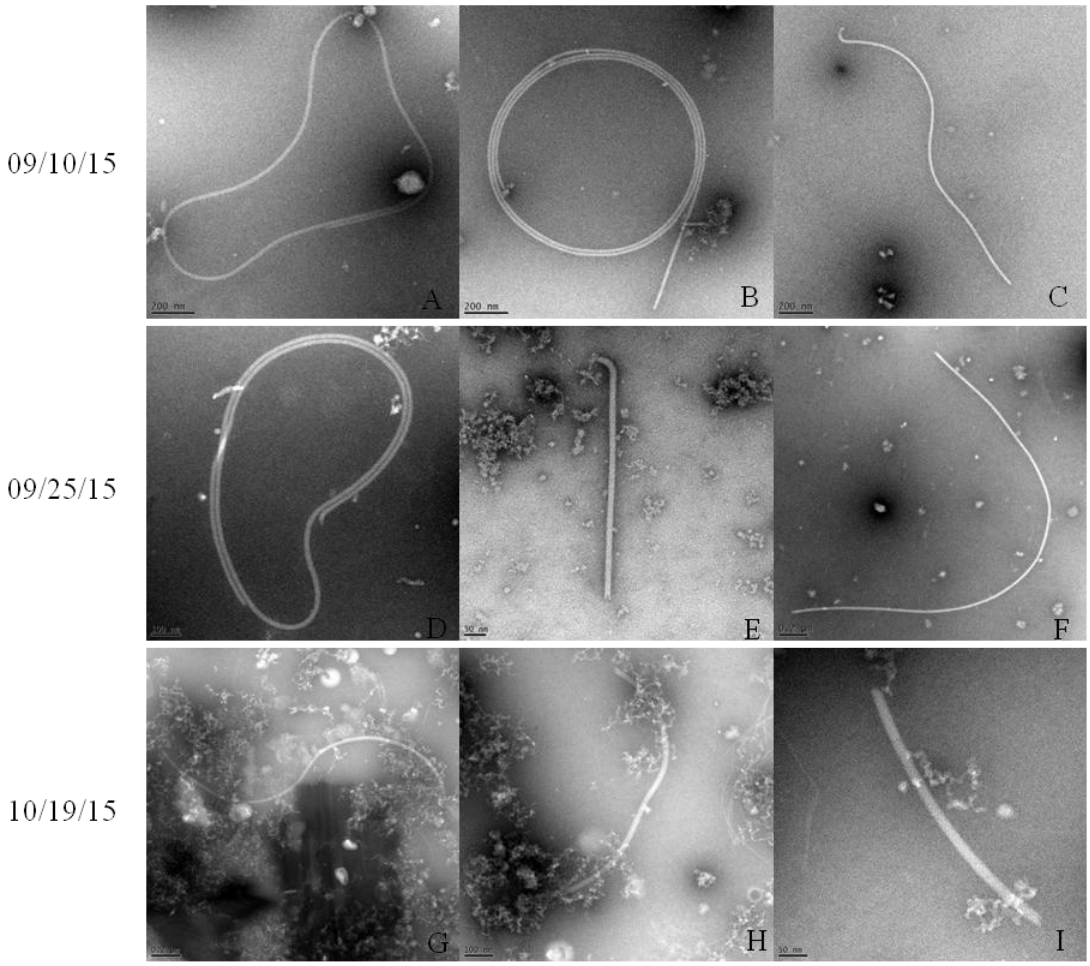

Fig. 4-12 Filamentous structure observed from symptomatic grape leaves. Dates indicate different replications of virion purification

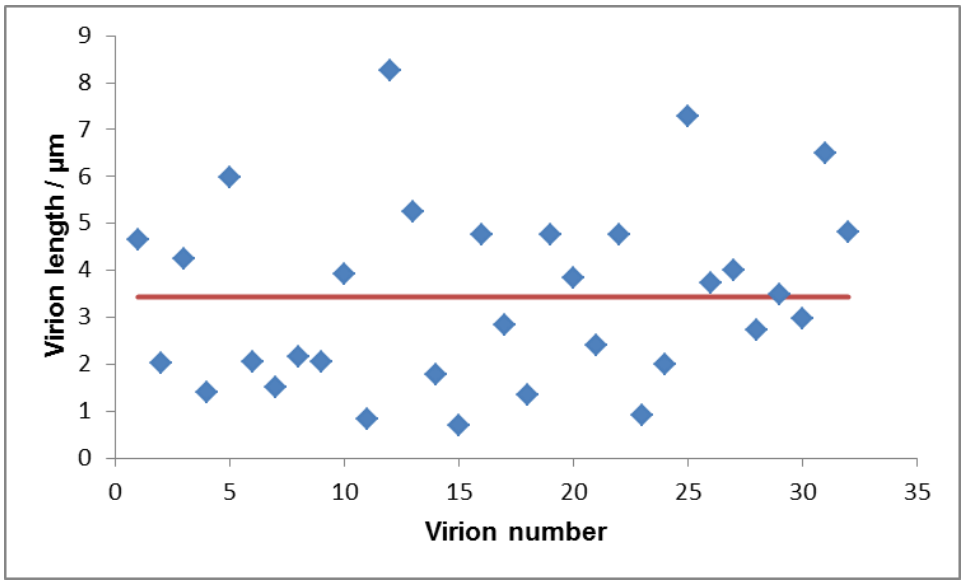

Fig. 4-13 lengths of virions purified from grapes with typical vein-clearing symptoms. 32 measurements indicated. Red line in the middle shows the average length. Red line indicates the average length.

average length of 160 nm (Fig. 4-14, Table 4-3).

To examine the possibility that the flexuous particles might be associated in some manner with healthy grapes, 200 grams of healthy grape leaves were collected and the virion purification protocol was applied. As with healthy *N. benthamiana* leaves, flexuous rod particles were observed (twenty-one flexuous rod particles observed from three individual preparations); however no bacilliform particles were found in the preparation from healthy plants. Further investigation is required to understand the source of the flexuous rod particles isolated from "healthy" plants.

2.5. Western blot failed to identify the GVCV CP due to the nonspecificity of GVCV CP antibodies

To further characterize GVCV, we attempted to create polyclonal antibodies against the GVCV CP. To identify GVCV CP amino acid sequences within ORF3, I used Vector NTI to align the CP sequences of putative *Banana streak MY virus* CP (Sharma *et al.*, 2014), putative C terminus of *Cacao swollen shoot virus* CP (Jacquot *et al.*, 1999), CaMV CP (Daubert *et al.*, 1982), putative C terminus of *Commelina yellow mottle virus* CP (Cheng *et al.*, 1996), and *Rice tungro bacilliform virus* CP (Marmey *et al.*, 1999) and the protein encoded by GVCV ORFIII (Fig. 4-15). The GVCV CP sequence was submitted to Genscript (Piscatawy NJ) and they synthesized three peptides to create three different antibodies.

Once we received the antibodies from Genscript, we first tested them against a

10/19/15

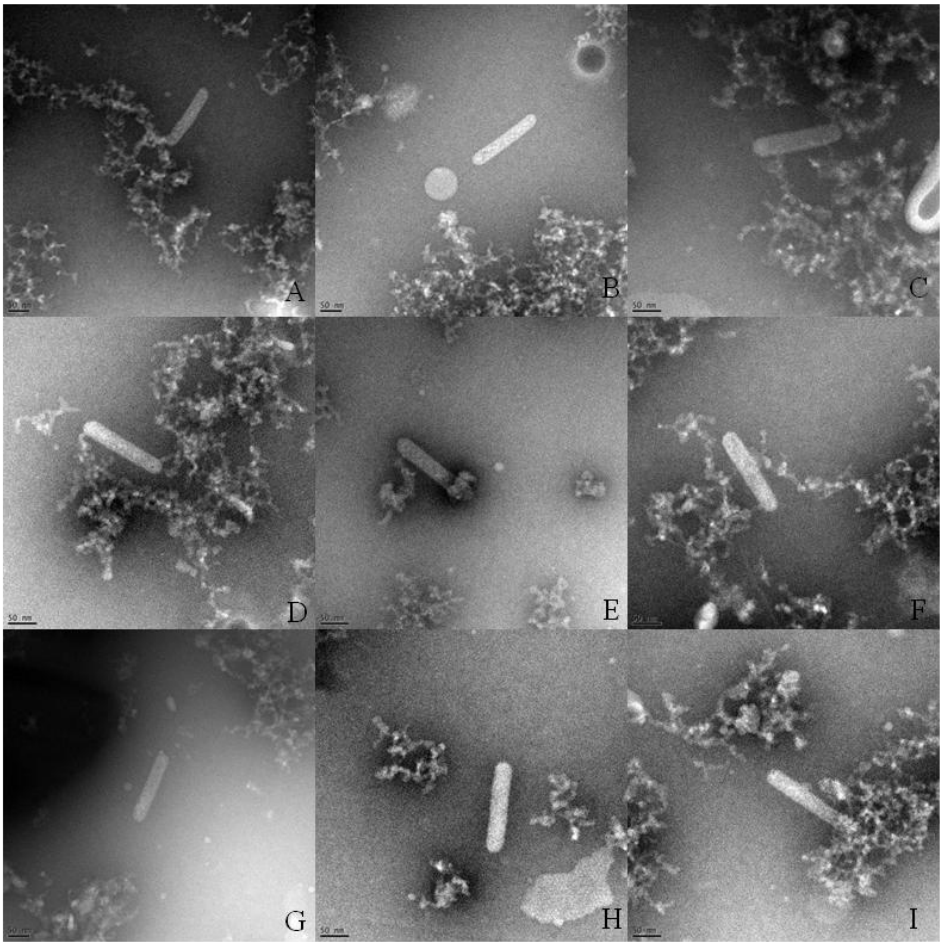

Fig. 4-14 Bacilliform virions observed from symptomatic grape leaves. All pictures were taken at Oct 19, 2015, from a single sample preparation.

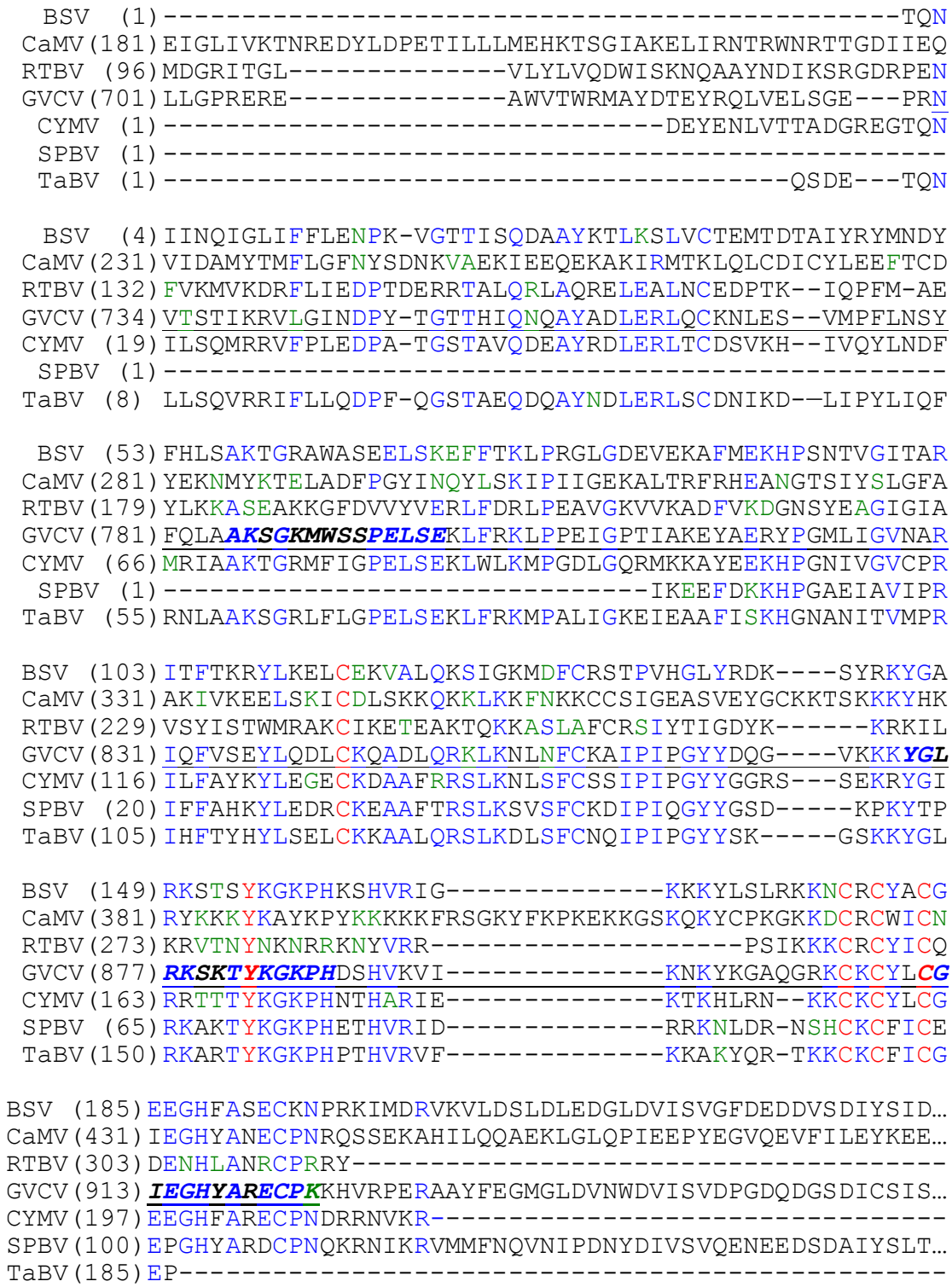

Fig. 4-15 Coat protein amino acid sequences alignment. Alignment was performed by Vector NTI. Blue: Conservative amino acids. Red: Identical amino

acids. Green: weakly similar amino acids. Sequences that are underlined are the predicted GVCV coat protein. Sequences with bold and italic letters are predicated antigen used in antibody production

virion preparation derived from 20 g of *N. benthamiana* agroinfiltrated with pGVCV-1 and a mock virion preparation created from 20 g of healthy *N. benthamiana* leaf tissue. Multiple protein bands were detected from the pGVCV-1 preparation and from healthy plant leaves with each of the three antisera. More importantly there was no difference between the virion preparation from pGVCV-1 inoculated leaves and from the healthy leaves (data not shown).

3. DISCUSSION

GVCV has been proven to be closely associated with vein clearing symptoms (Zhang *et al.*, 2011); however, Koch's postulates have never been completed due to the inability to purify GVCV virions and the difficulty to mechanically inoculate any plant virus to grape leaves. An infectious clone provides an alternative to the difficulties of purification and inoculation of GVCV virions and ultimately to determine whether GVCV is the causal agent of grapevine vein clearing disease observed in Midwest. Infectious clones have been made for five badnaviruses: *Rice tungro bacilliform virus* (RTBV) (Hay *et al.*, 1991), *Citrus yellow mosaic virus* (CYMV) (Huang & Hartung, 2001), *Cassava vein mosaic virus* (CsVMV) (De Kochko *et al.*, 1998), Rubus yellow net virus (RYNV) (Kalischuk *et al.*, 2013), *Cacao swollen shoot badnavirus* (CSSV) (Hagen *et al.*, 1994). In general, an infectious clone is constructed by cloning a greater-than-full-length (terminally redundant) genomic sequence into a binary Agrobacterium vector and then using Agrobacterium to deliver

the viral DNA into plant cells. In the case of the GVCV terminally redundant clone constructed in this chapter, the cloned sequences start at nt 7,185 and terminate at nt 30, resulting in a terminal redundancy of 598 bp.

I used Platinum High Fidelity Taq polymerase (Invitrogen) to amplify GVCV DNA from total DNA derived from symptomatic grape leaves in an attempt to avoid mutations during PCR. However, the DNA sequence cloned into the binary vector pKYLX7 still contained several base changes relative to the published GVCV isolate LBC0903. Most notably, there is a 16 bp deletion in the promoter region of DNA segment 4628-30 (Fig. 4-3). Given that the same mutations were detected in all sequenced colonies, there is no way to distinguish if these mutations were created during early steps of PCR, or if the nucleotide differences with the published sequence represent variation in the GVCV population in the leaf. Instead of continuing with cloning to try to identify a sequence that matched the published sequence, we decided to proceed with cloning these variant GVCV sequences into the binary vector pKYLX7 to create pGVCV-1 and test its infectivity by agroinfiltration into *N. benthamiana*. Our PCR assay for detection of GVCV viral DNA and the observation of systemic symptoms in some *N. benthamiana* plants confirmed the infectivity of pGVCV-1.

N. benthamiana is not a natural host of GVCV. As a result, there was always an inherent risk in testing the infectivity of pGVCV-1 through inoculation of *N. benthamiana*. If no encapsidated viral DNA was detected, it will be difficult to

distinguish between two possible explanations: it could be due to the inability of *N. benthamiana* to support the replication of pGVCV-1 or it could be due to the inability of pGVCV-1 to form functional GVCV virions. *N. benthamiana* was still chosen to test the infectivity of pGVCV-1 for the following three reasons: 1. in general, viruses are able to replicate and assemble within nonhosts cells; they typically are unable to move to adjacent cells and spread throughout the plant; 2. *N. benthamiana* can be infected by large number of diverse plant viruses (Goodin *et al.*, 2008), possibly due to its suppressed immunity. 3. *N. benthamiana* is the most widely used plant for agroinfiltration and we had previously shown that the GVCV promoter worked well upon agroinfiltration into *N. benthamiana* leaves (Zhang *et al.*, 2015). By contrast it is difficult to agroinfiltrate and express any gene in grape leaves, the natural host of GVCV. Consequently, for the purpose of initially testing the infectivity of pGVCV-1, *N. benthamiana* is a better choice than grapevine.

In addition to the PCR evidence for replication of pGVCV-1, I also found that some *N. benthamiana* plants developed a distinct vein-clearing symptom. The fact that systemic infection was induced in some but not all *N. benthamiana* infiltrated with GVCV infectious clone is very interesting. However, the reason why it cannot be consistently repeated in all tests is unknown. One possible explanation is that we may be selecting for mutated GVCV strains that have a higher infectivity and are able to cause systemic infections. Mutations might be introduced into the GVCV genome during replication, given the reverse transcriptase does not have a capacity for proof

reading. Another possibility is that specific environmental conditions might be required for systemic infection. For example, CaMV infections of *Nicotiana* species are influenced by light quality, light intensity, and duration (Qiu *et al.*, 1997; Wintermantel *et al.*, 1993). Further research will be necessary to determine whether the GVCV systemic infections of *N. benthamiana* are influenced by genetic or environmental conditions.

GVCV belongs to the family *Calimoviridae* genus *Badnavirus*, based on its sequence alignment (Zhang *et al.*, 2011) and badnaviruses generally form bacilliform virions with a diameter of 30 nm and a length of 120-150 nm (Tidona & Darai, 2011). The bacilliform virions observed from GVCV-infected grape leaves provided by Dr. Wenping Qiu (Missouri State University) fit this criteria, as they had a diameter of 30 nm and a length of 160 nm. However, only flexuous rod particles were observed from the virion preparation purified from Les Bourgeois vineyard. There are several possible explanations for this inconsistency: grape leaves provided by Wenping Qiu were collected from greenhouse, whereas grape leaves from Les Bourgeois vineyard might face a completely different environmental condition; alternatively, it might be that the GVCV collected from Les Bourgeois vineyard might have slight differences in its coat protein sequence that foster the formation of flexuous rods. It is significant that the GVCV preparations from Missouri State contained a mixture of both bacilliform virions and flexuous rods. Interestingly, the flexuous rods isolated from grape leaves exhibiting GVCV symptoms were much longer than the flexuous rods

isolated from *N. benthamiana* agroinfiltrated with pGVCV-1. The flexuous rods isolated from grape leaves had an average of 3,400 nm of length, which is far longer than most plant viruses. With a genome size of 7,753 bp (Zhang *et al.*, 2011), it is unlikely that a virion of 3,400 nm would contain GVCV DNA throughout its entire length unless this virion contained multimers of the GVCV genome. Further investigation is required to answer the questions raised by these observations.

Flexuous rod structures have been previously associated with badnavirus virion preparations. For example, flexuous rod particles with varied greatly in length were observed with other badnaviruses such as *Piper yellow mottle virus* (Lockhart *et al.*, 1997) and *Schefflera ringspot virus* (Lockhart & Olszewski, 1996). It was claimed that those protenaceous structures contain no nucleic acid detectable by ethidium bromide staining (Lockhart *et al.*, 1997; Lockhart & Olszewski, 1996), but an ethidium bromide staining procedure may not be as sensitive as a PCR assay. At this point, no conclusion can be made for questions such as: 1. Are these bacilliform and flexuous particles different forms of GVCV virions? 2. Do these particles contain GVCV DNA? 3. Why are the flexuous particles observed in grape much longer than those observed in *N. benthamiana*? Further investigation is required in the future.

On the other hand, the flexuous particles observed from both *N. benthamiana* leave tissue infiltrated with pGVCV-1 as well as symptomatic grape leaves may have a more mysterious nature. Significantly, flexuous particles were observed in both healthy *N. benthamiana* and healthy grape leaves. I attempted to eliminate any

sources of contamination from virus-infected leaves, treating all tubes, bottles, tips, stirring bars, and spatulas used in the experiment with either bleach or autoclaving before their use. Although contamination may remain a source for the flexuous rods, it may be that healthy plants contain these types of particles. Interestingly, many if not most plant genomes contain integrated caulimovirus sequence (Geering *et al.*, 2014), and in the case of petunia, *Arabidopsis thaliana* and *N. edwardsonii* it has been shown that these integrated sequences can be released, replicate episomally, and form virions (Lockhart *et al.*, 2000; Richert-Pöggeler & Shepherd, 1997; Squires *et al.*, 2011).

To confirm if the flexuous particles are a form of GVCV virions, I attempted to create a GVCV-specific antibody raised against three peptide sequences within the GVCV coat protein. However, all three of the coat protein antibody preparations were detecting non-specific proteins in healthy *N. benthamiana*. It may be that we are detecting non-specific interactions with host proteins. However, given that plants contain caulimovirus sequences and at least in some cases these sequences can be released to replicate and form virions, it is possible that we may be detecting an endogenous caulimovirus coat protein with our antibodies. Further research will be necessary to analyze the nature of the host proteins detected with the GVCV antibodies.

4. METHODS

4.1. Amplification of GVCV sequences and development of pGVCV-1

Three overlapping DNA fragments were amplified from DNA of symptomatic grape tissue using primers listing in Table 4-1. DNA fragment 7,185-2049 was amplified using primer 7185F-*Cla*I and 2049R with *Platinum*® *Taq* high fidelity DNA polymerase (Invitrogen by Life Technologies™, Carlsbad, CA) following the manufacturer's instructions. Primers 1945F and 4663R were used to amplify DNA fragment 1945-4663, and primers 4628F and 30R-*Eco*RI were used to amplify fragment 4628-30. The PCR program was: 94℃ for 2 min for initial denaturation, followed by 30 cycles of 94℃ for 30 s, 58℃ for 30 s and 68℃ for 4 min, and then 68℃ for another 10 min for a final extension. PCR products were analyzed in a 1% agarose gel and DNA bands were visualized using the Fotodyne™ FOTO/Analyst™ Investigator Eclipse UV Workstation photodocumentation system (Fotodyne, Hartland, WI). Amplified fragments were ligated into the pGEM-T easy plasmid vector (pGEM®-T Easy Vector System I, Promega, Madison, WI) following the manufacturer's protocol, and cloned fragments were sent to the University of Missouri DNA Core Facility for sequencing.

The multiclone sites of the intermediate vector pUC18 and the binary vector pKYLX7 were modified to add restriction enzyme sites *Cla*I, *Spe*I, and *Sal*I. Two reverse complementary polylinker primers, polylinker F2 and polylinker R2 (Table 4-1), were designed. Each primer has ten restriction recognition sites line in the order: *Hind*III, *Cla*I, *Sph*I, *Spe*I, *Pst*I, *Sal*I, *Bam*HI, *Kpn*I, *Sac*I, and *Eco*RI. Furthermore, either GGGG or CCCC nucleotide sequences were added to each end of the primer to

increase the terminal sensitivity of restriction enzymes. To replace the polylinker of pUC18 with the modified polylinker, 10 µl of 10 nM polylinker F2 and 10 µl of 10 nM polylinker R2 were mixed and boiled for 10 min, and the mixture was cooled down to room temperature for primer binding. Both pUC18 and the polylinker dimer were cut with *Eco*RI and *Hind*III at 37℃ for 1 hour, and ligated by T4 ligase (Promega, Madison, WI) at 4℃ overnight. The ligated DNA was transformed into *E. coli* strain JM101 and colonies were grown on LB plates with 100 µg/ml ampicillin for screening. The binary vector pKYLX7 was modified to remove its 35S promoter, present on an *Eco*RI-*Hind*III DNA fragment and replace it with the modified polylinker DNA following the same protocol, except colonies were selected on LB plates with 100 µg/ml kanamycin.

4.2. GVCV infectious clone assembly

Three fragments were assembled in the intermediate vector pUC18 containing the modified polylinker with the addition of *Cla*I, *Spe*I and *Sal*I. Fragment 7185-2049 and the modified pUC18 were digested by *Cla*I and *Spe*I, and DNA bands separated in a 1% agarose gel. DNA bands were recovered from the gel using a QIAquick® Gel Extraction Kit (Qiagen, Germantwon, MD) and ligated using T4 ligase (Promega, Madison, WI) at 4℃ overnight. The ligated DNA was transformed into JM101 and colonies were grown at LB plates with 100 µg/ml ampicillin for blue/white screening. The clone containing the GVCV insert was designated pUC7185-2041.

The GVCV DNA clone 1945-4663 was added into pUC7185-2041 in the following steps. Both the 1945-4663 GVCV DNA and pUC7185-2041 were cut with *Spe*I first, and then DNA was precipitated and recovered by ethanol precipitation, followed by a second digestion with *Sal*I. Bands were recovered from 1% agarose gel and ligated and transformed into JM101. The resulting clone was designated pUC7185-4644.

GVCV DNA fragment 4628-30 was added to pUC7185-4644 to complete the formation of a terminally redundant GVCV clone in a pUC derivative. The GVCV DNA fragment 4628-30 and pUC7185-4644 were digested with *Spe*I and *Eco*RI. The digested DNA was separated by agarose gel electrophoresis and individual bands were recovered from the gel before they were combined and ligated to make the terminally redundant clone, pUC7185-30. To form pGVCV-1, pUC7185-30 and pKYLX7 containing the modified polylinker were digested with *Cla*I and *Eco*RI, and the terminally redundant GVCV fragment 7185-30 was inserted into the modified binary vector pKYLX7. The negative control plasmid pGVCV-N was formed by insertion of the GVCV DNA fragment in pUC7185-4644 into the *Cla*I and *Eco*RI sites of the modified pKYLX7. The plasmids pGVCV-1 (also known as pKY7185-30) and pGVCV-N were electroporated into *Agrobacterium tumefaciens* strain Agl-1 as described previously (Lazo *et al.*, 1991). Transformants were selected on Luria Bertani (LB) medium supplemented with kanamycin (50μg/ml).

All restriction enzymes were purchased from either from New England Biolabs

(Ipswich, MA) or Promega (Madison, WI).

4.3. Growth and maintenance of plants, and agroinfiltration conditions

Plants were grown under greenhouse conditions, with sufficient water and controlled-release fertilizers. Plants were grown for at least two months before being agroinfiltrated. Agroinfiltration was performed following the standard lab protocol described in Chapter 3.

4.4. Virion purification, viral DNA isolation, and PCR for detection of GVCV viral DNA

The virion purification protocol for GVCV from *N. benthamiana* was modified from the CaMV virion purification protocol described in Chapter 3 with an additional ultracentrifugation step and a sucrose gradient centrifugation step. Two hundred grams of agroinfiltrated leaves were homogenized in 1X grinding buffer (200 mM Tris pH 7.0-7.4, 20 mM EDTA, 1.5 M urea) at 6 ml buffer per gram, and triton-X100 was subsequently added to a final concentration of 2%. The solution was stirred overnight to release virions from potential inclusion bodies, followed by centrifugation at 15,000 g for 10 min. The supernatant was poured through one layer of miracloth (Calbiochem, San Diego CA) to remove plant debris and the virions were pelleted through centrifugation at 190,000 g for 75 min at 8℃. Putative virion pellets were rinsed with dH_2O for three times before resuspension in 10 ml of autoclaved

dH_2O overnight with stirring. A second round of ultracentrifugation at 190,000 g for 75 min was performed to further concentrate virions prior to sucrose gradient centrifugation. The pellet was collected and resuspended in 2 ml of autoclaved dH_2O overnight with stirring. A sucrose step gradient was made by placing layers of 5 ml of 40% sucrose, 10 ml of 30% sucrose, 10 ml of 20% sucrose, and 10 ml of 10% sucrose in Ultra Clear centrifuge tubes (#344058, Beckman, Palo Alto, CA) from bottom to top. The sucrose gradient was stored at 4℃ overnight to equilibrate.

The concentrated virion pellet was loaded onto the surface of the sucrose gradient, and was centrifuged at 132,000 g for 2 hours with a Beckman SW27 swinging bucket rotor. Most debris was pelleted at the bottom of column, and there was no visible layer of GVCV virions, which we expected due to the low titer of GVCV. Approximately two thirds of the sucrose gradient was collected and the virions were pelleted in a final round at 190,000 g for 75 min. The pellet was resuspended in 1 ml of autoclaved water with overnight stirring. All tubes, beakers, bottles, tips, stirring bars, and spatulas used in the experiment were sterilized by either treatment with bleach or through autoclaving before use.

GVCV viral DNA was isolated following the standard lab protocol described in Chapter 3. In this procedure, virions were initially purified from 20 g agroinfiltrated *N. benthamiana* leaves at 7 dpi, followed by isolation of GVCV viral DNA. To detect GVCV viral DNA, I used primer pair 4628R and 30R-EcoRI (Table 4-1). PCR was performed using GoTaq® flexi DNA polymerase (Promega, Madison, WI) following

manufacturer's instructions. PCR cycles used for GoTaq were: 95℃ for 5 min for initial denaturation, followed by 35 cycles of 95℃ for 30 s, 58℃ for 30 s and 72℃ for 3 min, and then 72℃ for another 10 min for a final extension. DNA was separated in a 1% agarose gel.

4.5. Electron microscopy for virion observation and measurements

Virions were observed in University of Missouri Electron Microscopy core with negative staining as described in Chapter 3. Virion lengths were measured using the program Fiji (Schindelin *et al.*, 2012).

4.6. Antibody and western blot

The predicted GVCV CP amino acid sequences were submitted to Genscript (Piscataway, NJ) and Genscript was responsible for generating three polyclonal antibody preparations. Western blots were performed following standard lab protocol as described in chapter 3.

REFERENCES

Cheng, C.P., Lockhart, B. & Olszewski, N. E. (1996). The ORF I and II Proteins of Commelina Yellow Mottle Virus Are Virion-Associated. *Virology* **223**, 263-271.

Daubert, S., Richins, R., Shepherd, R. & Gardner, R. C. (1982). Mapping of the coat protein gene of *Cauliflower mosaic virus* by its expression in a prokaryotic system. *Virology* **122**, 444-449.

De Kochko, A., Verdaguer, B., Taylor, N., Carcamo, R., Beachy, R. & Fauquet, C. (1998). Cassava vein mosaic virus (CsVMV), type species for a new genus of plant double stranded DNA viruses. *Archives of virology* **143**, 945-962.

Gardner, R. C., Howarth, A. J., Hahn, P., Brown-Luedi, M., Shepherd, R. J. & Messing, J. (1981). The complete nucleotide sequence of an infectious clone of *Cauliflower mosaic virus* by M13mp7 shotgun sequencing. *Nucleic acids research* **9**, 2871-2888.

Geering, A. D., Maumus, F., Copetti, D., Choisne, N., Zwickl, D. J., Zytnicki, M., McTaggart, A. R., Scalabrin, S., Vezzulli, S. & Wing, R. A. (2014). Endogenous florendoviruses are major components of plant genomes and hallmarks of virus evolution. *Nature communications* **5**, 5269.

Goodin, M. M., Zaitlin, D., Naidu, R. A. & Lommel, S. A. (2008). *Nicotiana benthamiana*: its history and future as a model for plant-pathogen interactions. *Molecular Plant-Microbe Interactions* **21**, 1015-1026.

Grimsley, N., Hohn, T., Davies, J. W. & Hohn, B. (1987). Agrobacterium-mediated delivery of infectious maize streak virus into maize plants. *Nature* **325**, 177-179.

Hagen, L. S., Lot, H., Godon, C., Tepfer, M. & Jacquemond, M. (1994). Infection of Theobroma cacao using cloned DNA of cacao swollen shoot virus and particle bombardment. *Phytopathology* **84**, 1239-1243.

Hay, J. M., Jones, M. C., Blakebrough, M. L., Dasgupta, I., Davies, J. W. & Hull, R. (1991). An analysis of the sequence of an infectious clone of rice tungro bacilliform virus, a plant pararetrovirus. *Nucleic acids research* **19**, 2615-2621.

Hohn, T., Hohn, B., Lesot, A. & Lebeurier, G. (1980). Restriction map of native and

cloned *Cauliflower mosaic virus* DNA. *Gene* **11**, 21-31.

Huang, Q. & Hartung, J. S. (2001). Cloning and sequence analysis of an infectious clone of Citrus yellow mosaic virus that can infect sweet orange via Agrobacterium-mediated inoculation. *Journal of General Virology* **82**, 2549-2558.

Jacquot, E., Hagen, L., Michler, P., Rohfritsch, O., Stussi-Garaud, C., Keller, M., Jacquemond, M. & Yot, P. (1999). In situ localization of cacao swollen shoot virus in agroinfected Theobroma cacao. *Archives of virology* **144**, 259-271.

Jelly, N. S., Valat, L., Walter, B. & Maillot, P. (2014). Transient expression assays in grapevine: a step towards genetic improvement. *Plant biotechnology journal* **12**, 1231-1245.

Kalischuk, M. L., Fusaro, A. F., Waterhouse, P. M., Pappu, H. R. & Kawchuk, L. M. (2013). Complete genomic sequence of a Rubus yellow net virus isolate and detection of genome-wide pararetrovirus-derived small RNAs. *Virus research* **178**, 306-313.

Lazo, G. R., Stein, P. A. & Ludwig, R. A. (1991). A DNA transformation–competent Arabidopsis genomic library in Agrobacterium. *Nature Biotechnology* **9**, 963-967.

Lockhart, B., Kiratiya-Angul, K., Jones, P., Eng, L., De Silva, P., Olszewski, N., Lockhart, N., Deema, N. & Sangalang, J. (1997). Identification of Piper yellow mottle virus, a mealybug-transmitted badnavirus infecting Piper spp. in Southeast Asia. *European journal of plant pathology* **103**, 303-311.

Lockhart, B. & Olszewski, N. (1996). Schefflera ringspot virus, a widely distributed mealybug-transmitted badnavirus occurring in Schefflera and Aralia. In *IX International Symposium on Virus Diseases of Ornamental Plants **432***, 196-203.

Lockhart, B. E., Menke, J., Dahal, G. & Olszewski, N. (2000). Characterization and genomic analysis of tobacco vein clearing virus, a plant pararetrovirus that is transmitted vertically and related to sequences integrated in the host genome. *Journal of General Virology* **81**, 1579-1585.

Marmey, P., Bothner, B., Jacquot, E., de Kochko, A., Ong, C. A., Yot, P., Siuzdak, G., Beachy, R. N. & Fauquet, C. M. (1999). Rice tungro bacilliform virus open reading frame 3 encodes a single 37-kDa coat protein. *Virology* **253**,

319-326.

Qiu, S. G., WINTERMANTEL, W. M., SHA, Y. & SCHOELZ, J. E. (1997). Light-dependent systemic infection of solanaceous species by *Cauliflower mosaic virus* can be conditioned by a viral gene encoding an aphid transmission factor. *Virology* **227**, 180-188.

Richert-Pöggeler, K. & Shepherd, R. (1997). Petunia vein-clearing virus: a plant pararetrovirus with the core sequences for an integrase function. *Virology* **236**, 137-146.

Schindelin, J., Arganda-Carreras, I., Frise, E., Kaynig, V., Longair, M., Pietzsch, T., Preibisch, S., Rueden, C., Saalfeld, S. & Schmid, B. (2012). Fiji: an open-source platform for biological-image analysis. *Nature methods* **9**, 676-682.

Sharma, S. K., Kumar, P. V. & Baranwal, V. K. (2014). Immunodiagnosis of episomal Banana streak MY virus using polyclonal antibodies to an expressed putative coat protein. *Journal of virological methods* **207**, 86-94.

Squires, J., Gillespie, T., Schoelz, J. E. & Palukaitis, P. (2011). Excision and episomal replication of *Cauliflower mosaic virus* integrated into a plant genome. *Plant physiology* **155**, 1908-1919.

Tidona, C. & Darai, G. (2011). *The Springer index of viruses*: Springer. Berlin, Heidelberg, New York, 2011.

Wintermantel, W. M., Anderson, E. J. & Schoelz, J. E. (1993). Identification of domains within gene VI of *Cauliflower mosaic virus* that influence systemic infection of Nicotiana bigelovii in a light-dependent manner. *Virology* **196**, 789-798.

Zhang, Y., Angel, C., Valdes, S., Qiu, W. & Schoelz, J. (2015). Characterization of the promoter of *Grapevine vein clearing virus*. *Journal of General Virology* **96**, 165-169.

Zhang, Y., Singh, K., Kaur, R. & Qiu, W. (2011). Association of a novel DNA virus with the grapevine vein-clearing and vine decline syndrome. *Phytopathology* **101**, 1081-1090.

CHAPTER 5: TESTING MEALBUGS AS A POTENTIAL INSECT VECTOR OF *GRAPEVINE VEIN CLEARING VIRUS*

ABSTRACT

Two species of mealybugs, the longtailed mealybug (*Pseudococcus longispinus)*, and citrus mealybug (*Planococcus citri*), were tested for their ability to acquire and transmit *Grapevine vein clearing virus*. The longtailed mealybugs were collected from a cycad plant in Tucker greenhouse (University of Missouri), whereas a mixed population of longtailed and citrus mealybugs were collected from infested grapevines in the Ashland-Gravel greenhouses (University of Missouri). Both populations were able to acquire GVCV after short feeding periods of as little as three days. However, the tucker population was not able to persist on grapevines and was not tested for transmission of GVCV. The Ashland-Gravel population was allowed to feed on GVCV-infected grapevines for over one month, and then they were transferred to healthy grapevines for an additional month. The grapevines tested in 2015 were held for over one year for development of GVCV symptoms and were tested by PCR for GVCV infection. The grapevines tested in 2016 were tested two months after the end of the transmission tests. None of the plants developed symptoms indicative of GVCV, and PCR assays showed GVCV was not transmitted to any of the 31 grapevine plants. I conclude that the citrus and longtailed mealybugs are unlikely to be the vectors for GVCV.

1. INTRODUCTION

Unlike fungal, bacterial, and nematode pathogens, plant viruses are unable to be disseminated to plants without the assistance of some sort of vector. Most plant virus vectors are insects, but it is also possible for fungi and nematodes to serve as vectors. In general, a virus is transmitted by only a single type of vector. For example, a virus transmitted by aphids will not be transmitted by whiteflies, mites or thrips, much less by fungi or nematodes (Hull, 2002). On the other hand, viruses may be transmitted by multiple species within a genus. For example, some caulimoviruses may be transmitted by as many as 27 species of aphids (Schoelz, 2008).

GVCV belongs to genus *Badnavirus*, family *Caulimoviridae*. Most badnaviruses are transmitted by mealybugs, and only a few have been shown to be transmitted by aphids (Schoelz, 2008). The badnaviruses transmitted by mealybugs include *Banana streak virus (*BSV) (Su, 1998), *Cacao swollen shoot virus* (Dongo & Orisajo, 2007), *Citrus yellow mosaic virus* (Aparna et al., 2012), *Dioscorea alata bacilliform virus* (Phillips et al., 1999), *Kalanchoe top-spotting virus* (Hearon & Locke, 1984), *Pineapple bacilliform virus* (Sether et al., 2012), *Piper yellow mottle virus* (Lockhart et al., 1997), *Schefflera ringspot virus* (Lockhart & Olszewski, 1996), *Sugarcane bacilliform virus* (Lockhart & Autrey, 1991), and *Taro bacilliform virus* (Macanawai et al., 2005). Two Badnavirus species have been shown to be transmitted by aphids: *Gooseberry vein-banding associated virus*, *Rubus yellow net virus*, and *Spiraea yellow leafspot virus* (Hull et al., 2005). A list of badnavirus and their insect

vectors were shown in table 5-1.

In the case of BSV, Meyer *et al.* (2008) showed that this virus could be transmitted by three of four mealybugs species tested. *Planococcus citri* (Citrus mealybug), *P. ficus* (Vine mealybug), *Dysmicoccus brevipes* (Pineapple mealybug), and *Pseudococcus longispinus* (Longtailed mealybug) were allowed to feed on donor plants for 48 h for acquisition, and were moved to recipient plants for 120 h inoculation. Recipient plants were screened with ELISA and immunocapture-PCR at 3 and 6 months after inoculation to evaluate the transmission of BSV. Citrus mealybug, vine mealybug, pineapple mealybug were able to transmit BSV to the recipient plants, but all the plants inoculated with longtailed mealybugs remained BSV negative after six months.

Mealybugs have been shown to vector viruses to grapevine. For example, *Grapevine leafroll-associated viruses* (GLRaV- Closterovirus group), members of the *Closterovirus* genus that are associated with grapevine leafroll disease, were proven to be transmitted by mealybugs (Golino *et al.* 2002). Golino and coworkers (2002) tested four species of mealybugs for the transmission of GLRaV: *Pseudococcus longispinus* (longtailed mealybug), *Pseudococcus viburni* (obscure mealybug), *Pseudococcus maritimus* (grape mealybug), and *Planococcus citri* (Citrus mealybug). The feeding time ranged from 24 hours to 21 days, and plants were tested for GLRaV by ELISA at 3, 6 and 12 months. All four species were able to transmit GLRaV to healthy recipient plants with varied degrees of success. This study illustrates the type of mealybug

Virus	Vector	Citation
Banana streak virus	Mealybug	(Su, 1998)
Cacao swollen shoot virus	Mealybug	(Dongo & Orisajo, 2007)
Citrus yellow mosaic virus	Mealybug	(Aparna *et al*., 2012)
Dioscorea alata bacilliform virus	Mealybug	(Phillips *et al*., 1999)
Kalanchoe top-spotting virus	Mealybug	(Hearon & Locke, 1984)
Pineapple bacilliform virus	Mealybug	(Sether *et al*., 2012)
Piper yellow mottle virus	Mealybug	(Lockhart *et al*., 1997)
Schefflera ringspot virus	Mealybug	(Lockhart & Olszewski, 1996)
Sugarcane bacilliform virus	Mealybug	(Lockhart & Autrey, 1991)
Taro bacilliform virus	Mealybug	(Macanawai *et al*., 2005)
Rubus yellow net virus	Aphid	(Kalischuk *et al*., 2008) (Jones *et al*., 2002)
Spiraea yellow leaf spot virus	Aphid	(Lockhart & Geering, 2000) (Hull *et al*., 2005)

Table 5-1 Badnaviruses and their insect vector.

species that might be expected to transmit grape viruses, and the timeframe necessary for examining their vector capabilities.

In this chapter, I tested two mealybug species, the longtailed and citrus mealybugs, for their capacity to acquire and transmit GVCV. I found that GVCV DNA could be detected in both species after an acquisition feed, but neither was able to transmit GVCV to healthy grapevines in my tests.

2. RESULTS

2.1. Mealybug identification

To examine the potential for mealybugs to spread GVCV, two colonies of mealybugs were established on potatoes. One colony originated from mealybugs collected from a Cycad in Tucker greenhouse (University of Missouri-Columbia) and the other originated from mealybugs collected on grapes present in the Ashland-Gravel greenhouse (University of Missouri-Columbia). Mealybugs were identified to according to the procedure described in Daane *et al* (2011). Eight primers (PCa, PL, PF, PM, PC, PV, FG, MB-R) were generated (Table 5-2). PCa, PL, PF, PM, PC, PV, and FG were designed to be specific forward primers for the mealybug species *Pseudococcus calceolariae*, *Pseudococcus longispinus*, *Planococcus ficus*, *Pseudococcus maritimus*, *Planococcus citri*, *Pseudococcus viburni*, and *Ferrisia gilli*, respectively, and MB-R is a universal reverse primer. According to Daane *et al* (2011), for mealybugs of a certain species, only the primer set which contains the

GVCV2460F	AGACACAGGAGAAAGGGTAACT
GVCV3122R	GCTAAAACTTTCGAGCTAAC
GVCV4628F	CCATCACTGTACTTGGTCGACGTGC
GVCV30R	CCCAGATTTGAAACTGGAGCTCTGATACC
PCa	TGCAACAATAATTATTGCCATC
PL	CCATTTATCTTTGATCCACAG
PF	CTTTGTTGTAGCTCACTTTCAC
PM	CTGATTTCCTTTATTAATTAATTCAAC
PC	TAATCTATTTTTATCTATCAATTTAACC
PV	ATATTTCTTCTATTGGTTCATTC
FG	GAATCATTAATTTCTAAACGTTTACTAA
MB-R	CAATGCATATTATTCTGCCATATTA

Table 5-2 Primer list

species-specific forward primer and the universal reverse primer can amplify a band from mealybug DNA. Consequently, PCR amplification can serve as criteria of mealybug species identification.

Sets of forward and reverse primers were tested individually to determine mealybug species identity. As shown in Fig. 5-1, three bands were amplified from three primer combinations for mealybug colonies from both Tucker and Ashland greenhouse. Bands were labelled as Tucker 1, 2, 3 and Ashland 2, 3, 5, cloned into the bacterial plasmid pGEM-Teasy and their nucleotide sequence determined.

The nucleotide sequences showed allowed us to identify the mealybug species in each population, but in contrast to Daane *et al.,* (2011), the primers were not species specific. The mealybug nucleotide sequences isolated from the Tucker mealybugs were almost identical, with only a few mutations between them (Fig. 5-2), indicating these three fragments were amplified from the same template. these sequences showed that the forward primers for *P. calceolariae, P. longispinus*, and *P. ficus* were not species specific, as reported by Daane *et al*. (2011). A BLAST analysis (Altschul *et al.,* 1990) showed that all three sequences most closely matched that of mitochondrial COI gene for cytochrome c oxidase subunit 1 of *Pseudococcus longispinus* (Genebank: AB512118) (data not shown).

In the case of the population from Ashland Gravel-Greenhouse, the nucleotide sequences of the bands in lanes 3 and 5 were almost identical, whereas the nucleotide sequence of the band in lane 2 was obviously different (Fig. 5-3). An alignment

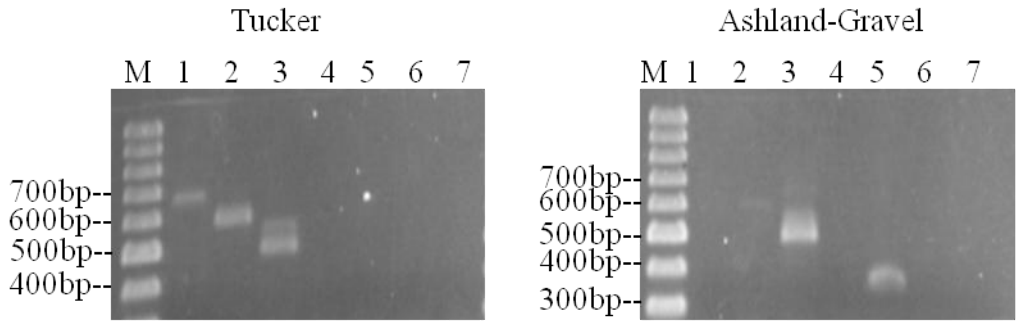

Fig. 5-1 Identification of mealybugs with species specific PCR primers. M:100bp. Lane 1: PCR with Pca and MB-R, with a band of 650 bp. Lane 2: PL+MB-R, 600 bp, Lane 3: PF+MB-R, 450 bp, Lane 4: PM+MB-R, 400 bp, Lane 5: PC+MB-R, 350 bp, Lane 6: PV+MB-R, 250 bp, Lane 7: FG+MB-R, 150 bp. DNA used in each PCR (from Tucker greenhouse colony or Ashland-Gravel greenhouse colony) was indicated on the top.


Tucker1 (1) TGCAACAATAATTATTGCCATCCCAACAAGAATCAAAATTTTTAGATGAA
Tucker2 (1) ----------
Tucker3 (1) ----------
Tucker1 (51) TAATAACTTTAAATGGAAAAAAAATTTTAAATTCATCTATTTATCTTTGA
Tucker2 (1) ----------CCATTTATCTTTGA
Tucker3 (1) ----------
Tucker1 (101) TCTACAGGATTTATTATTATATTTACATTAGGAGGATTAACTGGAATCAT
Tucker2 (15) TCCACAGGATTTATNATTATATTTACATTAAGAGGATTAACTGGAATCAT
Tucker3 (1) ----------
Tucker1 (151) TCTTTCTAATTCAATTATTGATATTAATCTACATGATACTTATTTTGTTG
Tucker2 (65) TCTTTCTAATTCAATTATTGATATTAATCTACATGATACTTATTTTGTTG
Tucker3 (1) ----------CTTTGTTG
Tucker1 (201) TGGCACATTTTCATTATGTACTATCAATAGGAGTAATTTTTTCAATTTTT
Tucker2 (115) TGGCACATTTTCATTATGTACTATCAATAGGAGTAATTTTTTCAATTTTT
Tucker3 (9) TAGCTCACTTTCACTATGTACTATCAATAGGAGTAATTTTTTCAATTTTT
Tucker1 (251) -CAAGTTTCATTTTTTGATCCCCTTTATTAATAAATATTAGATTAAACAA
Tucker2 (165) TCAAGTTTCATTTTTTGATCCCCTTTATTAATAAATATTAGATTAAACAA
Tucker3 (59) TCAAGTTTCATTTTTTGATCCCCTTTATTAATAAATATTAGATTAAACAA
Tucker1 (300) TAATTGATTAAAAGTTAATTTTTTTTAATTTATTTATTCCTATTAATTTAA
Tucker2 (215) TAATTGATTAAAAATTAATTTTTTTTAATTTATTTATTTCTATTAATTTAA
Tucker3 (109) TAATTGATTAAAAATTAATTTTTTTTAATTTATTTATTTCTATTAATTTAA
Tucker1 (350) CATTTTTTCCCCAACATTTCTTGGGAATTAATGGAATACCACGTCGATAC
Tucker2 (265) CATTTTTTCCCCAACATTTCTTGGGAATTAATGGAATACCACGTCGATAC
Tucker3 (159) CATTTTTTCCCCAACATTTCTTGGGAATTAATGGAATACCACGTCGATAC
Tucker1 (400) ATTATATATTCAGATTATTTTATTTTATGAAATAATATTTCTTCAATTGG
Tucker2 (315) ATTATATATTCAGATTATTTTATTTTATGAAATAATATTTCTTCAATTGG
Tucker3 (209) ATTATATATTCAGATTATTTTATTTTATGAAATAATATTTCTTCAATTGG
Tucker1 (450) TTCTTCAATAACTATTATTTTCACCATAATATTTATTTTTATTATTATTG
Tucker2 (365) TTCTTCAATAACTATTATTTTCACCATAATATTTATTTTTATTATTATTG
Tucker3 (259) TTCTTCAATAACTATTATTTTCACCATAATATTTATTTTTATTATTATTG

Fig. 5-2 Alignment of three fragments amplified using different primer sets from Tucker greenhouse. It is longtailed mealybugs.

```
 Ashland2  (1) CCATTTATCTTTGATCCACAGGGTTTATTATTATATTTACATTAGGAGGA
 Ashland3  (1) ----------------------------------------------------
 Ashland5  (1) ----------------------------------------------------

 Ashland2 (51) TTAACTGGAATCATTCTTTCTAATTCAATTATTGATATTAATCTACATGA
 Ashland3  (1) ----------------------------------------------------
 Ashland5  (1) ----------------------------------------------------

 Ashland2 (101) TACTTATTTTGTTGTGGCACATTTTCATTATGTACTATCAATAGGAGTAA
Ashland3   (1) ------CTTTGTTGTAGCTCACTTTCACTATGTATTATCTATAGGAGTAA
Ashland5   (1) ----------------------------------------------------

 Ashland2 (151) TTTTTTCAATTTTTTCAAGTTTCATTTTTTGATCCCCTTTATTATAATAAAT
 Ashland3  (45) TTTTCTCAATTTTTTCAAGATTTATTTTTTGATCACCATTACTATTTAAT
 Ashland5   (1) ----------------------------------------------------

 Ashland2 (201) ATTAGATTAAACAATAATTGATTAAAAATTAATTTTTTTAATTTATTTATT
 Ashland3  (95) GTTTCTTTAAATAATAATTGATTAAAAATTAATTTTTTTAATCTATTTTTT
 Ashland5   (1) ------------------------------------TAATCTATTTTTT

 Ashland2 (251) TTCTATTAATTTAACATTTTTTCCCCAACATTTCTTGGGAATTAATGGAA
 Ashland3 (145) ATCTATCAATTTAACCTTTTTTCCTTCAACATTTTTTAGGAATAAATGGAA
 Ashland5  (13) ATCTATCAATTTAACCTTTTTTCCTTCAACATTTTTTAGGAATAAATGGAA

 Ashland2 (301) TACCACGTCGATACATTATATATTCAGATTATTTTATTTTATGAAATAAT
 Ashland3 (195) TACCTCGTCGTTATATTATATATTCTGATTATTTTATTTTATGAAATAAT
 Ashland5  (63) TACCTCGTCGTTATATTATATATTCTGATTATTTTATTTTATGAAATAAT

 Ashland2 (351) ATTTCTTCAATTGGTTCTTCAATAACTATTATTTTCACCATAATATTTAT
 Ashland3 (245) ATTTCATCAGTTGGTTCATCTATAACAATTATTTTTACTCTAATTTTTAT
 Ashland5 (113) ATTTCATCAGTTGGTTCATCTATAACAATTATTTTTACTCTAATTTTTAT

 Ashland2 (401) TTTTATTATTATTGAATCTTTAATTTCTAAACGATTAATTATATTTAAAA
 Ashland3 (295) TTACATTATTATTGAATCATTTATATGTAAACGTTTAATTATATTTAAAA
 Ashland5 (163) TTACATTATTATTGAATCATTTATATGTAAACGTTTAATTATATTTAAAA

 Ashland2 (451) TAAAATTTTTCAATAGAGAATGATTAAATAATTCACCAAATTTAAATCAT
 Ashland3 (345) TAAAATTTTTTAATATTGAATGATTAAATAATTCACCTAATTTAAATCAT
 Ashland5 (213) TAAAATTTTTTAATATTGAATGATTAAATAATTCACCTAATTTAAATCAT
```

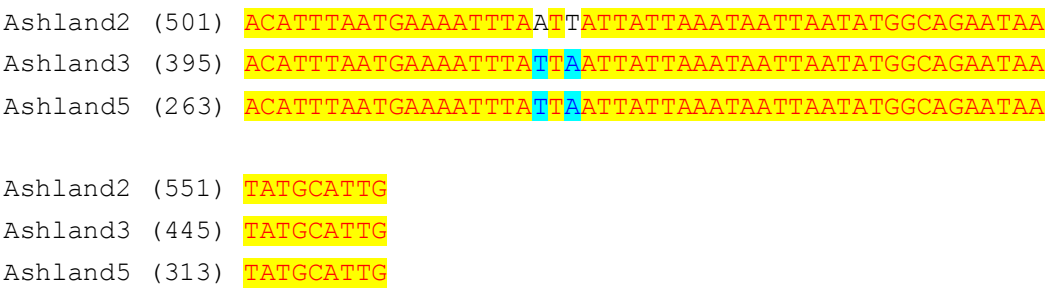

Fig. 5-3 Alignment of three fragments amplified using different primer sets. It is longtailed mealybugs.

between the Tucker 2 and Ashland 2 showed that they were almost identical (Fig. 5-4), indicating that this sequence was derived from the longtailed mealybug (*P. longispinus*); on the contrary, the alignment between the Tucker 3 and Ashland 3 showed that they were obviously different (Fig. 5-5). The nucleotide sequences of the bands in lanes 3 and 5 of the Ashland-Gravel mealybugs were closest to the mitochondrial COX1 gene and COX2 gene for cytochrome oxidase subunit 2 of the citrus mealybug (*Planococcus citri*) (Genebank AB439517) (data not shown). We concluded that the mealybug colony from the Ashland-Gravel greenhouse is a mixed colony, containing both the longtailed and citrus mealybugs.

2.2. Mealybugs are able to acquire GVCV

To determine if the longtailed and citrus mealybugs were able to acquire GVCV, both the Tucker and Ashland-Gravel populations were placed on GVCV-infected grapevines. One month later, The Ashland-Gravel population successfully established a colony on grapevines, whereas the Tucker mealybug population was unable to adapt to grapevines. Mealybugs from the Ashland-Gravel population that had been established on the GVCV-infected grapevine leaves were collected and combined for DNA isolation and subsequent testing for PCR using the primers GVCV2460F and GVCV3122R. Twelve out of 16 mealybug samples were positive for GVCV (Fig. 5-6), indicating that mealybugs could acquire GVCV.

To determine whether mealybugs could acquire GVCV after a short acquisition

```
Ashland2 (1)   CCATTTATCTTTGATCCACAGGGTTTATTATTATATTTACATTAGGAGGA
Tucker2  (1)   CCATTTATCTTTGATCCACAGGATTTATNATTATATTTACATTAAGAGGA

Ashland2 (51)  TTAACTGGAATCATTCTTTCTAATTCAATTATTGATATTAATCTACATGA
Tucker2  (51)  TTAACTGGAATCATTCTTTCTAATTCAATTATTGATATTAATCTACATGA

Ashland2(101)  TACTTATTTTGTTGTGGCACATTTTCATTATGTACTATCAATAGGAGTAA
Tucker2  (101) TACTTATTTTGTTGTGGCACATTTTCATTATGTACTATCAATAGGAGTAA

Ashland2(151)  TTTTTTCAATTTTTTCAAGTTTCATTTTTTGATCCCCTTTATTAATAAAT
Tucker2  (151) TTTTTTCAATTTTTTCAAGTTTCATTTTTTGATCCCCTTTATTAATAAAT

Ashland2(201)  ATTAGATTAAACAATAATTGATTAAAAATTAATTTTTTTAATTTATTTAT
Tucker2  (201) ATTAGATTAAACAATAATTGATTAAAAATTAATTTTTTTAATTTATTTAT

Ashland2(251)  TTCTATTAATTTAACATTTTTTCCCCAACATTTCTTGGGAATTAATGGAA
Tucker2  (251) TTCTATTAATTTAACATTTTTTCCCCAACATTTCTTGGGAATTAATGGAA

Ashland2(301)  TACCACGTCGATACATTATATATTCAGATTATTTTATTTTATGAAATAAT
Tucker2  (301) TACCACGTCGATACATTATATATTCAGATTATTTTATTTTATGAAATAAT

Ashland2(351)  ATTTCTTCAATTGGTTCTTCAATAACTATTATTTTCACCATAATATTTAT
Tucker2  (351) ATTTCTTCAATTGGTTCTTCAATAACTATTATTTTCACCATAATATTTAT

Ashland2(401)  TTTTATTATTATTGAATCTTTAATTTCTAAACGATTAATTATATTTAAAA
Tucker2  (401) TTTTATTATTATTGAATCTTTAATTTCTAAACGATTAATTATATTTAAAA

Ashland2(451)  TAAAATTTTTCAATAGAGAATGATTAAATAATTCACCAAATTTAAATCAT
Tucker2  (451) TAAAATTTTTCAATAAAGAATGATTAAATAATTCACCAAATTTAAATCAT

Ashland2(501)  ACATTTAATGAAAATTTAATTATTATTAAATAATTAATATGGCAGAATAA
Tucker2  (501) ACATTTAATGAAAATTTAATTATTATTAAATAATTAATATGGCAGAATAA

Ashland2(551)  TATGCATTG
Tucker2  (551) TATGCATTG
```

Fig. 5-4 Tucker 2 and Ashland 2 are almost identical.

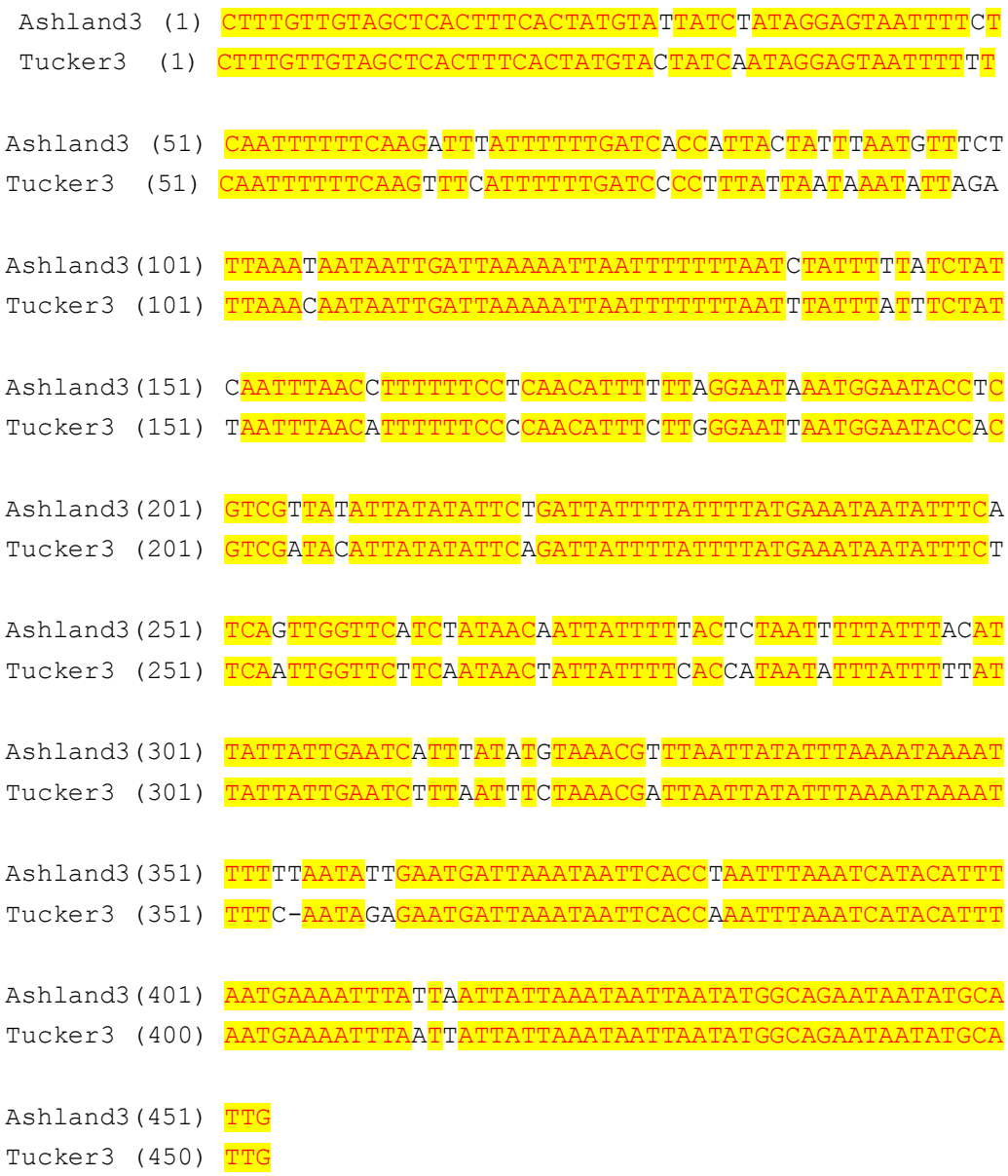

Fig. 5-5 Ashland 3 and Tucker 3 are different.

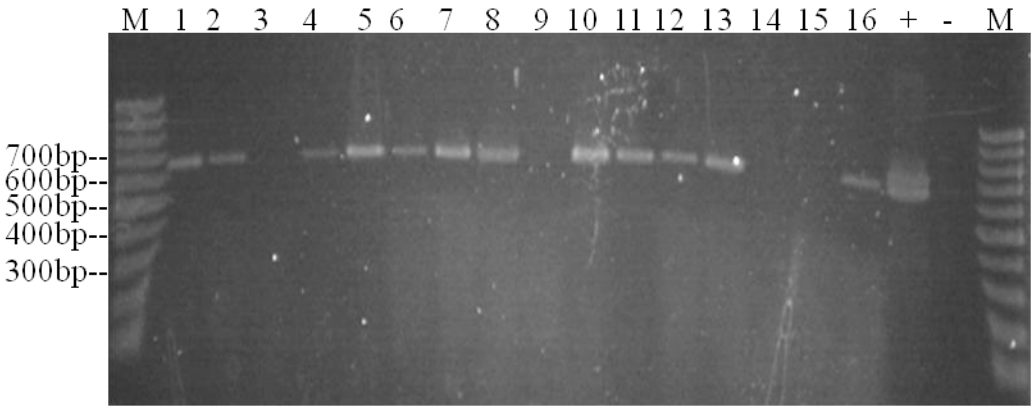

Fig. 5-6 PCR results show that the Ashland-Gravel mealybug population can acquire GVCV after extended feeding on GVCV-infected grapevines. M: 100bp ladder (Fermentas, Pittsburg PA); 1-16: DNA of mealybugs from 16 GVCV-infected grapevine leaves; +: positive control, DNA of GVCV-infected grapevine leaf; -: negative control, H_2O was added in PCR cycle as template. PCR was done with primers GVCV2460F and GVCV3122R.

feed, both the Tucker and Ashland-Gravel populations were placed on detached GVCV-infected grapevine leaves and DNA was purified from mealybugs at different time points. As shown in Fig. 5-7, GVCV was amplified from the Ashland-Gravel mealybug population after three days of feeding, indicating that the GVCVacquisition time might be as short as three days. In this test, the longtailed mealybug (Tucker population) was unable to acquire GVCV. However, in a repeated short term GVCV acquisition test, the GVCV was successfully amplified from the longtailed mealybug population (data not shown).

2.3. Mealybugs are not able to transmit GVCV to healthy grape

The acquisition tests showed that GVCV DNA was present in mealybugs that fed on GVCV-infected grape leaves. To test whether mealybugs could transmit GVCV to healthy grapevines, we first established mealybugs on GVCV-infected grapes. GVCV-infected grapevines were moved into Bugdorms (Taichung, Taiwan, China) and were infested with mealybugs from the Ashland-Gravel population. One month later, healthy grapevines were moved into the same Bugdorms and mealybugs were allowed to spread to the healthy plants. One month after the mealybugs were observed to colonies the healthy grapevines, plants were removed from the bugdorms and insecticide was sprayed to kill the mealybugs. Grapevines were observed for typical GVCV symptoms for over one and were tested at nine months by PCR for GVCV viral DNA utilizing the pair, GVCV4628F and GVCV30R.

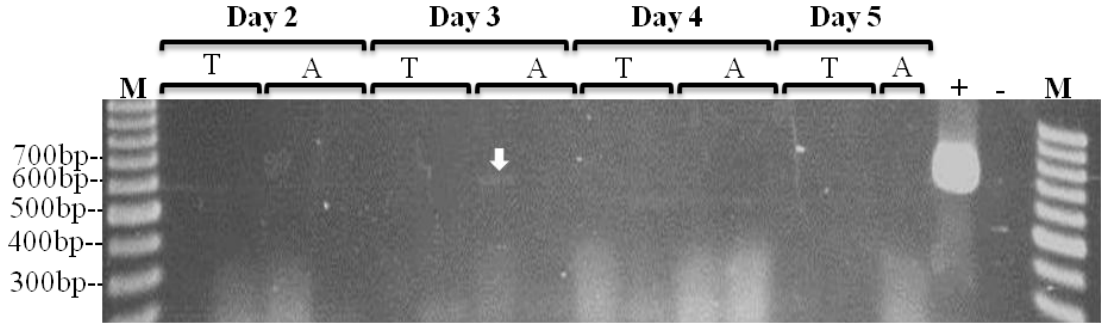

Fig. 5-7 The Ashland-Gravel mealybug population is able to acquired GVCV from symptomatic grape leaves after three days of feeding. DNA purified from two mealybug populations (labeled as T for Tucker or A for Ashland-Gravel) at different time points, as illustrated. PCR was done with primer GVCV2460F and GVCV3122R . M: 100bp DNA ladder (Fermentas, Pittsburg PA); +: positive control consists of DNA from a GVCV-infected grapevine leaf as template; -: negative control, no DNA template added.

The transmission test was repeated three times during the growing season in 2015, using six plants per test for a total of 18 plants. No GVCV symptoms were present at any point during the 2015 growing season. A leaf was selected from each grapevine for DNA isolation and PCR analysis for the presence of GVCV DNA. All of the grapevines were negative for GVCV. A typical result is illustrated in Fig. 5-8. The 18 grapevines were overwintered in a cooler set at 4 C, moved back to the greenhouse in the spring of 2016, and observed for GVCV symptoms throughout the 2016 season. No GVCV symptoms were apparent in these plants during the 2016 growing season. In July of 2016, two leaves from each of the 18 plants were selected for DNA isolation followed by a PCR test for the presence of GVCV. All 36 samples were negative for GVCV. The same transmission test was repeated again in the summer of 2016, in an attempt to transmit GVCV to 15 healthy grapevines. At the end of the growing season, none of the grapevines exhibited any symptoms typical of GVCV (data not shown).

3. DISCUSSION

Mealybugs have been shown to be the most common vector for members of the badnavirus genus (Schoelz, 2008). In this chapter I examined the capacity of the longtailed and citrus mealybugs to transmit GVCV. Although the citrus mealybug was shown to acquire GVCV, in several independent tests we were unable to show that the citrus mealybugs could transmit GVCV from infected to healthy grapevines.

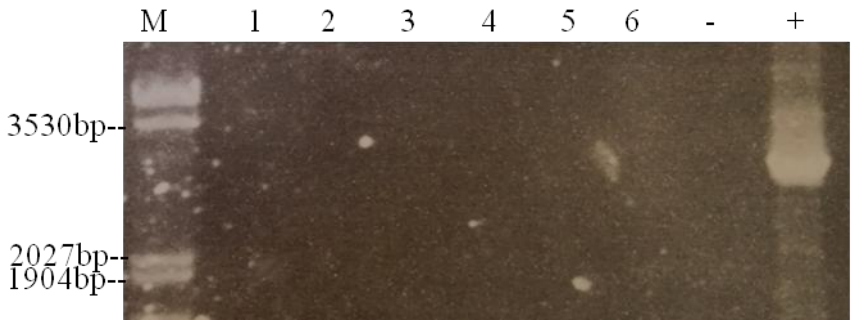

Fig. 5-8 Typical PCR results of grapes in transmission experiments. M: λ DNA marker, land 1-6: DNA of six grapevine involved in transmission experiment. - : negative control, DNA of healthy grapevine leaf. +: positive control, DNA isolated from GVCV-infected grapevine leaf. PCR was performed with primers GVCV4628F and GVCV30R

We were able to locate two populations of mealybugs for our transmission tests. Taxonomic identification for mealybug species can be difficult, particularly for the nymphal stages that are primarily involved with dispersal (Beuning *et al.*, 1999; Gullan, 2000; Hardy *et al.*, 2008). As a result, a mealybug species-specific PCR would be very helpful for a fast and accurate mealybug classification. Daane *et al.* (2011) proposed a multiplex PCR with a universal reverse primer and species-specific forward primer and tested them on 104 mealybug samples from US, Chile, Australia, Mexico, Argentina, Italy, Portugal, Spain, Greece, Israel, and Pakistan. Ninety five out of 104 samples were successfully identified by multiplex PCR. However, most of the mealybug samples from the U.S. (54 out of 63 samples) were from California, and another 9 samples were from Washington, Oregon, North Carolina, and Nebraska. None were from Missouri.

As the sequencing results showed in Fig. 5-2, 5-4, 5-5, and 5-6, it is reasonable to assume that Daane *et al* (2011) underestimated the diversity of mealybug population in Missouri. We found that primers that were supposed to be species specific actually amplified the same template of a single species, and that the differences in sizes of the PCR products did not reflect different species.

One difficulty of working with GVCV is that no GVCV antibody is available; the only method to screen for GVCV is by PCR. When screening for GVCV by PCR, proper controls are required to avoid a false positive, and proper primers have to be selected to avoid contamination. In this experiment, we found that primers that

amplify longer fragments are better in terms of GVCV screening. Primers GVCVF1 and GVCVR1 (sequences not shown) amplify a 500 bp band; they were first selected for GVCV screening and they were able to repeatedly amplify GVCV DNA from samples without any amplification of the negative controls. However, ghost bands started to appear with GVCVF1 and GVCVR1 over time (data not shown), and re-dilution of both primers did not solve the problem. Primers GVCV2460F and GVCV3122R, which amplify a band with approximately 650 bp length, were used to replace GVCVF1 and GVCVR1 in GVCV screening. They were able to successfully amplify GVCV from samples at the beginning without false positives. For this reason, I believe the acquisition tests conducted with this primer set in Figs 5-6 and 5-7 are reliable. However, the same contamination problems eventually happened again with GVCV2460F and GVCV3122R (data not shown). To avoid the problem with false positives, I chose the primer set, GVCV4628F and GVCV30R, which amplify a band with approximately 3,000 bp length, were then selected, and the contamination problem never occurred with this primer set. In Fig. 5-8, grapevines were tested for GVCV by PCR with primers GVCV4628F and GVCV30R for the purpose of eliminating any chance of a false positive.

Another difficulty of working with GVCV is that GVCV is not evenly distributed in infected plants. Not all the leaves from GVCV-infected plants are symptomatic, and the non-symptomatic leaves from GVCV-infected grapevines could be negative for GVCV in a PCR assay. In fact, in most infected grapevines, only a

small portion of leaves exhibit typical GVCV symptoms. Furthermore, the vein clearing symptoms can be difficult to distinguish, especially when plants are under heat stress during summer. It is possible that when mealybugs were placed on a "symptomatic" leaf, they were actually placed on a GVCV-negative leaf on a GVCV-infected plant. This might be part of the reason why the transmission tests to healthy grapes failed.

Mealybugs of different species may have varied efficiency of virus transmission. Citrus mealybug, Vine mealybug, and Pineapple mealybugs are able to transmit BSV but longtailed mealybug does not appear to be a vector for BSV (Meyer *et al*., 2008). In the transmission experiment of GLRaV, the Obscure mealybug, Longtailed mealybug, Citrus mealybug, and Grape mealybug had transmission efficiencies of 19% (65 plants), 35% (100 plants), 5% (40 plants), and 90% (10 plants), respectively (Golino *et al*., 2002). It is possible that longtailed mealybugs and citrus mealybugs are not able to transmit GVCV or have a very low efficiency in GVCV transmission. Finally, it may be that another species of mealybugs not included in my test could still transmit GVCV.

To conclude, in this experiment, we could not prove that mealybugs are the insect vector of GVCV. Further investigation, such as testing other species of mealybugs with a larger number of plants in each test, may be required to answer this question.

4. MATERIALS AND METHODS

4.1. Maintenance of Grapevines and mealybug populations

Healthy and GVCV-infected grapevines with were generously provided by Dr. Wenping Qiu from Missouri State University. The GVCV grapevines were clonally propagated from a single GVC-infected Grapevines (LBC0903, Zhang *et al.*, 2011). Grapevines were grown under greenhouse conditions with sufficient water and controlled-release fertilizers. They were vernalized from at 4 C from approximately mid-December until early March.

Two colonies of mealybugs were collected from two greenhouses at University of Missouri: one from cycad in Tucker greenhouse and the other one from grapevines in Ashland greenhouse. The two colonies of mealybugs were maintained separately on potato sprouts.

When grapevines were inoculated with mealybugs, plants were moved into BugDorm (Taichung, Taiwan, China), which has a fine mesh to allow air flow but prevents mealybugs from escaping to nearby healthy plants in the greenhouse.

4.2. DNA isolation from plants and mealybugs

DNA was isolated from grape leaves using DNeasy® Plant Mini Kit (Qiagen, Germantown MD) following the manufacturer's instructions. DNA was eluted in 100 µl of autoclaved H_2O. Agarose gel electrophoresis (1% agarose in Tris-Borate EDTA buffer) was performed to determine whether DNA was present and to make

a rough, quantitative assessment of DNA concentration.

The protocol for mealybug DNA isolation was modified from Dellaporta *et al* (1983). Mealybugs or aphids were ground in 400 µl of extraction buffer (100 mM Tris pH=8, 50 mM EDTA pH=8, 500 mM NaCl, 10 mM mercaptoethanol) in a 1.5 ml eppendorf tube. Twenty seven µl of 20% SDS were added to the solution, the solution was mixed thoroughly by vigorous shaking, and then incubated at 65℃ for 10 min. To precipitate protein, 133 µl of a 5 M potassium acetate solution was subsequently added. The tube was shaken vigorously and incubated on ice for 20 min, followed by a 13,000 rpm for 20 min centrifugation at room temperature. The supernatant was collected and the pellet was discarded, and 270 µl of isoproponal was added to precipitate the DNA. The solution was mixed and incubated at -20 ℃ overnight, and the DNA was pelleted by centrifugation at 13,000 rpm for 20 min at room temperature on the second day. The DNA pellet was redissolved in 19 µl H_2O. 1% agrose gel electrophoresis was performed to assess DNA quality. DNA was isolated from a group of mealybugs as well as from individual mealybugs.

4.3. PCR

Two sets of GVCV-specific primers were used for GVCV detection: GVCV2460F and GVCV3122R, which amplify the region between nt 2,460 to nt 3,122 of the GVCV genome and generate a 663 bp band; GVCV4628F and

GVCV30R, which amplify the region between nt 4628 and nt 30 and generate a 3,156 bp band. PCR was performed with GoTaq® Flexi DNA polymerase (Promega, Madison WI) following the manufacturer's instruction. The PCR program for GVCV2460F and GVCV3122R was: 94℃ 1min before first round of DNA denaturation, 35 cycles of amplification (94℃ for 30s, 52.3℃ for 30s, 72℃ for 1min), and final elongation at 72℃ for 10min. the PCR program for GVCV 4628F and GVCV30R was: 95 ℃ for 5 min for initial denaturalization, 35 cycles of amplification (95℃ for 30s, 58℃ for 30s, and 72℃ for 3 min), and final elongation at 72℃ for additional 10 min. PCR products were assessed in 1% agarose gel electrophoresis.

PCR for mealybug species identification was modified from the multiplex PCR procedure described by Daane *et al* (2011). Instead of performing multiplex PCR, I tested samples with primer sets for individual species.

4.4. GVCV acquisition tests

A mealybug colony originated from the Ashland-Gravel greenhouse was established on three GVCV symptomatic grapevines. GVCV detection was performed on mealybugs that had fed on GVCV-positive grapevines for approximately one month for the long-term GVCV acquisition test. Five to 10 mealybugs from were collected from a single leaf, depending on the size of the mealybugs, and ground together for DNA isolation as described above.

For the short-term acquisition test, 20 grapevine leaves with GVCV symptoms were collected from Les Bourgeois vineyard (14020 W. Highway BB - Rocheport, MO 65279). GVCV-free mealybugs collected from potato colonies were used in this assessment. The absence of GVCV in the colony had previously been confirmed by PCR. Mealybugs originated from Tucker greenhouse were placed onto 10 leaves, with 5 mealybugs per leaf; mealybugs originated from the Ashland-Gravel greenhouse were placed onto another 10 leaves, with 5 mealybugs per leaf. Grapevine leaves were kept in 15ml plastic tubes, and water was added repeatedly to keep the petiole covered in water for the duration of the study. Mealybugs fed on the grapevine leaves for 2-5 days before DNA isolation. PCR described above was applied to detect GVCV.

4.5. GVCV transmission test

GVCV-infected grapevines were inoculated with mealybugs originated from the Ashland-Gravel greenhouse and placed in bugdorms. Mealybugs spread to the whole plant in about one month. Two healthy grapevines were moved into the same bugdorm to let mealybugs naturally spread to healthy grapevines. One month after the mealybugs settled on healthy grapevines, insecticide was applied to kill all mealybugs. DNA was isolated from leaves of healthy grapevine for GVCV screening. The PCR primers, GVCV4628F and GVCV 30R, were used to amplify GVCV DNA. Grapevines were moved into a cooler (4℃) during winter, and the

same PCR test was repeated again in spring of the second year.

REFERENCES

Altschul, S. xF., Gish, W., M iller, W., Myers, E. W. & Lipman, D. J. (1990). Basic local alignment search tool. *Journal of molecular biology* **215**, 403-410.

Aparna, G. S., Kotakadi, V. S., Saigopal, D. & Reddy, M. (2012). Citrus yellow mosaic: a transmissible virus of citrus species in India. *The bioscan* **7**, 283-287.

Beuning, L., Murphy, P., Wu, E., Batchelor, T. & Morris, B. (1999). Molecular-based approach to the differentiation of mealybug (Hemiptera: Pseudococcidae) species. *Journal of economic entomology* **92**, 463-472.

Daane, K. M., Middleton, M. C., Sforza, R., Cooper, M. L., Walton, V. M., Walsh, D. B., Zaviezo, T. & Almeida, R. P. (2011). Development of a multiplex PCR for identification of vineyard mealybugs. *Environmental entomology* **40**, 1595-1603.

Dellaporta, S. L., Wood, J. & Hicks, J. B. (1983). A plant DNA minipreparation: version II. *Plant molecular biology reporter* **1**, 19-21.

Dongo, L. & Orisajo, S. (2007). Status of cocoa swollen shoot virus disease in Nigeria. *African Journal of Biotechnology* **6**, 2054-2061.

Golino, D., Sim, S., Gill, R. & Rowhani, A. (2002). California mealybugs can spread grapevine leafroll disease. *California Agriculture* **56**, 196-201.

Gullan, P. J. (2000). Identification of the immature instars of mealybugs (Hemiptera: Pseudococcidae) found on citrus in Australia. *Australian Journal of Entomology* **39**, 160-166.

Hardy, N. B., Gullan, P. J. & Hodgson, C. J. (2008). A subfamily-level classification of mealybugs (Hemiptera: Pseudococcidae) based on integrated molecular and morphological data. *Systematic Entomology* **33**, 51-71.

Hearon, S. & Locke, J. (1984). Graft, pollen, and seed transmission of an agent associated with top spotting in Kalancho ë blossfeldiana. *Plant disease* **68**, 346-350.

Hull, R. (2002). Matthews' Plant Virology, 4th edition. Academic Press, London.

Hull, R., Lockart, B.E., Reddy, D.V.R. and Schoelz, J.E. **(2005)**. Family

Caulimoviridae. In: *Virus Taxonomy. Seventh Report of the International Committee on Taxonomy of Viruses* (Edited by van Regenmortel, M.V.H., Fauquet, C.M., Bishop, D.H.L., Carstens, E.B., Estes, M.K., Lemon, S.M., Maniloff, J., Mayo, M.A., McGeoch, D.J., Pringle, C.R. and Wickner, R.B.), pp335-347, Academic Press, San Diego.

Jones, A. T., McGavin, W. J., Geering, A. & Lockhart, B. (2002). Identification of Rubus yellow net virus as a distinct badnavirus and its detection by PCR in Rubus species and in aphids. *Annals of applied biology* **141**, 1-10.

Kalischuk, M. L., Fusaro, A. F., Waterhouse, P. M., Pappu, H. R. & Kawchuk, L. M. (2013). Complete genomic sequence of a Rubus yellow net virus isolate and detection of genome-wide pararetrovirus-derived small RNAs. *Virus research* **178**, 306-313.

Lockhart, B. & Autrey, L. (1991). Mealy bug transmission of sugarcane bacilliform and sugarcane clostero-like viruses. In: III International Society of Sugarcane Technologist Pathology Workshop, 17.

Lockhart, B. & Geering, A. (2000). Partial characterization of two aphid-transmitted viruses associated with yellow leafspot of Spiraea. In *X International Symposium on Virus Diseases of Ornamental Plants **568***, 163-168.

Lockhart, B., Kiratiya-Angul, K., Jones, P., Eng, L., De Silva, P., Olszewski, N., Lockhart, N., Deema, N. & Sangalang, J. (1997). Identification of Piper yellow mottle virus, a mealybug-transmitted badnavirus infecting Piper spp. in Southeast Asia. *European journal of plant pathology* **103**, 303-311.

Lockhart, B. & Olszewski, N. (1996). Schefflera ringspot virus, a widely distributed mealybug-transmitted badnavirus occurring in Schefflera and Aralia. In *IX International Symposium on Virus Diseases of Ornamental Plants **432***, 196-203.

Macanawai, A. R., Ebenebe, A. A., Hunter, D., Devitt, L., Hafner, G. & Harding, R. (2005). Investigations into the seed and mealybug transmission of Taro bacilliform virus. *Australasian Plant Pathology* **34**, 73-76.

Meyer, J., Kasdorf, G., Nel, L. & Pietersen, G. (2008). Transmission of activated-episomal banana streak OL (badna) virus (BSOLV) to cv. Williams banana (Musa sp.) by three mealybug species. *Plant Disease* **92**, 1158-1163.

Ng, J. C. & Perry, K. L. (2004). Transmission of plant viruses by aphid vectors.

Molecular Plant Pathology **5**, 505-511.

Palacios, I., Drucker, M., Blanc, S., Leite, S., Moreno, A. & Fereres, A. (2002). Cauliflower mosaic virus is preferentially acquired from the phloem by its aphid vectors. *Journal of General Virology* **83**, 3163-3171.

Phillips, S., Briddon, R., Brunt, A. & Hull, R. (1999). The partial characterization of a badnavirus infecting the greater asiatic or water yam (Dioscorea alata). *Journal of phytopathology* **147**, 265-269.

Schoelz, J. E. (2008). Caulimoviruses: General Features. In *Encyclopedia of Virology*, 5 vols. (Edited by Mahy, B.W.J. and Van Regenmortel, M.H.V.). Oxford: Elsevier pp. 457-464.

Sether, D., Melzer, M., Borth, W. & Hu, J. (2012). Pineapple bacilliform CO virus: diversity, detection, distribution, and transmission. *Plant Disease* **96**, 1798-1804.

Su, H.-J. (1998). First occurrence of banana streak badnavirus and studies on its vectorship in Taiwan. In: *Banana streak virus: a unique virus Musa interaction? Proceedings of a workshop of the Promusa Virology Working Group* (Edited by Frison, E.A. and Sharrock, S.L), Montpellier, France, pp. 20-25.

Zhang, Y., Singh, K., Kaur, R. & Qiu, W. (2011). Association of a novel DNA virus with the grapevine vein-clearing and vine decline syndrome. *Phytopathology* **101**, 1081-1090.

Appendix

Complete sequences of GVCV isolate LBC0903, accession number: JF301669

>JF301669.2 Grapevine vein-clearing virus isolate LBC0903, complete genome

TGGTATCAGAGCTCCAGTTTCAAATCTGGGAAATCTCTACAATTATTCCTTCAAGAT

TATGATGAGGAACTAACTCTCATAATCGTGTAGGGAATCGTTAGTAGGATCTCAGAA

CAAGGTTCTTATCCCCTCATACTACTGATTCTGGTATATAGGCTGGAAACACGACAC

TGTTACGATCCCACTTCTGTTGGAGTGGTAGTAGCCCGTTGTGAGACAACGCCACGT

ACCATTTTCAGTTTTCCTAGCCCAAATCCCCATGAACAGAACTCCCACGGTCAATAA

GTTTCAACAGGATCCCTAGCCCAACAATACTGAAAGTCCTAGGACAGGCTGCGACGC

GAAGTACCACCAGTTCAGGCGATGCTGTTCCGCCGATTGTTTGTGGGAAAACTGCAG

TAGGAGAGGACGGACAACTATTCAAGGGAACGGAACCTGGAGACACCGGCCGAGTTC

TTAGTAAGCGGTTCAAGGAAGGAGACTGATGCAAAGTATAGAACAACAACAGTTTGA

GGCGGAGATAGAATCTTGGGAGAGATCTGAACGCACACCCCTACACGGTTACCGTGA

TCTTGTGGAATATCCCCGTTACGAAAGAAATCAGCATTTCCCATCTGCAAAGTTCCC

CTGCTACCACTTTGTTGCTGAGAAAGACAACGTTCACGCCACTTACACCAAGGGAGA

TAGAATCCCTCAGCTGCTGAATACACTGTACGACCTACAAGTCAACCAGTGTCATAA

CCAGGCAGTGATCTACGATCGGATCCAACTCCTTTCGAGGTATACGGTCCGAAAGGG

TAAGCCTTTACCGGCTATCCCTGAGGAATCTGTCCTCAAGGAACCAGAAGAAAGCTC

AACTGAGCTTAAGCACCAGATCGAGCTCCTTCGAGCAGATCTAAGGGAGATCAAGGC

TAATCAGTCAAGCCTCCGACTTGCCATCTCTGAAATCCGTGAATCCATCACAGATCT

AACGGCAAGAGAATCGGCACCTAAGCCGATTGAAGCAGAGACAGCCTACCTGACCGC

CCAGCTAAAGGTTCAGGTTCAAGAGATCAAAACAGCTTTAACAGAGATCAAAACCTT

TGCCAGGACTTTGGTTCCTGAAAGGTAGATGTCCACGTGGCAAATTGCTGCTGCCGC

AGAGGAATACAAAAACGCCATAAAGGCAACTGCAACCCTCACCAAGGACGAAAGAGC

TGTTGGCTTTGTTAAGCCCCACGAGTTCGAGCCAAATTTCAGTGACACCAACATTCA

AAGGCAAAACAATACTTTGATCCACTTGCTAATTCAAAGCCTTGAAGAAATCAAAGA

GCTCCGCGCTCAGGTTCAGACCCTCAACGATCGTATTATAACTTTGGAAAAGGGAAA

GGCTCCAGTCACTCTTCCTGATAACGTGGTAGAACAAATATCCACTCAACTCAAGGA

AGCCAAGTTTGGACAACCAAAAGAAGGTTTGGTCAAAGGGACAAAAGGCACCTTCCG

GGTCTGGAAGTGATGTCTAGGTCCAGGACTCAGACCACTGAGTTGCCTCGTGCAACC

AGAAGATCCACTAGCCCAGTAGAAAGGCTAGACGACCAGATCCGCGGCTACCGACGG

ATGGCCCGTGCCCGCTACCTTGCGGAGCAACGAATACGTAGGTCCTTTTCAAGGAAC

TACAGGGAAACTCTGGAAAGACGCCTAGATCCAGAGGCTGAACTACAGCTCAGTCGA

AGACGAAGAGCTAACTTAGTACCAGCAGAAGTACTATACTCCCTCAACTACAATGAA

CCCCAGAATAGGGTTTATCAACACTATGAAGAGGTGAGATCCCATGTCATAGACCGG

CAGCAAGATTTCCGGTTTATTGAAGAACAGTCCTACCGCACCCTTGTGCAAGAAGGC

ATGCAGCATATCCACCCTGGAATGCTGATGGTGAGAATACAAGTGCTACACCGAGTA

GACGCAGGAATTAGCGCCATGATCGTGTTCCGAGACACGAGGTGGAATGATGAAAGA

CAAATTATCAGTGCTATGACTGTTGATATGGCCAGAGGGGCACAACTAGTCTACGCC

ATCCCAGATCTCATGATGTCAATCCATGATTTCTACCACCACCTGCAAGTCAGCATT

ACCACCAGAGGATACGGTACCGGTTGGGTAGGAGGTGAAAGCAACCTCATAGTGACT

AGGTCACTCACCGGAAGGATCACAAATACCAGTCAGGCCAACTTCAATTATCAAATT

GAAGGAGTAGCTGACTACCTGGCAAGCCATGGCGTGCAGAGTATACCAGGACAGCCA

TGGAGGGACATAAACCAGGAAGGATCCTGGAACCTAAGGCCTTCATCAATACAGGCC

CCTACTCAGGTCCCCACAGGCCTTGTCTCAAGACAATCTGCCACCGGCAATATCAGC

CTAAGGTTCACTGGTTTTCAGGACCAGGTCCAGACGGTTGAAACTGAGGAAGAGTCT

GGTATGACAGACACAGGAGAAAGGGTAACTCATTATGCCCTTGTTGGAACCTTCGAA

TGGTTGGAGGAATGTCCTTCATATCAACAAAGAAGGAATCAAGAAACAGAGGAAAAT

GGCTGGGTGAAACATGTGGAAGGAGATAAGGGGTTCAACTTCAAAGTCCGTATGACC

CCTCCAGCATGGAGCCATGACCCGCAGCCCATCATAGCTACGGGATGGGGAGATGAT

TTTAATAATCCTCCGCCACCTCCACCTCCTAAAACTGAAGAGGAGGAAATATTGGAG

TTATACCCAGTAAGAAGAAGACCCGACCCTGTGCAGATAGCCAGGAAAGAAAAGGCG

GCAGTTTTCTCTCAAGCTGTCAACACTATCTTCGAGCACGAAGGGAAGGATGTCTCA

AGGATGAAACCATCAGGGGAAGCCCCTGACTCGGATCCAGACAGCCCAGTCTGGAAG

GTAAAGAAAAGCCCTTATCCTCATAAGCCAATGAAGCTGAAGGATGAGAAGGGTAAA

AGTCCTTTTGAGGACTTGGAACTAAAACAAGACCTAGTTCAAAGCTGGATAGCTCAA

CTAGGAAGTGGCTCAGGAAGCAGAACGGAGAAACCTATCTTCGACACTACCAGCAGT

GACTCAGACTCTGATCTGTCTGATGTTAGCTCGAAAGTTTTAGCCTATGCTGGAGTT

GAAGAAGCGGTAATGGAATACCCACGGAGGGTAAAAACTGCGACGGCTAAGCTAGCA

GACATGGAAAAGGCTTTTGCCGGAGAAACAACCGCAGCAGTAGGAGGAGATTCGGAG

ATGACAACTGGTCAGTCTTCTAGATCTACTCTCATACCACCAAATGAAGGAGGAGGA

CCTATACGGTATCCACCAGCAGAAAGACCGTCCACATCGGCCTCTACATACAACACT

ACAGCCCCACCTCTTTTTGAAGGGACTGTTAGGCCCGGAAGGTATGGTCGCCCCTTG

GCACCATGGTCTCTACCATCAGCACAGCACTCTCAAGGAGCTTTGCTGATCCTCCCT

CCTGAAGTAGCAAGTCACGCTGACGCCATCACTACATGGGAAACAATCACCCTAAAT

CATTTGATGAATATATCATTTGATTCCCTCCAAGACAGGGTTGATTACATTGAAAAT

CTCCTTGGACCAAGGGAAAGAGAAGCTTGGGTCACTTGGAGAATGGCGTACGATACG

GAATACAGACAGCTGGTTGAGCTCTCTGGAGAGCCAAGAAATGTTACCAGCACCATC

AAAAGAGTTCTGGGTATCAATGACCCTTATACAGGAACTACTCACATCCAGAATCAA

GCCTATGCGGATCTTGAGCGCCTGCAGTGCAAAAATCTGGAATCAGTAATGCCATTC

CTGAACTCTTATTTCCAACTCGCAGCTAAGAGTGGGAAAATGTGGAGTAGCCCTGAA

CTCTCAGAAAAGCTTTTCAGAAAGCTTCCCCCAGAAATCGGTCCTACTATAGCAAAG

GAGTATGCTGAGCGATACCCTGGCATGTTAATCGGAGTTAATGCCAGAATACAGTTC

GTCTCTGAGTATCTCCAGGACCTGTGTAAGCAAGCAGATCTTCAAAGAAAATTGAAG

AATTTGAATTTCTGCAAGGCAATTCCTATTCCTGGTTACTATGACCAAGGAGTAAAG

AAGAAATACGGCCTACGCAAATCCAAAACTTATAAGGGTAAACCTCATGACTCTCAT

GTCAAGGTTATCAAAAATAAGTACAAAGGGGCCCAAGGTCGTAAATGCAAATGCTAC

CTCTGTGGTATTGAAGGCCACTATGCTCGAGAATGCCCAAAGAAGCATGTCAGACCA

GAACGTGCAGCCTACTTTGAAGGCATGGGCTTGGATGTCAACTGGGATGTAATAAGT

GTTGACCCAGGAGATCAAGATGGATCAGACATCTGCTCAATTTCTGAAGGAGAAGCC

CAACATGGAATGGAGGACCTAGCCGCGTTCAAAGCCCAACTTCCATATCCAGTGGAA

GCCCAATATGAGCAGCACCAGGCCCTTGTGGTTATCCAAACAACCTTTAAAAAGGAA

GATAAGCCCCAAGGCTCTTGGCGCATGTCAAAGCCCATTCCCGAAACCCAACAGCAA

TGCCAGCACACATGGGATGACATGTATGCCCTAGCAGAAGGACAACAAGCGTGCAGC

ACTTGCCAGACCATCACTGTACTTGGTCGACGTGCTACTTGCACCCTTTGCCTACTC

AACCTCTGCTCACTATGCGCTGGCTTAGACTTCGGTCTCAAAATAGTTCCTAAGACT

GCCACACGTGCTGACTGGAAATTCCAAGATCGCGATTCTCTTATCGCTTCCCTCTAC

GAGCACAATGCATTCCTTCTACGTCAAGTTGAAGGATTAAAACAGGAACTCCAAGCT

GCTAAAGAACAGCTTCAACTGCTACACTCGGTTGACATGATCAACCTCTCTGATGAT

GGATTAGAGAATTTTTCCCTTGAGGAAAAATCCTTTTTAAGAGGGGGAGGGGGTACC

AGTAGCAGTTCAATCAAAATCTCATCAACAACCACACCCCCTGGTTTTCCTACAACA

CCCAACAGATTCCAGCCTCTTGCGCAGGAAAAACTTAAAGGAATACAGGAAGACCTA

TCTCTGGCAGTACAGTTTGATGATGTCAGACAACAAGAACAGGCGTATACTGAAATG

CCTCGAGGAGCTCACAACAAGCTATACCACGTGGTGGTAACCTTCAGAATCCCTGAT

GCTAAGGGACAGCTCCTTGAATTTGATATCAACGCCATCATAGACACTGGCTGCACC

TGTTGCTGCATCAACCTCACAAAGGTACCCGATGGAGCAATTGAGAACGCCTCCATA

ATCCAAGAAGTCTCTGGGATTAACAGCAAAACAGTAGTCACCAAGAAACTCAGGCAA

GGCAAGATGATCCTCGCAGGGAATGATTTCTACATTCCTTATGTCTCAGCCTTTGAG

ATGAACATGCCTGGAATTGACATGCTGATAGGCTGCAACTTCATCAGAGCAATGAAG

GGAGGAATACGGTTGGAAGGAACTGAGGTCACCTTCTACAAAACCATCACCAGGATT

CAAACTACCCTGGAACCTCAAAAGATAGCATACTTGGAAGAGCTAGTAGAAGCAGAA

GACCTACACTATGAGCTCGCAGCTGCAAGTATGCCTGAGCCTACTGCTGAAGGACTC

AGAAACACCAAACTCCTAGCCGAACTGAAAGATCAAGGCTACATAGGAGAAGAGCCT

CTCAAACACTGGTCAAAGAATAGGGTACGATGCAAGCTTGACATCATTAACCCTGAT

ATCACCATTGAGGCAAAGCCACCTGGACACCTAACTCTGGAGGATAAGGTCAAATAT

CAGAAGCACATTGACGCCCTCCTAGACCTTGGAGTCATCAGACCTAGCAAGAGCAGA

CATAGGTCCGCAGCTTTTATAGTTGCCTCTGGGACCTCTGTAGATCCCAAAACTGGC

AAAGAAACCCGCGGTAAGGAAAGAATGGTGATTGACTACCGCATGCTAAACGACAAC

TGCCATAAGGATCAATACAGTCTGCCTGGAATCACCTCCATCATCAAATCTCTTGGG

CAAGCTAAAATCTTCAGTAAATTTGACCTGAAGTCTGGCTTCCACCAAGTTATGATG

GAAGAAGAAAGCATCCCCTGGACTGCTTTTATCAGCCCCGCAGGTCTATACGAATGG

CTAGTCATGCCATTTGGAATCCAAAATGCACCTGCCATATTTCAAAGAAAGATGGAT

GAATGCTTCAAAGGAACCGAGGATTTCATCGCCGTCTATATTGATGATATTCTGGTA

TTCTCAAACTCCATCAGAGAGCATGAAAAGCACCTGCAGAGAATGCTGAGTATCTGC

AAGGAACATGGGCTCGTCCTTAGCCCAACAAAAATGAAGATTGCTGTCCCAGGAATT

GATTTCCTTGGTGCCCACATCAGAAATAGCAGAGTGAGTCTGCAACCGCACATCATC

AAGAAGATTGCTGACAAGAAAGATGATGAGCTGATGACCCTCAAAGGCCTCAGAAGC

TGGTTAGGGGTAATCAACTATGTCAGACAATACATCCCTAAGTGCGGAACACTTCTC

GGTCCTCTCTATGCTAAAACCTCTGAGCATGGTGATCGAAGATGGCACCCCAAAGAC

TGGGAAATTGTAAGACAGATCAAGAAGATGGTCCAATCCCTTCCTGATCTAGAACTT

CCTCCACCCCACGCAGTTATCATCATTGAATCTGACGGTTGCATGGAAGGATGGGGA

GGAATCTGCAAATGGAAGAACTCAAAGGGGGAGTCCAAAGGCAAGGAGCGAATCTGT

GCTTACGCCAGCGGAAAATTCCCAACAGTCAAATCCACCATAGATGCTGAAATTTAT

GCAGTCATGGCATCCCTGGAGAATTTTAAGATTTACTATCTTGATAAGCGGGAAATC

ACCATTAGAACTGACTGCCAGGCCATAATCAGCTTCTATGATAAGACGGCTATCAAG

AAACCCAGCAGAGTTCGCTGGATTAATTTTTGTGATTACATCACTAACACAGGGATT

AAAGTCCAGTTTGAACATATAAAAGGCCAAGATAATCAGCTTGCAGACCAGCTCTCA

AGGCTTGCCCAGAATGTCTGCGCAATCCAGGTCATCCCTGAATCAGCCCATGAAGCC

CTCAGTATAATTCTAGAACAAGACTGCACGGCCCAAGAATTAATGGCCCAGTTCAAC

TCTATGCTTCAGGCAAACCTCAGGCTCAACCATGGAAGGCCCAACACTACTTGGTAC

TCAAGGACCAAGCCCAAGAAATCCAAAGCCCGTAAGCAAGCCCAAGTCCAGCTACGC

TTTGACGTAAGCAATGACGACTAGGGATAATAATGGAGGAATCTTGTAAGGACAGCA

CATGGTCCTTCTTTCCTCTTTTCTTTTGTAATTTTTGTCTTCTTGTGTCGGCAACCG

CTCCTTTTGTAAAGAGGAATCTGCTTTTGAGCTGTCGATGGGGCCCAATGTGTGTAC

CCGAGCTCTAAAAGTAACTTACCTCTAGTTGCTTTTGTAAACCTTAGTTAAGTTTGT

TTTCCTTTCTCCCCTATAAAAGGGAGCCCCTCAGTTGTAAGAAGGCATCGAACAGAG

CAATACCTCTGAGCGCTTCCTTCTCTCTAGATTTCAAGTTTTCTTGTATCTTTCCAG

TTCCAGTGTTCTTAATGCAATTTGAAGTCTTCATACTCTATGTCATTCTGTTCATAG

TTCTTTTCCGCTACCTATACTCTGTGATCCAAATTTTTAATTTGTGATCTGTTTAAT

C

VITA

Yu Zhang was born August 6th, 1989 in Yingtan, Jiangxi, China. She received the following degrees: B.S. in Life Science from China Agricultural University (2009), and M.S. in Plant Sciences from Missouri State University (2011). In January 2012, she arrived in Columbia, MO, and started her doctoral studies at the Division of Plant Sciences, University of Missouri.